AN EXPERIMENTAL STUDY OF FLOW CHARACTERISTICS IN A COMPOUND MEANDERING CHANNEL

MD. ABDULLAH AL AMIN

DEPARTMENT OF WATER RESOURCES ENGINEERING

BANGLADESH UNIVERSITY OF ENGINEERING AND TECHNOLOGY (BUET), DHAKA-1000, BANGLADESH

MARCH 2013

AN EXPERIMENTAL STUDY OF FLOW CHARACTERISTICS IN A COMPOUND MEANDERING CHANNEL

by

MD. ABDULLAH AL AMIN

Student No. 100716025

In partial fulfillment of the requirement for the degree of

MASTER OF SCIENCE IN WATER RESOURCES ENGINEERING

DEPARTMENT OF WATER RESOURCES ENGINEERING

BANGLADESH UNIVERSITY OF ENGINEERING AND TECHNOLOGY (BUET), DHAKA-1000

MARCH 2013

DECLARATION

This is to certify that the thesis on **"An Experimental Study of Flow Characteristics in a Compound Meandering Channel"** has been performed by me and neither this thesis nor any part thereof has been submitted elsewhere for the award of any other degree or diploma.

--	--
(Dr. Md. Sabbir Mostafa Khan)	(Md. Abdullah Al Amin)
Countersigned by the Supervisor	Signature of the Candidate

CERTIFICATE OF APPROVAL

The thesis titled **"An Experimental Study of Flow Characteristics in a Compound Meandering Channel"**, submitted by **Md. Abdullah Al Amin**, Roll No. 100716025F, Session: October 2007, has been accepted as satisfactory in partial fulfillment of the requirement for the degree of Master of Science in Water Resources Engineering on 18th March, 2013.

____

Dr. Md. Sabbir Mostafa Khan — **Chairman**
Professor — (Supervisor)
Department of Water Resources Engineering
BUET, Dhaka-1000, Bangladesh.

____

Dr. Umme Kulsum Navera — **Member**
Professor and Head — (Ex-Officio)
Department of Water Resources Engineering
BUET, Dhaka-1000, Bangladesh.

____

Dr. Anika Yunus — **Member**
Assistant Professor
Department of Water Resources Engineering
BUET, Dhaka-1000, Bangladesh.

____

Dr. M.R. Kabir — **Member**
Pro-Vice Chancellor — (External)
University of Asia Pacific
Dhaka-1000, Bangladesh.

March 2013

ACKNOWLEDGEMENT

At first, the author acknowledges the blessings as of almighty for enabling him to carry out the study successfully.

The author expresses his profound gratitude and sincere appreciation to his supervisor Dr. Md. Sabbir Mostafa Khan, Professor, Department of Water Resources Engineering, BUET, who introduced the author to the interesting field of compound meandering channels. The author is really greatful to the supervisor for his cordial supervision, intellectual guidance, valuable suggestions, constant support and encouragement at every stage of this study.

The author is also indebted to the members of the examination committee Dr. Umme Kulsum Navera, Professor and Head, Department of Water Resources Engineering, BUET, Dr. Anika Yunus, Assistant Professor, Department of Water Resources Engineering, BUET and Dr. M. R. Kabir, ProVice-Chancellor, The University of Asia Pacific for their valuable comments and constructive suggestions regarding this study.

The author is also thankful to Mr. Mozaffar Hossain, Director and Mohammad Ali, Executive Engineer, O & M Directorate, Bangladesh Water Development Board for their help and support.

The last but not the least, acknowledgement goes to the author's family for their kind advice, support and inspiration.

MD. ABDULLAH AL AMIN

ABSTRACT

Most of the river flows in Bangladesh can be characterized as compound meandering channel in which the flow characteristics are very complex. Engineers, Planners and Researchers are highly interested in predicting accurately as well as reliably the quantitative estimates of flow parameters in a compound meandering channel. Experiments have been conducted in a compound meandering channel with symmetric cross-sections having floodplain width ratio 1, 1.67, 2.33, 3 using the large-scale open air facility in the Department of Water Resources Engineering, Bangladesh University of Engineering and Technology (BUET), Dhaka. The aim of the research was to explore the physics of flow phenomenon in the compound meandering channel with varying floodplain width. Point velocity data have been collected using an ADV (Acoustic Doppler Velocity Meter) by four runs in every setup (four setups) at five locations of a compound meandering channel.

The analysis of velocity profile and isovels show that the velocity is increasing in the inner bend and decreasing in the outer bend of a bend section in a compound meandering channel. Maximum and minimum velocity is obtained nearest to the inner bend and outer bend respectively. But in the crossover section maximum velocity is obtained nearest to the mid section of a compound meandering channel. There is a significant effect of depth and width ratio on the percentage of flow in a compound meandering channel. The percentage of flow in the main channel is decreasing with the increase of depth ratio and the percentage of flow in the main channel is increasing with the decrease of width ratio. Shear stress is increasing with the increase of depth ratio. Low magnitude of boundary shear stress is obtained at the outer bend as compare to that at the inner bend. Due to non-uniform distribution of velocities over the channel sections of a compound meandering channel, velocity distribution coefficients are introduced. The value of energy and momentum coefficient of a compound meandering channel decrease with the increase of depth ratio at the same relative width ratio.

TABLE OF CONTENTS

LIST OF FIGURES

LIST OF TABLES

LIST OF SYMBOLS

Symbol	**Meaning**
a	Amplitude
B	Overall semi-width
Bt	Total width of the mixing region
b	Semi-width of the main channel
b_t	Width of shear layer
D_r	Depth ratio (H/h)
g	Gravitational acceleration
H	Total water depth
h	Height of the main channel
H'	Depth of water above floodplain bed
k	Von Karman constant
M_B	Meander Width
M_L	Meander Length
Mr	Meander Ratio
P	Wetted perimeter of the channel section
Q	Total Discharge
Q_{mc}	Discharge in the main channel
Q_{fp}	Discharge in the floodplain
R	Hydraulic radius of the channel cross section
S_b	Channel bed slope
S_f	Floodplain bed slope

Notation	Meaning
S_r	Sinuosity
U	Mean velocity
Vx	Longitudinal Velocity
Wr	Width ratio[B/b]
Z	Height above bed
Zo	Height of hydraulic roughness
ρ	Density of flowing fluid
λ	Wave length
τ_o	Bed shear stress
α	Energy Coefficient
β	Momentum Coefficient

LIST OF ABBREVIATIONS

Abbreviation	Meaning
ADV	Acoustic Doppler Velocity-meter
BUET	Bangladesh University of Engineering and Technology
BWDB	Bangladesh Water Development Board
COR	Correlation Coefficient
LFP	Left Flood Plain
MC	Main Channel
RFP	Right Flood Plain
PVC	Polyvinyl Chloride
UK	United Kingdom

CHAPTER ONE

INTRODUCTION

1.1 General

Natural rivers, streams and man made surface drainage channels often overflow their banks during episodes of high flooding resulting in a huge potential damage to life and property as well as erosion and depositions of sediments. Many rivers have meandering compound channels possessing a main channel, which always carries flow and one or two floodplains, which only carry flow at above bankful stages. It has been established that a strong interaction between the faster moving main channel flow and slower moving floodplain flow takes place in a compound channel. This interaction results in a lateral transfer of a significant amount of longitudinal momentum which affects the velocity, discharge and bed shear stress distribution. These hydraulic parameters, in turn, affect the transport of sediments and pollutants through the compound channel system. The flow characteristics in a compound meandering channel, with the faster moving main channel and slower moving floodplain is very complex than in a straight compound channel due to three dimensional (3D) nature of the flow. Engineers, planners and researchers are highly interested in predicting accurately as well as reliably the quantitative estimates of flow parameters in a compound meandering channel. As a result, an adequate knowledge of the hydraulics of compound meandering channel flow is required for the proper design and management of rivers, drainage and irrigation canals.

1.2 Background of the Study

Most of the river flow can be characterized as compound meandering channel flow i.e. consisting of a meandering main channel flanked by one or two side flood plains. In fact, Bangladesh is one of the biggest Deltas in the world which is composed in the world of three major compound river systems, namely the Ganges, the Brahmaputra-Jamuna and the Megna. Proper quantification of the flow parameters for the main channel and flood plain flow of such rivers still has been a subject of considerable research. A systematic study is of utmost importance from the view point of better understanding of the flow phenomena in a compound meandering channel. Though Bangladesh is criss-crossed by so many rivers having meandering mechanism i.e. erosion in the outer bend and deposition in the inner bend but unfortunately research documents related to this are hard to come by. Considering the importance and scope for research, the present study is undertaken.

1.3 Objectives of the Study

The objective of the research is to understand the physics of flow phenomenon in the compound meandering channel with varying floodplain width. The specific objectives of the research are as follows:

1. Computation of discharge in the compound meandering section for various depths (Stage-Discharge Curves)
2. Velocity Distribution for different depths of flow and formulation of Isovels.
3. The Percentage of flow distribution between the main channel and the flood plain.
4. Shear stress distribution in the compound meandering channel
5. Computation of Energy Coefficient (Coriolis Coefficient) and Momentum Coefficient (Boussinesq Coefficient)

1.4 Organization of the Thesis

This thesis comprises of five chapters. General description is given in Chapter 1, Literature review is presented in Chapter 2, Experimental works are focused in Chapter 3, Results and Discussions of the research work is described in Chapter 4 and finally the Conclusions are in the Chapter 5.

The first chapter of the study gives a brief description of the flow characteristics in a compound meandering channel. It also includes the main objectives of the present study.

The second chapter gives a short account of previous studies and literature available for the present study.

The chapter three describes the experimental work as a whole. This chapter discusses about the experimental set up, construction of the channel, data collection procedures and methodology.

The chapter four describes the experimental results concerning flow parameters such as distribution of discharge, velocity, shear stress, energy coefficient and momentum coefficient.

The chapter five summarizes the conclusions drawn from the present research. A guideline for the future work is also outlined in this chapter.

In the concluding part of the thesis, results in the form of figures, tables and photographic view of a compound meandering channel are presented in the Appendix-A, Appendix-B, Appendix-C and Appendix-D. References are provided to take a look at the relevant literatures that were consulted.

CHAPTER TWO
LITERATURE REVIEW

2.1 General

A main channel flanked with one or two shallow flood plains is usually referred to as a compound channel system. The most obvious aspect of a compound channel is that the flow depths on the flood plain are often significantly smaller than the depths in the main channel especially during small floods and channel flow is known to have a distorted 3-dimensional nature mainly due to the velocity difference between the main channel and the flood plain. A shear layer is formed at the junction of the main channel and the flood plain, and fluid exchange takes place through this junction region. In case of meandering channel such flow structure is more complex. When the flow goes over bank in the compound meandering channel, the 3-dimensional (3D) flow mechanisms in the bend of a main channel are further enhanced by the interaction that may occur between the main channel and flood plain flow. An illustration of the flow field, stream wise components of main channel and flood plain flow in meandering compound channels are given in the Figure 2.1 (Ervine *et al.*, 1993), Figure 2.2 (Wormleaton *et al.*, 2004) and Figure 2.3 respectively.

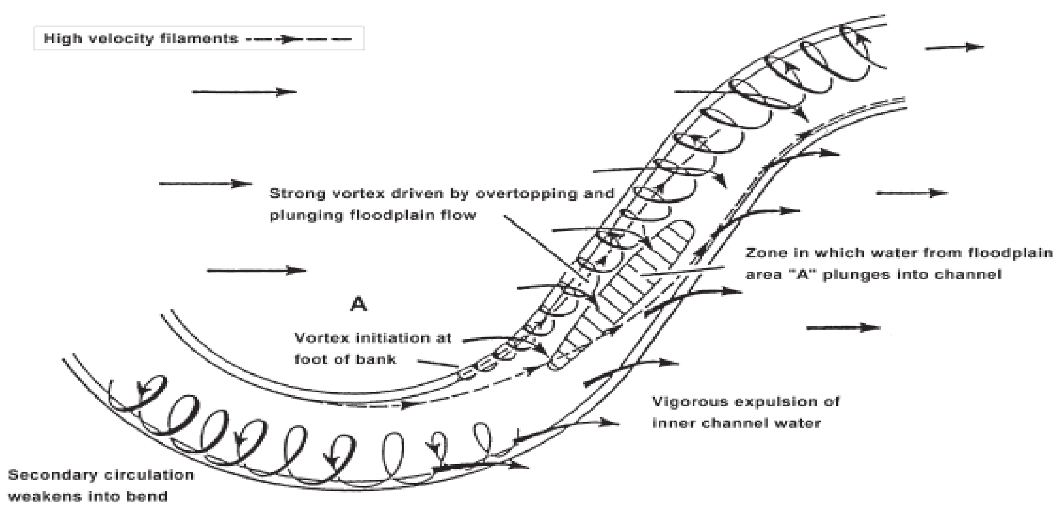

Fig 2.1: Flow Features within a flooded meandering channel

(Source: Ervine *et al.*, 1993).

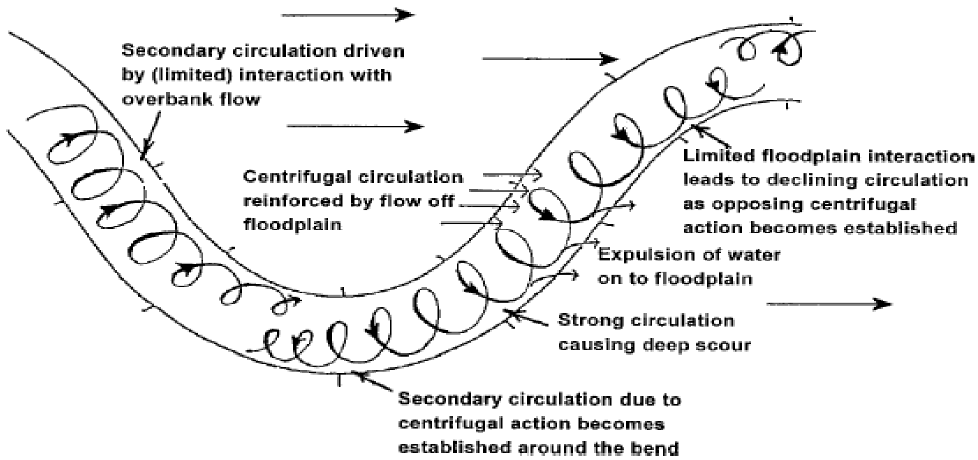

Fig 2.2: Flow Features within a flooded meandering channel

(Source: Wormleaton *et al.*, 2004).

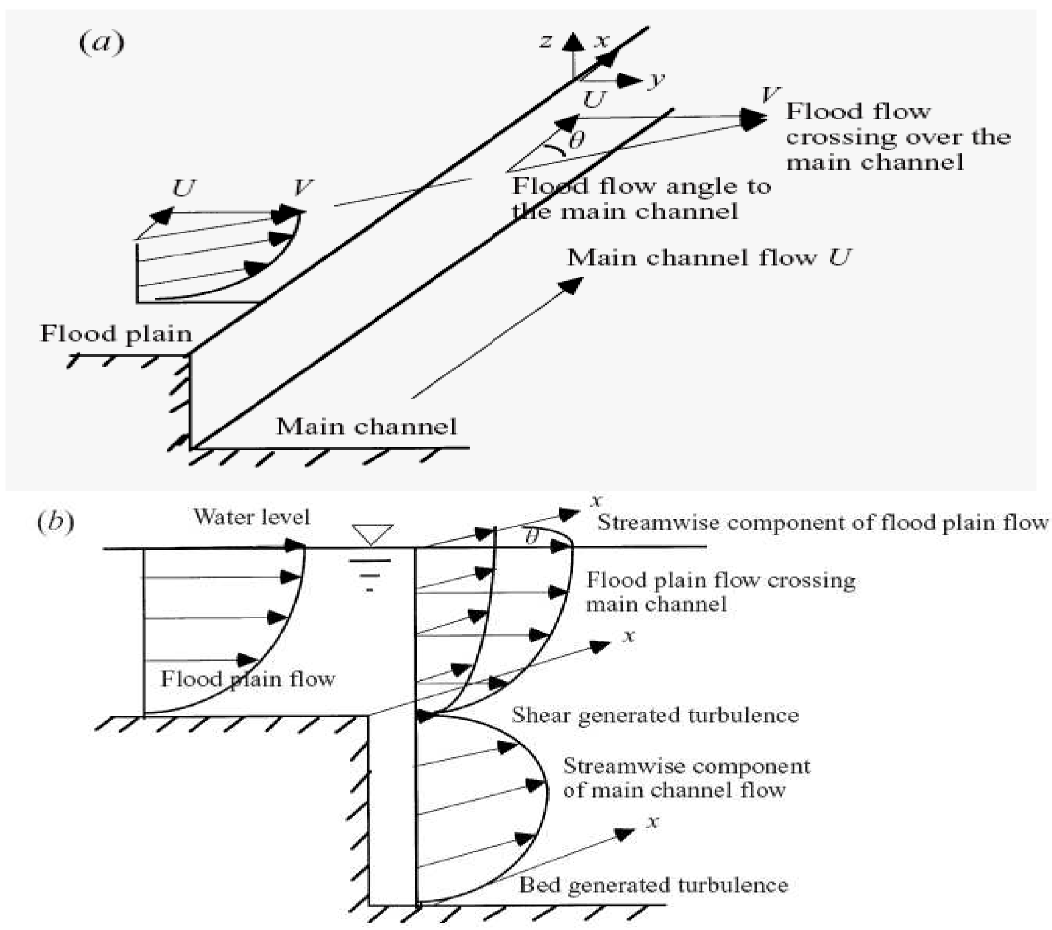

Fig 2.3: Illustration of stream wise components of main channel and floodplain flow

2.2 Preview of the Past Studies

In this section, as part of literature review a brief summary of the relevant papers are introduced. The materials reviewed may be categorized as experimental investigations of compound channel in straight reaches and compound meandering channel.

2.2.1 Compound Channels in Straight Reaches

Khatua et al. (2012) investigated the stage-discharge prediction for straight and smooth compound channels width wide floodplains and proposed a new method i.e. Modified Divided Channel Method (MDCM) for calculating the discharge in compound channels. An equation for interaction length of interface is developed for the calculation of momentum transfer between the main channel and floodplain. They found that MDCM gave satisfactory discharge results for both small-scale and large-scale experimental data. Considering all the data sets, the standard error is found to be minimum when compared with all other approaches and also compares favorably with that estimated using Conveyance Estimation System.

Ching and Luo (2012) in a paper entitled "Energy and Momentum Coefficients in Straight Symmetric Compound-Channel Flows." investigate the relationship of the energy coefficient and momentum coefficient in straight compound channel with the change of Reynold's number and cross-section shape. They showed that the value of both the energy coefficient and momentum coefficient in main channel, flood plain and total section decrease with the increase of water depth and Reynold's number at the same relative width and at the same Reynold's number, the value of both the energy coefficient and momentum coefficient in main channel and total section increase with the increase of main channel width.

Mohaghegh and Kouchakzadeh (2007) in a paper entitled "Evalution of Stage-Discharge relationship in Compound Channels." compared the experimental results with the computed results obtained from the nine most well-known methods for computation of discharge in a compound channel. The results demonstrate a high accuracy of the divided channel method with the horizontal division lines, while the length of division line is included within the calculation of the wetted perimeter. In addition, as relative depth increases, the results of the all methods converge to each other and also in case of steeper slopes in lower relative depths, more agreements between different calculated methods and experimental results were observed. Furthermore, the results show the effects of the maximum momentum transfer on the horizontal interface between the main channel and floodplains, while further angular distance from the horizontal interface toward the vertical interface between main channel and floodplains causes gradual decrease of momentum transfer effects.

Proust et al. (2006) investigated experimentally the flow in an asymmetrically compound channel transition reach in an abrupt floodplain contraction (mean angle 22°). They compared three 1D models and one 2D simulation to their experimental data to know whether the models, developed for straight and slightly converging channels, are equally valid to their geometry. They showed that the error on the level of water is moderated due to lateral mass transfer but increased error of discharge distribution in the sub-areas. They suggested for further work to understand the phenomena of severe mass transfers in non-prismatic compound channels.

Tominaga and Knight (2004) conducted numerical simulation to understand the secondary flow effect on the lateral momentum transfer with a standard k-ε model linked artificially with a given secondary flow. This simulation reproduced the typical linear distribution of momentum transfer term. The simulated secondary flow decreased the bed shear in main channel and increased the flood plain shear.

Ozbek et al. (2003) used limited experimental results from the FCF at Wallingford, for computing apparent shear stress and discharge in symmetrical compound channels with varying floodplain widths. They considered three assumed interface planes (vertical, horizontal, and diagonal) between the main channel and the floodplain sub-sections for computation of apparent shear stresses across the interfaces. They evaluated the discharge values for each sub section and for the whole cross-section. They showed that the performance of these computation methods depend on their ability to accurately predict apparent shear stress. The diagonal and horizontal division methods provided better results than the vertical division method, with the diagonal method giving the most satisfactory results.

Atabay and Knight (2002) presented some stage discharge relationship of symmetrical compound channel section using the experimental results of the Flood Channel Facility (FCF). They examined the influence of flood plain width and main channel aspect ratio to the stage discharge relationship. They derived simple empirical relationships between stage and total discharge, and stage and zonal discharge for uniform roughness and varying flood plain width ratio. The broad effects on the stage-discharge relationship due to flood plain width ratio were examined.

Myers et al. (2001) presented the experimental results of both fixed and mobile main channel boundaries together with two types of flood plain roughness compound channel using FCF data. On the basis of mathematical modeling, they proposed the velocity and discharge ratio relationships which was helpful for discharge assessment in over-bank flows and compared their results well with the data from a prototype natural compound river channel. They found that the ratios of main channel to floodplain average velocities and discharge plot logarithmically for the laboratory data, and linearity with the natural river data. The “divided channel method”(DCM) of discharge estimation overestimated the discharge in all cases and exhibited reasonable accuracy when applied to laboratory data with smooth floodplains, but showed significant errors up to 35% for rough floodplain data, and up to 27% for river data. The single channel method (SCM) significantly underestimated compound discharge for all cases for low flow depths, but became more accurate at larger depths for the smooth boundary laboratory data as well as the river data.

Thornton et al. (2000) performed series of eight experiments in a physical model of a compound channel to quantify the apparent shear stress at the interface between main channel and both vegetated and non-vegetated floodplain. They analyzed the data by using a turbulence-based method to calculate the apparent shear stress as a function of the fluctuation in channel velocities. They presented an empirical relationship for the estimation of the apparent shear stress at the main channel-floodplain interface which was found to be the function of the bed shear stress, average velocity, flow depth, and the blockage caused by floodplain vegetation. They also presented an empirical relationship to incorporate a quantitative measure of the density of vegetation within a floodplain.

Bousmar and Zech (1999) presented a theoretical 1D model of compound channel flow known as the exchange-discharge model (EDM) which is suitable for stage-discharge computation as well as practical water-profile simulations. The momentum transfer is estimated as the product of velocity gradient at the interface by the mass discharge exchanged through this interface resulting from the turbulence. Similarly, the turbulent exchange discharge is estimated by a model analogous to the mixing length model including a proportionality factor ψ that is found to be reasonably constant. They summarized that the model predicts well the stage-discharge both for the experimental data and natural data. They applied their models successfully for flow prediction in a prototype River Sambre in Belgium.

Khan (1999) in a paper entitled “A study of flow characteristics in a compound channel.” described the total discharge increases with the increase in depth and width of the compound section. The discharge decreases with the increase of flood plain roughness for the same depth ratio. Discharge in both the flood plain and main channel decreases with the increase in flood plain roughness.

Pang (1998) conducted experiments on compound channel in straight reaches under isolated and interacting conditions. It was found that the distribution of discharge between the main channel and floodplain was in accordance with the flow energy loss, which can be expressed in the form of flow resistance coefficient. In general, Manning's roughness coefficient *n* not only denoted the characteristics of channel roughness, but also influenced the energy loss in the flow. The value of *n* with the same surface in the main channel and floodplain possessed different values when the water depth in the section varied.

Myers and Lyness (1997) studied the behavior of two key discharge ratios, namely total to bank full discharge and main channel to floodplain discharge in compound channels for smooth and homogeneously roughened channels of various scales. The total to bank full discharge ratio was shown to be independent of bed slope and scale and was function of cross section geometry only. The other ratio was also independent of bed slope and scale but was influenced by the lateral floodplain bed slope. They evaluated the coefficients and exponents in the equations relating to flow ratios to flow depths.

Ackers (1993) deduced a design formula for straight two stage channels by taking into account the interaction effects between floodplain and main channel. A parameter representing the coherence between the hydraulic condition of floodplain and main channel zones was proposed. The formulations were tested in large-scale experimental channels covering a wide range of geometry.

Stephenson and Kolovopoulos (1990) in a paper entitled “Effects of Momentum Transfer in Compound Channels” discussed four different methods of subdivision of compound channels on the basis of consideration of shear stress between floodplain and main channel to evaluate a method of discharge calculation. Based on the published data, they concluded that their 'area method' was the most promising alternative of discharge computation and that Prinos-Townsend (1984) equation gave better results for apparent shear stress at floodplain and main channel interface. They incorporated channels with fairly wide range of bed roughness and floodplain widths in their computations.

Myers (1987) presented theoretical considerations of ratios of main channel velocity and discharge to the floodplain values in compound channel. These ratios followed a straight-line relationship with flow depth and were independent of bed slope but dependent on channel geometry only. Equations describing these relationships for smooth compound channel geometry were presented. The findings showed that at low depths, the conventional methods always overestimated the full cross sectional carrying capacity and underestimated at large depths, while floodplain flow capacity was always underestimated at all depths. He underlined the need for methods of compound channel analysis that accurately model proportions of flow in floodplain and main channel as well as full cross-sectional discharge capacity.

Wormleaton and Hadjipanos (1985) studied flow distribution in compound channels and showed that even though a calculation method may give satisfactory results of overall discharge in a compound channel, the distribution of flow between floodplain and main channel may be badly modeled. In general, the floodplain flow was found to be underestimated and the main channel flow overestimated.

Knight and Hamed (1984) extended the work of Knight and Demetriou (1983) to rough floodplains. The floodplains were roughened progressively in six steps to study the influence of different roughness between floodplain and main channel to the process of lateral momentum transfer. Using four dimensionless channel parameters, they presented equations for the shear force percentages carried by floodplains and the apparent shear force in vertical, horizontal, diagonal, and bisector interface plains. The apparent shear force results and discharge data provided the strength and weakness of these four commonly adopted design methods used to predict the discharge capacity of the compound channel.

Knight and Demetriou (1983) conducted experiments in straight symmetrical compound channels to understand the discharge characteristics, boundary shear stress and boundary shear force distributions in the section. They presented equations for calculating the percentage of shear force carried by floodplain and also the proportions of total flow in various sub-areas of compound section in terms of two dimensionless channel parameters. For vertical interface between main channel and floodplain the apparent shear force was found to be more at low depths of flow and also for high floodplain widths. On account of interaction of flow between floodplain and main channel, it was found that the division of flow between the subareas of the compound channel did not follow the simple linear proportion to their respective areas.

Wormleaton et al. (1982) undertook a series of laboratory tests in straight channels with symmetrical floodplains and used "divide channel" method for the assessment of discharge. From the measurement of boundary shear, apparent shear stress at the vertical, horizontal, and diagonal interface plains originating from the main channel-floodplain junction could be evaluated. An apparent shear stress ratio was proposed which was found to be a useful yardstick in selecting the best method of dividing the channel for calculating discharge. It was found that under general circumstances, the horizontal and diagonal interface method of channel separation gave better discharge results than the vertical interface plain of division at low depths of flow in the floodplains.

Rajaratnam and Ahmadi (1981) in a paper entitled "Hydraulics of channels with floodplains." studied the interaction of the flow in a main channel and a wide floodplain experimentally. They observed that because of the interaction the bed shear stress of the floodplain is increased and the bed shear stress of the main channel is decreased and that depth ratio of the flow in the main channel and floodplain determines the level of interaction. They also found that the apparent shear stress is also a function of depth ratio. They noticed that the eddy viscosity varies strongly across the flow. They defined the total width of the mixing region as:

$Bt=5.97(H-d)$; where H and d are the depths in the main channel and floodplain respectively. This width starts in the main channel where U begins to decrease with lateral distance(y) to the section in the floodplain where U reaches the steady floodplain value of U_∞.

Rajaratnam and Ahmadi (1979) studied the flow interaction between straight main channel and symmetrical floodplain with smooth boundaries. The results demonstrated the transport of longitudinal momentum from main channel to flood plain. Due to flow interaction, the bed shear in floodplain near the junction with main channel increased considerably and that in the main channel decreased. The effect of interaction reduced as the flow depth in the floodplain increased.

Myers and Elswy (1975) studied the effect of interaction mechanism and shear stress distribution in channels of complex sections. In comparison to the values under isolated condition, the results showed a decrease up to 22 percent in channel shear and increase up to 260 percent in floodplain shear. This indicated the possible regions of erosion and scour of the channel and flow distribution in alluvial compound sections.

2.2.2 Compound Meandering Channel

Prabir et al. (2012) in a paper entitled "Flow Investigations in a Wide Meandering Compound Channel" investigated the flow characteristics in a meandering compound channel that were conducted in a smooth meandering compound channel having width ratio ($W_r \approx 12$) under different values of relative depth (D_r) and velocity contours were shown. It is seen that with increased relative depth the primary velocity gradient decreases in both sides of bend apex in a meandering compound channel. However the velocity magnitude remains higher in inside of bend and adjacent floodplain than in outside zone of the bend.

Jing (2010) presented a three-dimensional (3D) numerical model to investigate the turbulent flow in meandering compound open channels with trapezoidal cross-sections. The velocity magnitude, tangential velocity, transverse velocity and Reynolds stress are calculated for various flow conditions. Good agreement between the simulated and available laboratory measurements was obtained. Comparison of the calculated secondary currents of four cases(one being inbank flow and other three being overbank flow) with different water depths reveals that the inbank flow exhibits different flow behaviors from that of the overbank flow does and the water depth has significant effects on the magnitude and direction of secondary currents.

Afzalimehr and Singh (2009) carried out field experiments on five reaches of the meandering cobble-bed Beheshtabad River in central Iran and showed that the position of the maximum velocity was independent of the relative submergence (h/d_{50} less or more than 4) and relative curvature (R/W), where h is the flow depth, d_{50} is the median diameter of sediment, R is the radius of curvature, and W is the river width. A new method, called the boundary-layer characteristic method, was employed for the determination of shear velocity. The shear velocity values estimated with this method were in agreement with those obtained using the parabolic law. The law of the wall was valid for low and high relative curvatures in the inner, outer, and central zones of the meandering reaches. However, this law was not suitable for determining the shear velocity for the relative submergence range of $2.7 < h/d_{50} < 9.6$ due to its high sensitivity to near bed velocities.

Shiono,Chan, Rameshwaran and Chandler (2008) investigated the flow characteristics in meandering channels with non-mobile and mobile beds for overbank flows measuring flow rates, velocities, turbulent kinetic energies, bed forms and sediment transport rates at overbank flows condition. The behavior of bed form in meandering channels with overbank flows was observed using digital photogrammetry, with velocity measurements taken with a Laser Doppler Anemometer. The bed form structure and velocity distributions along the meandering channel were obtained for bank full flow and three overbank flow depths. Important interactions between the flow structure and bed form were observed along the meandering channel. The sediment transport rates collected during the experiment showed three phases; an increase in the sediment transport rate up to the bankfull level, a small decrease as the flow goes overbank up to a relative depth ratio of 0.3 and then an increase again for higher flow depths. The regions of higher turbulent kinetic energy were identified. The total energy losses due to friction, secondary flow and interfacial turbulence in the lower layer flow of the main channel were compared in both the non-mobile and mobile bed cases.

Patra K.C. (2005) in a paper entitled ”Discharge Assessment for Two Stage Meandering and Straight Compound Channels.” analyzed the discharge characteristics of compound sections composed of a rectangular main channel and one or two floodplains disposed off to its sides. A set of smooth and rough sections is studied with aspect ratio varying between 2 and 5. The assumed vertical, diagonal, and horizontal interface plains are used to separate the compound channel section to subsections, the discharge for each subsection are calculated using Manning's equation. These subsection discharges are then added to give the total discharge carried by the meandering and straight compound channels. However, all these interface planes give results that are different from the observed values. A variable-inclined interface is proposed for which apparent shear force is calculated as close to zero. Equations are presented giving proportion of discharge carried by the main channel and floodplain. The equations agree well with experimental and river discharge data. Using a variable-inclined interface, the error between the measured and calculated discharges for the meandering compound sections is found to be the minimum when compared to that using other interfaces.

Wormleaton et al. (2005) investigated velocity distributions, depth variation and sediment transport under bankfull and overbank flow conditions in meandering channels with a graded sand bed using the large-scale U.K. Flood Channel Facility. They concluded that the influence of overbank flow on the morphology of the bend depended upon the roughness of the floodplain, which determined the intensity of the interaction circulation generated around the crossover. This counteracted the centrifugal circulation around the bend which in the case of both smooth and rough floodplains led to erosion of the inner point bar. However, in the case of smooth floodplain the interaction circulation was strong enough through the bend to cause deposition around the outside bank. With the rough floodplain, the net circulation around the bend was not strong enough either to maintain the point bar or cause deposition around the outside of the bend. This led to increased net erosion of bed material around the apex which was deposited downstream to form an enhanced point bar.

Patra et al. (2004) in a paper entitled “Flow and Velocity Distribution in Meandering Compound Channels.” investigated the flow and velocity distribution in meandering compound channels with over bank flow. Using power law they presented equations concerning the three-dimensional variation of longitudinal, transverse, and vertical velocity in the main channel and floodplain of meandering compound sections in terms of channel parameters. The results of formulations compared well with their respective experimental channel data obtained from a series of symmetrical and unsymmetrical test channels with smooth and rough surfaces. They also verified the formulations against the natural river and other meandering compound channel data.

Morvan et al. (2003) in a paper entitled “Three-Dimensional Hydrodynamics of Meandering Compound Channels.” investigated the velocity field in meandering compound channels with over bank flow using the Flood Channel Facility (FCF) data, and simulated the flow field using computational fluid dynamics. They predicted the velocities, secondary velocities and the helical motion of the water flowing within the main channel and compared their results with the experimental data.

Patra and Kar (2000) in a paper entitled “Flow Interaction of Meandering River with Floodplains.” reported the test results concerning the boundary shear stress, shear force, and discharge characteristics of compound meandering river sections composed of a rectangular main channel and one or two floodplains disposed off to its sides. They used five dimensionless channel parameters to form equations representing the total shear force percentage carried by floodplains. A set of smooth and rough sections were studied with aspect ratio varying from 2 to 5. Apparent shear forces on the assumed vertical, diagonal, and horizontal interface plains were found to be different from zero at low depths of flow and changed sign with increase in depth over floodplain. They proposed a variable-inclined interface for which apparent shear force was calculated as zero. They presented empirical equations predicting proportion of discharge carried by the main channel and floodplain.

Ervine et al. (2000) presented a practical method to predict depth-averaged velocity and shear stress for straight and meandering over bank flows. They also presented an analytical solution to the depth-integrated turbulent form of the Navier-Stokes equation that includes lateral shear and secondary flows in addition to bed friction. They applied this analytical solution to a number of channels, at model, and field scales, and compared with other available methods such as that of Shiono and Knight and the lateral distribution method (LDM).

Shiono et al. (1999) in a paper entitled "Stage-Discharge Assessment in Compound Meandering Channels." reported the effect of bed slope and sinuosity on discharge of two stage meandering channel. Basing on dimensional analysis, an equation for the conveyance capacity was derived which was subsequently used to obtain the stage-discharge relationship for meandering channel with over bank flow. It was found that the channel discharge increased with an increase in bed slope and it decreased with increase in sinuosity for the same channel. An error of 10% in discharge estimation was reported for relative depths exceeding 0.01.

Shiono et al. (1999) in a paper entitled "Bed shear stress in meandering channels for overbank flows" investigated boundary shear stress in meandering channels for overbank flow using a Preston tube and a heated thin film sensor. Measurements of secondary flow were also carried out using a Laser Doppler Anemometer. The distributions of the boundary stress and secondary flow along the meandering channels for over bank flow show that locations of peak and dip on the boundary shear stress distribution well correspond to those of the secondary flow downwards and upwards motion respectively.

Shiono et al. (1999) in a paper entitled “Energy Losses due to Secondary Flow and Turbulence in Meandering Channels with Overbank Flow.” presented the secondary flow and turbulence data using two components Laser- Doppler anemometer. They developed the turbulence models, and studied the behavior of secondary flow for both in bank and over bank flow conditions. They divided the channel into three sub areas, namely (i) the main channel below the horizontal interface (ii) the meander belt above the interfaces and (iii) the area outside the meander belt of the flood plain. They investigated the energy losses for compound meandering channels resulting from boundary friction, secondary flow, turbulence, expansion and contraction. They reported that the energy loss at the horizontal interface due to shear layer, the energy loss due to bed friction and energy loss due to secondary flow in lower main channel have the significant contribution to the shallow over-bank flow. They also concluded that the energy loss due to expansion and contraction in meander belt have the significant contribution to the high over-bank flow.

Shiono and Muto (1998) in a paper entitled “Complex flow mechanisms in compound meandering channels with overbank flow” investigated the most important feature of the compound meandering channel flow as the behavior of the secondary flow. Turbulence and secondary flow measurements were undertaken using a two component laser-Doppler anemometer in meander channels with straight flood plain banks. The difference in direction of rotation of the flow before and after inundation at a bend section was confirmed by the detailed velocity measurements. In addition, by performing the measurements over a half wavelength of meander, the originating and developing processes of the secondary flow were also clarified. In contrast to the centrifugal force for in bank flow, the interaction between the main channel flow and the flood plain flow in the cross-over region was found to play an important role in developing a shear produced secondary flow in the overbank cases. In such channels, large interfacial shear stresses were induced at around the bankfull level, especially in the cross-over region, and were found to be larger than the bed shear stress in magnitude. The influence of secondary flow on eddy viscosity was found also to be significant.

Fares (1995) in a paper entitled "Boundary Shear in Curved Channel with Side Overflow." investigated the characteristic changes in the boundary shear stress field of a channel bend at the intersection with a side overflow. On the basis of a field survey on bottom topography changes of the meandering river Allan Water at the cut-off section, a detailed study of boundary shear stresses in an idealized rigid bed model was undertaken. Both mathematical and experimental approaches were employed in the idealized model study. The analysis of results showed that continual reductions in shear stresses occurred in the bend at the side overflow region. The maximum reduction of shear stresses was 37% in cases of low side overflows and 82% in cases of high side overflows. These reductions were attributed to the development of stagnation and separation zones at the intersection associated with strong lateral outward currents. Based on the idealized model study, the features observed in the bed topography of Allan Water at the cutoff section are most likely to develop in cases of combined bend and high side overflows.

Wark and James (1994) developed a procedure to calculate conveyance in meandering channels with over bank flow based on the horizontal division of the cross section. It represented a significant change to the current practice of using vertical division of separating the floodplain from main channel. The non-friction energy losses were shown to be less important as the floodplain was roughened. The bed friction remained the most significant source of energy loss in the channels with over bank flow. The work was tested against the field data collected from the river Roding at Abridge in Essex and found to predict the measured stage-discharge relations reasonably well.

Sellin et al. (1993) in a paper entitled "Behavior of Meandering Two Stage Channels." studied the influence of channel geometry, floodplain widths and roughness on the stage-discharge relationship. They found that the interaction mechanism associated with over bank flow in straight channels had very little influence on meandering two stage channels. For compound channel with smooth boundary, the loss of energy at various flow depths was expressed in terms of the variation of Manning's n and Darcy-Weisbach friction factor f. They suggested that considerably more work is needed to establish a sufficiently robust calculation method to reflect adequately the range of circumstances found in the field. The influence of floodplain roughness, main channel cross section, and sinuosity on the flow structures required further studies.

Ervine et al. (1993) reported the influence of parameters like sinuosity, boundary roughness, main channel aspect ratio, width of meander belt, flow depth above bank full level, and cross sectional shape of main channel affecting the conveyance in the meandering channel. They quantified the effect of each parameter through a non-dimensional discharge coefficient F^* and reported the possible scale effects in modeling such flows.

Willetts and Hardwick (1993) in a paper entitled "Stage Dependency for Over Bank Flow in Meandering Channels." studied the measurement of stage-discharge relationship and observation of velocity fields in small laboratory two stage channels. It was found that the zones of interaction between the channel and floodplain flows occupied the whole or at least very large portion of the main channel. The water, which approached the channel by way of floodplain, penetrated to its full depth and there was a vigorous exchange of water between the inner channel and floodplain in and beyond the downstream half of each bend. This led to consequent circulation in the channel in the whole section. The energy dissipation mechanism of the trapezoidal section was found to be quite different from the rectangular section and they suggested for further study in this respect. They also suggested for further investigation to quantify the influence of floodplain roughness on flow parameters.

Mekeogh and Kiely (1989) in a paper entitled “Experimental study of the mechanisms of flood flow in meandering channels” discussed the flow mechanism and derived the following conclusions:

1) Conveyance of a meandering channel floodplain is greater than that of a straight channel floodplains
2) Boundary shear is higher in meandering flood flow than straight channel flood flow
3) The flow mechanisms of expansion and contraction are shown to occur in meandering flood flow
4) At high depth ratio, the direction of flood flow over the meandering channel is essentially parallel with the floodplain flow.
5) The longitudinal turbulence intensities were higher in magnitude for meandering channels than straight channels.
6) The maximum turbulence intensity was observed to occur on the floodplains, adjacent to the downstream interface of the crossover sections and at the inner bend of the main channel,
7) Turbulence transfer from the floodplain to the main channel was observed in straight and meandering channels.

Johannesson and Parker (1989) in a paper entitled “Velocity Distribution in Meandering Rivers.” presented an analytical model for calculating lateral distribution of depth averaged primary flow velocity in meandering rivers. Using an approximate "moment method" they accounted for the secondary flow in the convective transport of primary flow momentum, yielding satisfactory results of the redistribution of primary flow velocity.

Ervine and Ellis (1987) carried out experimental investigation for the different sources of losses of energy in the meandering compound channel. They divided the compound channel into three sub areas, namely (i) the main channel below the horizontal interface from the junction, (ii) the meander belt above the interface, and (iii) the area outside the meander belt of the flood plain. They identified the different sources of losses of energy in each sub-area and proposed a discharge estimation method.

Ghosh and Kar (1975) in a paper entitled "River Flood Plain Interaction and Distribution of Boundary Shear in a Meander Channel with Flood Plain." presented the evaluation of interaction effect and the distribution of boundary shear stress in meander channel with floodplain. Using the relationship proposed by Toebes and Sooky (1967) they evaluated the interaction effect by a parameter (W). The interaction loss increased up to a certain floodplain depth and there after it decreased. They concluded that the channel geometry and roughness distribution did not have any influence on the interaction loss.

Toebes and Sooky (1967) in a paper entitled "Hydraulics of Meandering Rivers with Floodplains." investigate the hydraulics of meandering rivers with floodplains under laboratory conditions. They attempted to relate the energy loss of the observed internal flow structure associated with interaction between main channel and floodplain flows. The significance of helicoidally channel flow and shear at the horizontal interface between main channel and floodplain flows were investigated. It was found that energy loss in compound meandering channel was more than the sum of simple meandering and uniform channel carrying the same total discharge and same wetted perimeter. The interaction loss increased with decreasing mean velocities and exhibited a maximum when the depth of flow over the floodplain was less. For the purpose of analysis, a horizontal fluid boundary located at the level of main channel bank full stage was proposed as the best alternative to divide the compound channel into hydraulic homogeneous sections. Helicoidal currents in meander floodplain geometry were observed to be different and more pronounced than those occurring in a meander channel carrying in bank flow. It was reported that Reynold's number (R) and Froude number (F) had significant influence on the meandering channel flow.

2.3 Comments on the Literature Review

From the literature review, it is apparent that most of the research in a compound meandering channel concentrated on the different methods of discharge and shear stress estimation for different width and depth ratio. But research documents related to flow characteristics i.e. velocity distribution, stage-discharge curve, flow distribution, shear stress distribution and velocity distribution coefficients in a compound meandering channel are rare not only in Bangladesh but also in the world. Velocity distribution as well as stage-discharge curve, shear stress distribution is essential for the design, operation and maintenance of a compound meandering channel and more importantly for the prediction of flood and flood protection measures. So the study of flow characteristics in a compound meandering channel is an important issue now-a-days.

CHAPTER THREE

METHODOLOGY AND DATA COLLECTION

3.1 General

The experimental study has been conducted in the open air facility of Water Resources Engineering Department, Bangladesh University of Engineering and Technology (BUET), Dhaka. In an elaborate sense, the objective of the research is to understand the physics of flow phenomenon in a compound meandering channel with different flood plain width. Required data have been collected from 20 experimental runs in four different setups of the compound meandering channel. The details of the experimental setup as well as the measuring techniques are described in the following articles.

The experimental setup consists of two parts, the permanent part and the temporary part. The permanent part is the experimental facility necessary for the storage and regulation of water circulating through the experimental reach. The temporary part is mainly brick walls which are used to vary the floodplain width for different setups.

3.2 Theory of Meandering Channel

3.2.1 Introduction

The flow in the bend of a meandering channel is of the free-vortex type where the velocity varies inversely with the radius of curvature. Because of secondary current in a bend, the flow is of helical-screw type and since the secondary current near the bed is from the outer to the inner bank, the outer bank is constant erosion and the eroded materials are deposited at the inner bank. This process causes increasing curvature of the outer bank, leading to horse shoe type loop formation. Deep channel is maintained at the outer bank and the inner bank gets shallower. In meandering channel, large interfacial shear stresses were induced at around the bankfull level, especially in the cross-over region.

3.2.2 Geometry of Meandering Channel

In general a meander is a bend in a sinuous watercourse or river. The geometry of a meandering channel (Fig 3.1) is usually described by the meander length (M_L) and meander width (M_B). Various parameters that are used to define the characteristics of the meanders are as follows:

Meander Length (M_L): The meander length is the axial length of one meander, i.e. the tangential distance between the two consecutive corresponding points of a meander.

Meander Width (M_B): The meander width is the distance between the outer edges of the one clockwise loop and the adjacent anti-clockwise loop of the meander.

Meander Ratio (M_r): The meander ratio is the ratio of the meander width to the meander length.

Sinuosity (Sr): The sinuosity is the ratio of the thalweg length to the valley length. The thawleg length is the length of the river along the line of the maximum depth.

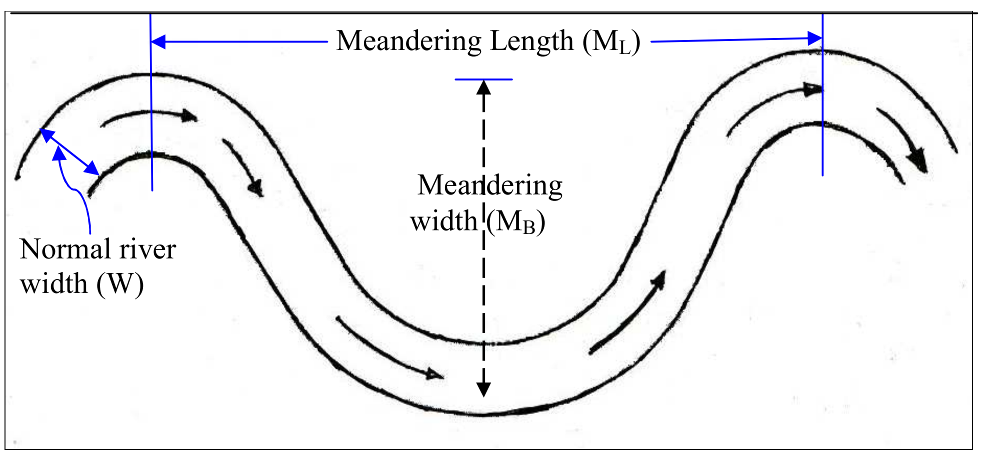

Figure 3.1: Geometry of a Meandering Channel

3.2.3 Mechanism of Meander Development

Development of a meander is a highly complex phenomenon. Various investigators studied the problem in the past and gave their own theories. Some of these theories are explained below.

1. Inglis theory: According to Inglis, when there is heavy load of bed material in the river, excess turbulent energy is developed due to unevenness of the bed. The flow does not remain axial and it it tends to concentrate towards one of the banks. When the flow concentrates at a bank that bank resists the component of velocity causing flow towards it and a part of the velocity energy is converted into pressure energy. This results in an increase in the water surface near that bank. This increased pressure causes a cross-current of the bottom water towards the other bank and there is deposition of the material at the inner bank.

2. Friedkin's Theory: According to Friedkin, meandering occurs because of local bank erosion and consequent overloading and deposition by the river of the heavier sediments which move along the bed. In other words, a bank is locally scoured which results in the excess silt charge. This excess silt charge is deposited on the same bank a little further downstream because it cannot be carried by the river. Meandering occurs because of this deposition.

3. Joglekar's Theory: According to Joglekar and his associates, the primary cause of meandering is excess of sediments in river during floods. This sediment load being in excess of the load-carrying capacity of the river is deposited on the bed. Consequently, the river tends to build up a steeper slope which causes a reduction in the depth of water. There is a corresponding increase in the width of the river channel if the banks do not resist erosion. Even when there is a slight deviation from uniform axial flow, more flow occurs towards one bank than the other. Additional flow is immediately attracted towards that bank. It leads to shoal formation at the other bank. This accentuates the curvature of flow and finally a meander is formed.

3.3 Description of Different Components

3.3.1 Outline of the Experimental Reach

The experimental reach consists of a 670 cm long symmetric compound meandering channel, set at a constant bed slope 0.001845 with fixed bed and banks. The cross sectional dimension of a compound meandering channel is 45.70cmx24.10cm and the maximum floodplain width is 45.70cm. The entire reach is constructed by brick, cement and sand. The experimental reach of this compound meandering channel has wavelength, λ=365.70cm, amplitude, a=137.2 cm, giving sinuosity ratio of 1.20. A schematic diagram of the experimental reach and experimental setup are presented in the figure 3.2 and figure 3.3 respectively.

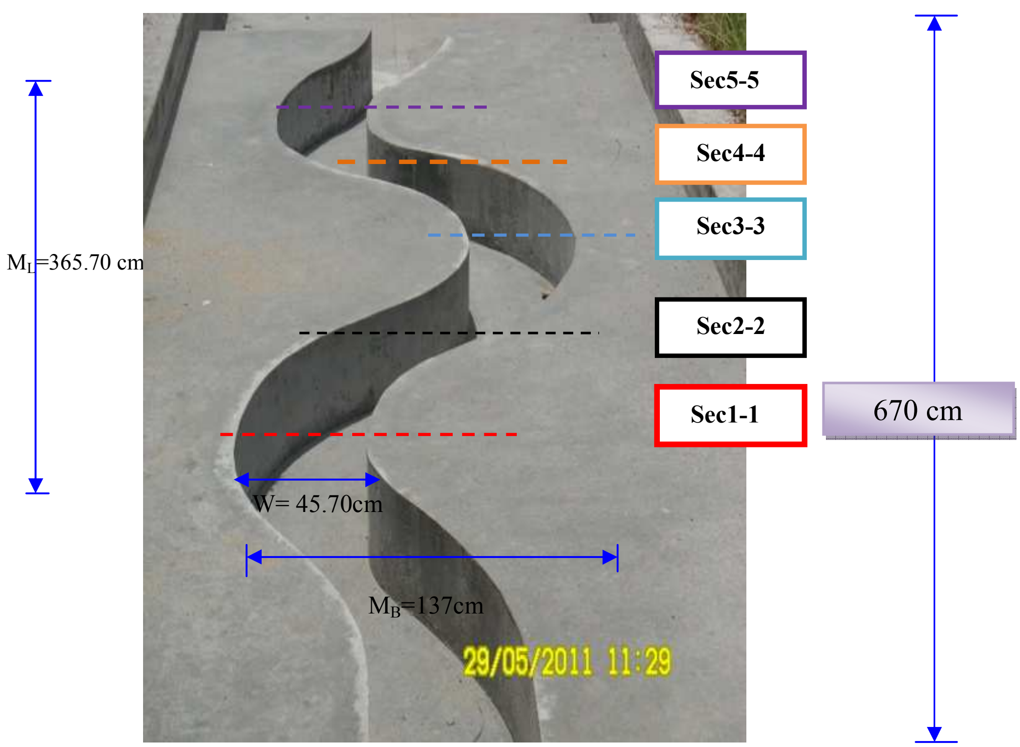

Figure 3.2: A Schematic diagram of the Experimental Reach

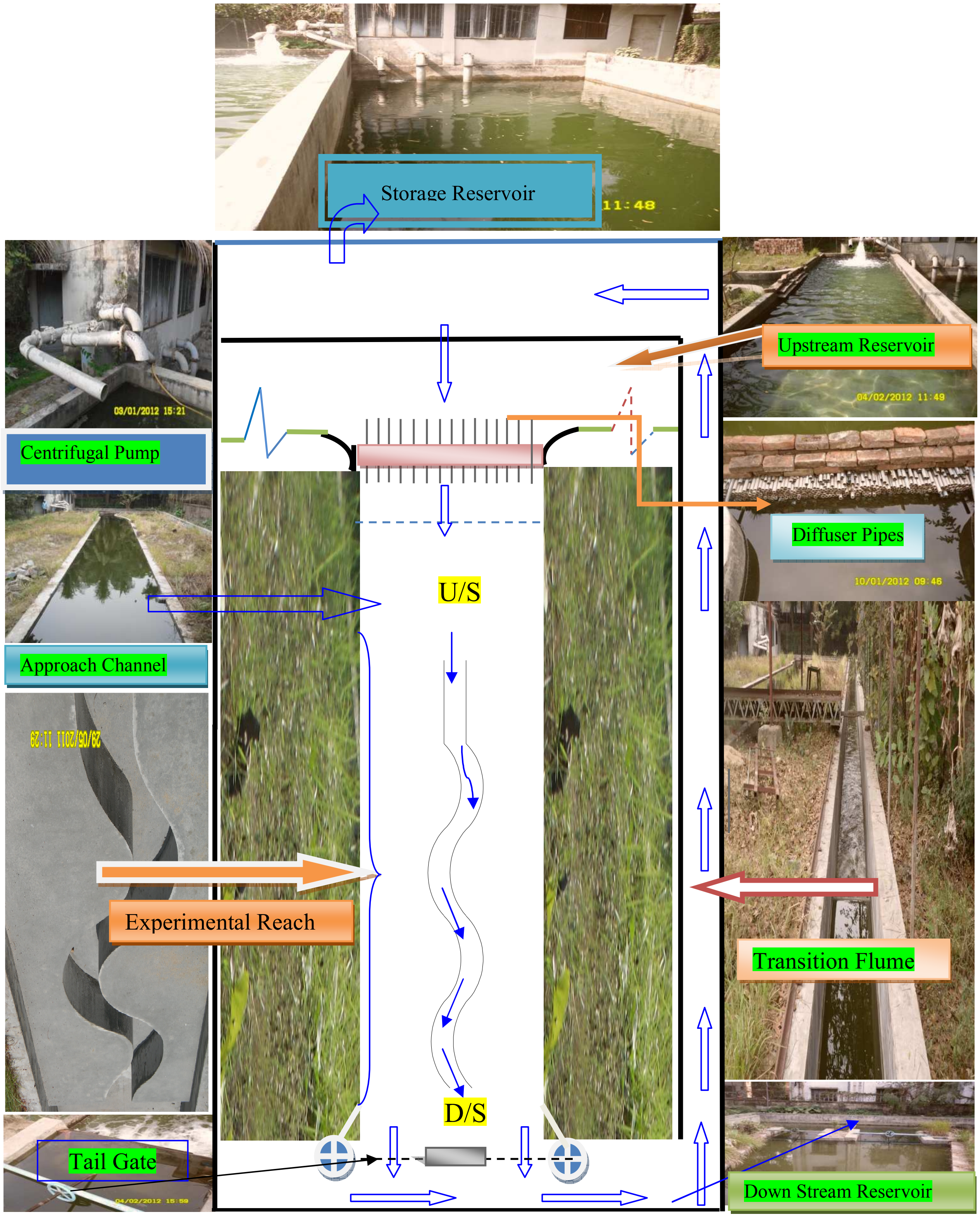

Figure 3.3: A Schematic Diagram of the Experimental Setup

3.3.2 The Water Supply System

3.3.2.1 The Storage Reservoir

The storage reservoir has a cross sectional dimension 12mx5.8m and a height of 5.6m. From the storage reservoir water is intake by the pump and discharge to the upstream reservoir. On every third day the reservoir was emptied, cleaned and refilled again. The valve attached to the reservoir is used to empty the reservoir for cleaning or repairing purpose.

3.3.2.2 The Upstream Reservoir

The upstream reservoir is located between the storage reservoir and the approach channel where water is stored from the direct supply of the pump. The reservoir has a cross sectional dimension 11.2mx3.2m and a height of 1.5m.Water from the upstream reservoir passes through a flexible wall built in bricks and PVC pipes into the approach channel. This is done to ensure undisturbed and uniform flow in the experimental reach.

3.3.2.3 The Approach Channel

The approach channel conveys water to the experimental channel. This channel is 30m in length and 3.1m in width. The walls of the channel are made of bricks, sand and cement. The sharp crested weir is located in the upstream of the channel. This channel carries water as a uniform flow.

3.3.2.4 The Downstream Reservoir

The downstream reservoir serves as the transition reservoir. At the entrance of the reservoir, there is a tail gate and a spillway is used to remove excess water at the end.

3.3.2.5 The Centrifugal Pump

The centrifugal pump draws water from the storage reservoir and supplies to the upstream reservoir. The pump has a maximum discharge capacity of 80 l/s.

The pump is primed before the motor is started. A small hole is provided in the sides of the centrifugal pump to assist the priming operation.

3.3.2.6 The Tail Gate

The water regulating function of the downstream end is provided by tail gate. The tail gate rotates around a horizontal axis. It is operated to maintain desired water level in the experimental reach. At the end of the experimental channel, water is allowed to flow freely so that backwater has no effect in the experimental reach.

3.3.2.7 The Transition Flume

Behind the tail gate, the water falls into the stilling basin and passes through a transition flume which allows water for recirculation.

3.3.2.8 The Guide Vanes and Tubes

To ensure a more smooth flow towards the approach channel guide vanes and tubes are placed between the upstream reservoir and the approach channel which are at right angle to each other. In order to prevent turbulence in the approach channel, PVC pipes (Diffuser) are used.

3.4 Measuring Equipments

3.4.1 Measuring Line and Measuring Bridge

To indicate the co-ordinate system and the location of various measurements, both side walls are equipped with parallel measuring lines, indicating the X direction. As the experimental reach is a meandering channel, so the actual X direction for main channel is taken as the flow direction and by using a set-square, the perpendicular direction is determined. During data collection, the measuring bridge (frame) is to be moved in the predefined location along the channel manually. A small steel strand is fitted on the bridge and operated manually. The measuring instrument is kept fixed on this strand.

3.4.2 The Point Gauge and Reference Point

The point gauge is used to measure water level in the approach channel. The gauge is installed at the approach channel that helps to maintain water level in the experimental reach for different runs in a setup.

3.4.3 The Acoustic Doppler Velocity Meter

The Acoustic Doppler Velocity meter (ADV) is a single point current meter that accurately measures the three components of water velocity in both high and extremely low flow conditions. Velocities are measured in a sampling volume located a distance away from the probe head. The probe head is made up of a single transmitter located in the center of the probe head and either two or three receivers mounted on arms. The transmitter generates a narrow beam of sound that is projected through the water. Reflections from particles or scatters such as suspended sediment, biological matter or bubbles in the water are reflected and sampled by the highly sensitivity receivers. The intersection of the receiver axes designates the location of the sampling volume. The 10-MHz ADV (figure3.12) is suitable for a wide range of applications ranging from laboratory, to field, to full oceanographic applications. The 10-MHz ADV has the following features

- Three-axis velocity measurement
- Sampling Rate 0.1 to 25Hz
- Sampling Volume 0.25cc
- Distance to sampling volume 5 or 10cm
- Resolution 0.01cm/s
- Accuracy 1% of measured velocity, ±0.25cm/s
- Programmable velocity (cm/s) 3, 10, 30, 100, 250.

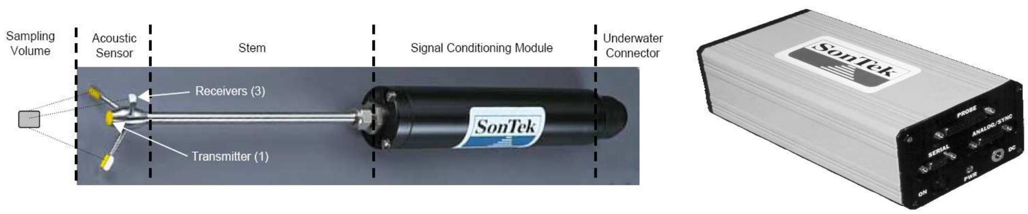

Figure 3.4: Acoustic Doppler Velocity Meter

3.5 Experimental Procedure

3.5.1 Construction of the Compound Meandering Channel

An extensive works has been done for the construction of the compound meandering channel in the physical laboratory i.e. open air facility in the Water Resources Engineering department, BUET. At first the experimental reach of the physical lab is developed by sand filling. The channel bed is prepared by brick flat soling and net finishing is done by cement layer. The required drawing is setup by a handmade large compass with a permanent marker. The construction phase of the channel is shown in figure 3.5. At every step of the construction, the required dimensions were checked thoroughly and from starting to end the entire construction process was under regular supervision.

Figure 3.5: Construction Stage of Compound Meandering Channel

3.5.2 Determination of Channel Slope

The average channel bottom slope and floodplain slope were determined by measuring the elevations of bed level at different intervals by a level and staff. By dividing the difference of bed level elevation to the length difference, the bed slope of main channel for each segment is obtained and then averaging all the values the channel bed slope, S_b is determined. Similarly by dividing the difference of elevation to the length difference of floodplain bed and then averaging all the values, the floodplain bed slope, S_f is determined. Table 3.1 shows the determination of channel bottom slope and flood plain slope.

Table 3.1: Determination of bed slope

Location	Distance(cm)	Elevation(cm)	Slope	Average Slope
Main Channel	0.000	421.975	-	0.001823
	83.82	421.975	0.000000	
	167.64	422.140	0.001970	
	251.46	422.390	0.002980	
	335.28	422.410	0.000242	
	419.10	422.490	0.000956	
	502.92	422.850	0.004202	
	586.74	423.00	0.004204	
	670.56	423.20	0.001791	
Right floodplain and Left floodplain	0.000	397.85	-	0.001821
	83.82	397.85	0.000000	
	167.64	398.09	0.002860	
	251.46	398.26	0.002032	
	335.28	398.28	0.000243	
	419.10	398.36	0.000956	
	502.92	398.72	0.004291	
	586.74	398.87	0.001790	
	670.56	399.07	0.002390	

3.5.3 Data Collection and Processing

The entire experiment consists of four setups for different width ratio i.e. Wr=3, Wr=2.33, Wr=1.67, Wr=1. Each setup has four runs i.e. depth ratio Dr=0.40, Dr=0.35, Dr=0.30, Dr=0.20. Each run consists of five cross sections. Each cross section is divided into 19 zones starting from left floodplain to right floodplain. The main channel is equally divided into nine zones (zone MC1 to zone MC9), the left floodplain is equally divided into 5 zones (zone LFP1 to zone LFP5) and right floodplain is divided into 5 zones (zone RFP1 to zone RFP5). Table 3.2 shows the laboratory test scenarios and cross-sectional location for data collection is shown in the figure 3.6(a) and figure 3.6(b) represents the layout of Bend Section.

Table 3.2 Laboratory Test Scenarios

Run No	Meaning of Run No
C1S1R1	Case1(Wr=1) Section1(U/S Bend) Run1(Dr=0.20)
C1S1R2	Case1(Wr=1) Section1(U/S Bend) Run2(Dr=0.30)
C1S1R3	Case1(Wr=1) Section1(U/S Bend) Run3(Dr=0.35)
C1S1R4	Case1(Wr=1) Section1(U/S Bend) Run4(Dr=0.40)
C1S2R1	Case1(Wr =1) Section2(U/S Cross-over) Run1(Dr =0.20)
C1S2R2	Case1(Wr =1) Section2(U/S Cross-over) Run2(Dr =0.30)
C1S2R3	Case1(Wr =1) Section2(U/S Cross-over) Run3(Dr =0.35)
C1S2R4	Case1(Wr =1) Section2(U/S Cross-over) Run4(Dr =0.40)
C1S3R1	Case1(Wr =1) Section3(Middle Bend) Run1(Dr =0.20)
C1S3R2	Case1(Wr =1) Section3(Middle Bend) Run2(Dr =0.30)
C1S3R3	Case1(Wr =1) Section3(Middle Bend) Run3(Dr =0.35)
C1S3R4	Case1(Wr =1) Section3(Middle Bend) Run4(Dr =0.40)
C2S1R1	Case2(Wr =1.67) Section1(U/S Bend) Run1(Dr =0.20)
C2S1R2	Case2(Wr =1.67) Section1(U/S Bend) Run2(Dr =0.30)
C2S1R3	Case2(Wr =1.67) Section1(U/S Bend) Run3(Dr =0.35)
C2S1R4	Case2(Wr =1.67) Section1(U/S Bend) Run4(Dr =0.40)

Contd. Table 3.2

Run No	Meaning of Run No
C2S2R1	Case2(Wr =1.67) Section2(U/S Cross-over) Run1(Dr =0.20)
C2S2R2	Case2(Wr =1.67) Section2(U/S Cross-over) Run2(Dr =0.30)
C2S2R3	Case2(Wr =1.67) Section2(U/S Cross-over) Run3(Dr =0.35)
C2S2R4	Case2(Wr =1.67) Section2(U/S Cross-over) Run4(Dr =0.40)
C2S3R1	Case2(Wr =1.67) Section3(Middle Bend) Run1(Dr =0.20)
C2S3R2	Case2(Wr =1.67) Section3(Middle Bend) Run2(Dr =0.30)
C2S3R3	Case2(Wr =1.67) Section3(Middle Bend) Run3(Dr =0.35)
C2S3R4	Case2(Wr =1.67) Section3(Middle Bend) Run4(Dr =0.40)
C3S1R1	Case3(Wr =2.33) Section1(U/S Bend) Run1(Dr =0.20)
C3S1R2	Case3(Wr =2.33) Section1(U/S Bend) Run2(Dr =0.30)
C3S1R3	Case3(Wr =2.33) Section1(U/S Bend) Run3(Dr =0.35)
C3S1R4	Case3(Wr =2.33) Section1(U/S Bend) Run4(Dr =0.40)
C3S2R1	Case3(Wr =2.33) Section2(U/S Cross-over) Run1(Dr =0.20)
C3S2R2	Case3(Wr =2.33) Section2(U/S Cross-over) Run2(Dr =0.30)
C3S2R3	Case3(Wr =2.33) Section2(U/S Cross-over) Run3(Dr =0.35)
C3S2R4	Case3(Wr =2.33) Section2(U/S Cross-over) Run4(Dr =0.40)
C3S3R1	Case3(Wr =2.33) Section3(Middle Bend) Run1(Dr =0.20)
C3S3R2	Case3(Wr =2.33) Section3(Middle Bend) Run2(Dr =0.30)
C3S3R3	Case3(Wr =2.33) Section3(Middle Bend) Run3(Dr =0.35)
C3S3R4	Case3(Wr =2.33) Section3(Middle Bend) Run4(Dr =0.40)
C4S1R1	Case4(Wr =3) Section1(U/S Bend) Run1(Dr =0.20)
C4S1R2	Case4(Wr =3) Section1(U/S Bend) Run2(Dr =0.30)
C4S1R3	Case4(Wr =3) Section1(U/S Bend) Run3(Dr =0.35)
C4S1R4	Case4(Wr =3) Section1(U/S Bend) Run4(Dr =0.40)
C4S2R1	Case4(Wr =3) Section2(U/S Cross-over) Run1(Dr =0.20)
C4S2R2	Case4(Wr =3) Section2(U/S Cross-over) Run2(Dr =0.30)
C4S2R3	Case4(Wr =3) Section2(U/S Cross-over) Run3(Dr =0.35)
C4S2R4	Case4(Wr =3) Section2(U/S Cross-over)e Run4(Dr =0.40)
C4S3R4	Case4(Wr =3) Section3(Middle Bend) Run4(Dr =0.40)

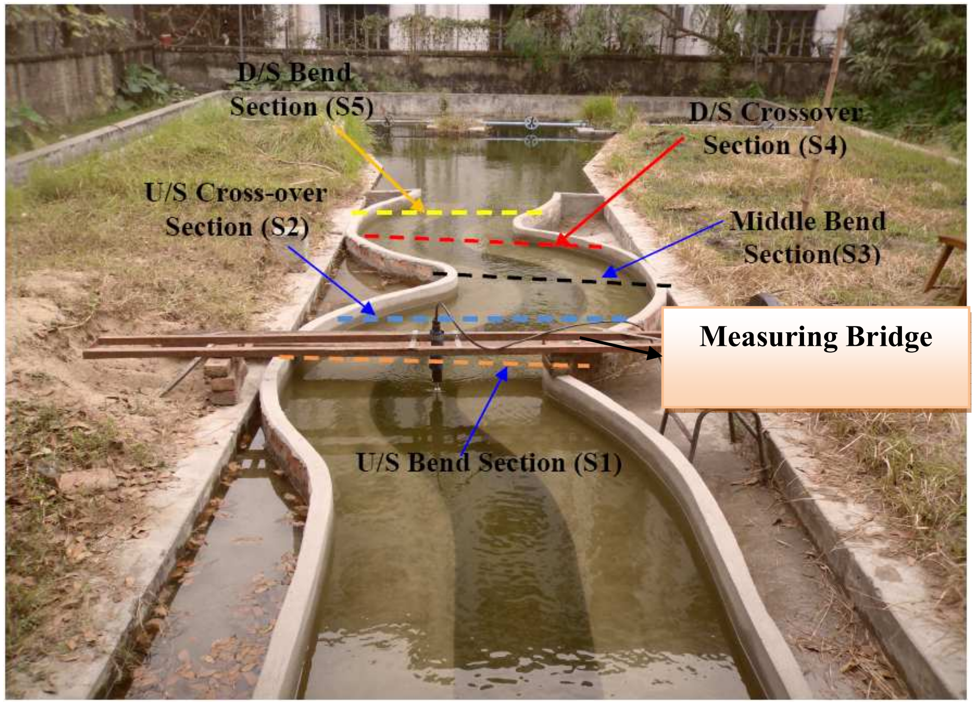

Figure 3.6(a): The Cross-sectional location for data collection

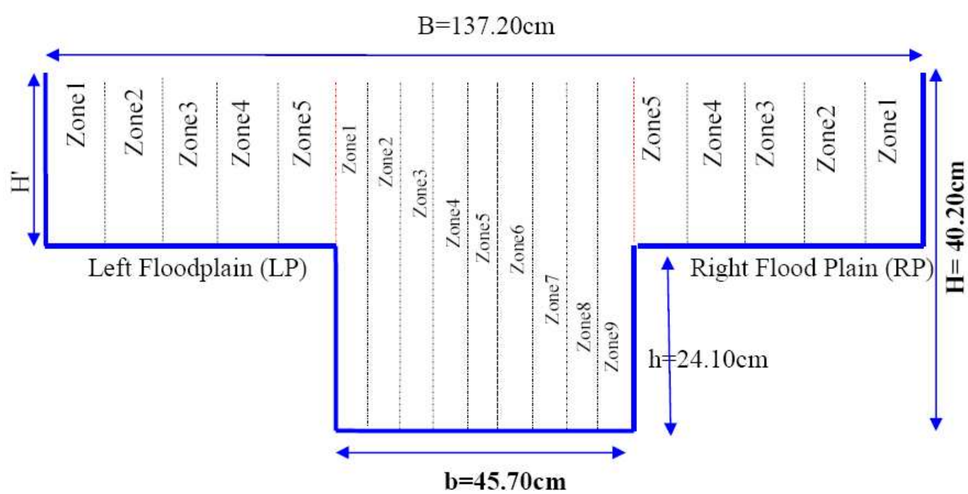

Figure 3.6(b): Layout of U/S Bend Section

In each zone 3D point velocity readings are taken by ADV at five vertical points i.e. 0.1H, 0.2H, 0.4H, 0.6H, 0.8H for main channel and 0.1H', 0.2H', 0.4H', 0.6H', 0.8H' for floodplain. In each vertical point 60 seconds point velocity readings are taken. Sample of data collection by ADV is shown in figure 3.7.

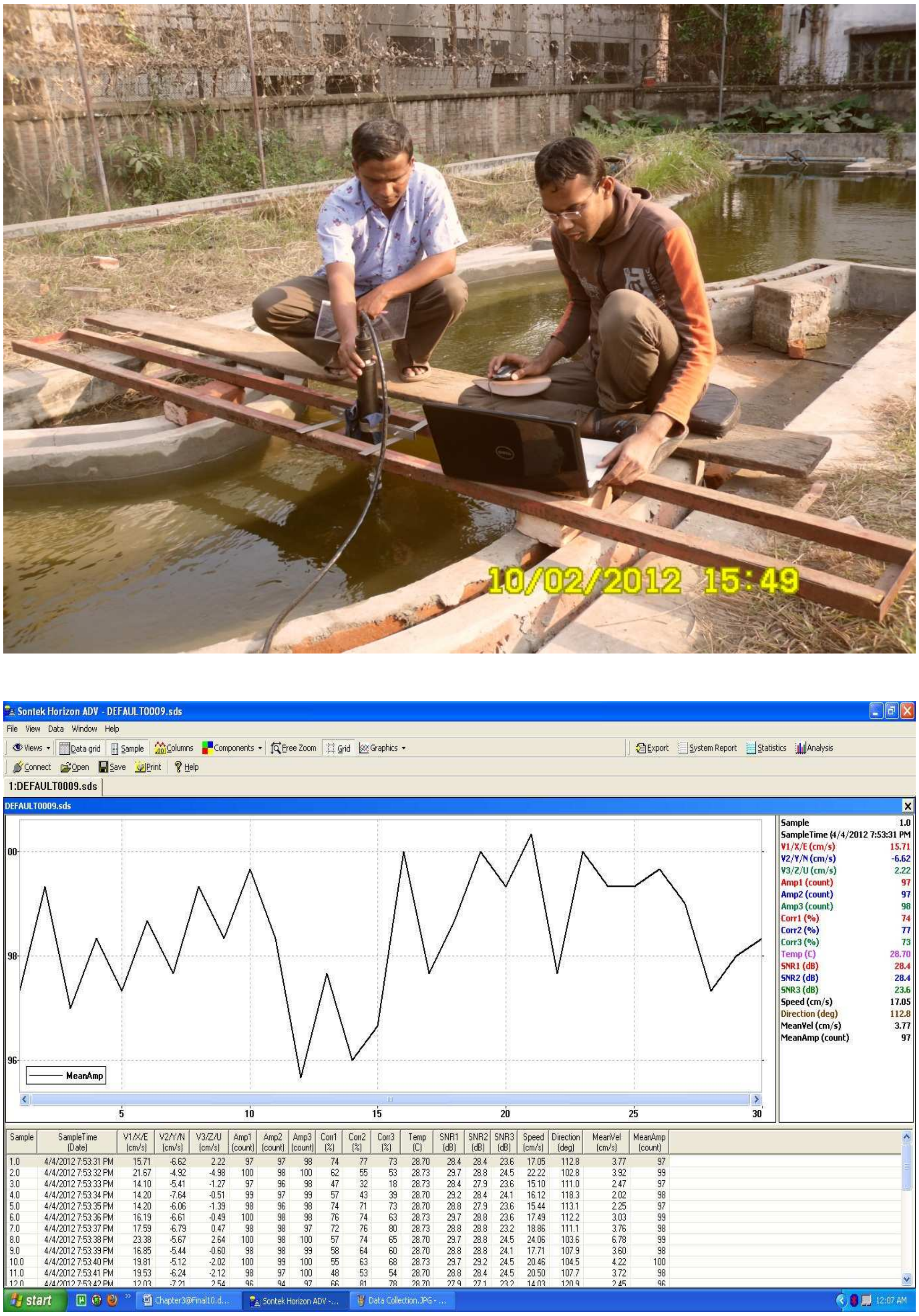

Figure 3.7: Data Collection by ADV

3.5.4 Measurement of Velocity

Owing to the presence of the free surface and the friction over the channel bed and banks, the velocities are not uniformly distributed in an open channel flow section. The velocity along a vertical varies from zero at the stream bed and maximum at or near the surface. The average velocity along a vertical is determined by measuring the velocities at 0.2 and 0.8 of the depth below the free surface when the depth is more than 0.61m or at 0.6 of the depth when the depth is less than 0.61m, i.e.

$$\bar{U} = \frac{U_{0.2} + U_{0.8}}{2} \approx U_{0.6} \qquad \textbf{3.1}$$

3.5.5 Measurement of Discharge

Different methods are available for the measurement of discharge in an open channel flow and of them area velocity method is the familiar one. In this method a channel section is subdivided into a number of segments by a number of successive intervals. Then by using the average velocity determined according to the previous article, the discharge of the segment is calculated as follows

$$\Delta Q_i = \Delta A_i . U_i \qquad \textbf{3.2}$$

Where ΔQ_i the discharge in the ith segment, ΔA_i is the cross-sectional area of the ith segment and U_i is the average velocity at the ith vertical.

The total discharge is computed as

$$Q = \Sigma \Delta Q_i \qquad \textbf{3.3}$$

The cross-sectional mean velocity of a stream is equal to the discharge divided by the area, i.e.

$$U = \frac{Q}{\Sigma \Delta A} \qquad \textbf{3.4}$$

3.5.6 Estimation of Bed Shear Stress

Shear Stress is a measure of the force of friction from a fluid acting on a body in the path of that fluid .In the case of open channel flow; it is the force of moving water against the bed of the channel. Estimation of bottom shear stress is important because it controls the erosion and deposition of sediments at the bed as well as their diffusion in the water column. For simple ideal conditions, bottom shear stress could be measured directly using a Floating Plate element or a Preston tube. In turbulent flows the estimation of bed shear stress may be linked to the first moment statistics (mean) or second moment statistics of the turbulence. Different methods available are Logarithmic velocity profile method, Covariance or Reynolds stress method, Turbulent kinetic energy method and Inertial dissipation method. The bed shear stress can be calculated by the following equation

$$\tau_0=\rho gRS_0 \qquad \textbf{3.5}$$

Where, g=gravitational acceleration,

ρ= density of flowing fluid,

R= hydraulic radius of the channel cross-section

S_0=channel bottom slope.

Velocity profiles are often used as an indirect method to determine mean boundary shear stress in natural rivers (Wilcock 1996).While several methods are available to determine the time-averaged local boundary shear stress(e.g.Biron et al.2004,Dietrich & Whiting 1989), this study employs the theoretical log-law, given as:

$$U/U^*=(1/k)\ln(Z/Zo) \qquad \textbf{3.6}$$

Where U is the mean velocity, U* is the friction velocity, k is von Karman's constant (k=0.4), Z is the height above bed, Zo is the height of hydraulic roughness.

The above equation applies within a near bed region that is both well below the free surface and above the local influence of individual bed roughness elements.

For steady uniform sub critical flow in a wide straight channel with roughness dominated by grains on the bed surface, a log profile is found to closely approximate velocity throughout the flow depth.

3.5.7 Velocity Distribution Coefficients

Due to non-uniform velocity distribution in a channel section, the kinetic energy and the momentum of flow computed from the cross-sectional mean velocity are generally less than their actual values. To get the actual kinetic energy of flow, the kinetic energy based on the mean velocity is multiplied by the coefficient,α known as the kinetic energy coefficient or the Coriolis coefficient. Similarly to get the actual momentum, the momentum based on the mean velocity is multiplied by the coefficient,β known as the momentum coefficient or the Boussinesq coefficient. The energy and momentum coefficients α and β together are known as the velocity distribution coefficients. The energy and momentum coefficients are always positive and never less than unity. For uniform velocity distribution in the channel section, α= β=1. From the experimental results the value of α varies from 1.03 to 1.36 and β varies from 1.01 to 1.12 for fairly straight prismatic channel, but it changes due to many factors such as meander parameters and roughness criteria of the channel. In channels of complex cross-section, the coefficient for energy and momentum can easily be as great as 1.6 and 1.2 and can vary quite rapidly from section to section in case of irregular alignment. In regular channels, flumes, spillways the average value of energy and momentum coefficient are 1.15 and 1.07. On the other hand in the river valley over flooded condition the average value of energy and momentum coefficient are 1.75 and 1.2 (After Chow, 1958).

Energy Coefficient (α) and Momentum Coefficient (β) can be expressed as:

$$\alpha = \frac{\Sigma u^3 \Delta A}{U^3 A} \qquad 3.7$$

$$\beta = \frac{\Sigma u^2 \Delta A}{U^2 A} \qquad 3.8$$

CHAPTER FOUR
RESULTS AND DISCUSSSIONS

4.1 General

A detailed analysis of experimental data is presented in this chapter. At first, the flow parameters that are involved in a compound meandering channel are identified. The analysis of the results is based on highlighting the individual flow parameter separately and analyzing them individually. In this chapter, the results of the following experimental flow parameters will be discussed successively in separate sections.

- Velocity Distribution
- Discharge
- Flow Distribution
- Shear Stress
- Velocity Distribution Coefficients

4.2 Velocity Distribution

Velocity distribution in a compound meandering channel is affected by many factors such as width ratio, depth ratio, roughness of the channel, geometry of the channel, presence of bends etc. Here velocity distribution with respect to depth ratio and width ratio are analyzed. Investigations of velocity distribution in the compound meandering channel are discussed in the following articles.

4.2.1 Individual Velocity Profiles

In this study, three dimensional point velocities in several sections for the different depth ratios and width ratios are measured. Here, the longitudinal velocity distribution curve of different depth and width ratio for some locations is presented and all other velocity distribution curves are given in the figures A-1 to A-31 at Appendix-A.

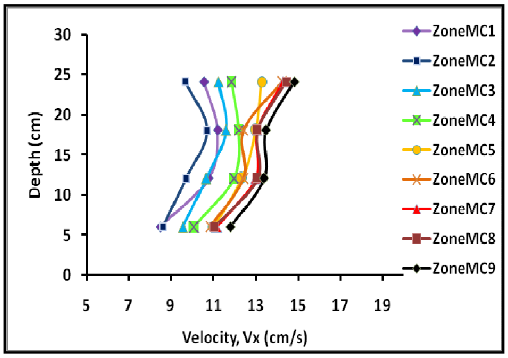

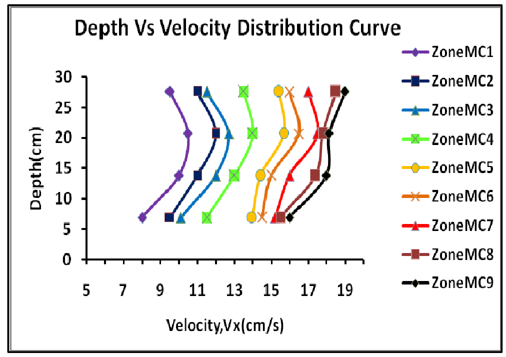

U/S Bend Section, Depth ratio 0.20
C1S1R1

U/S Bend Section, Depth ratio 0.30
C1S1R2

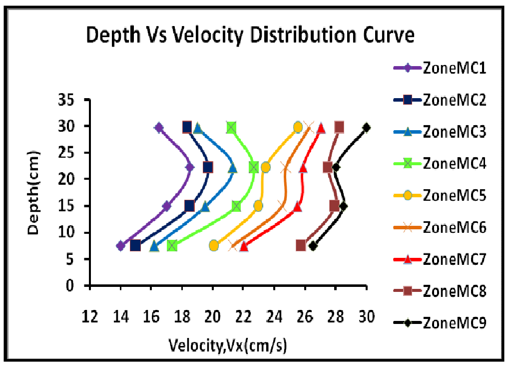

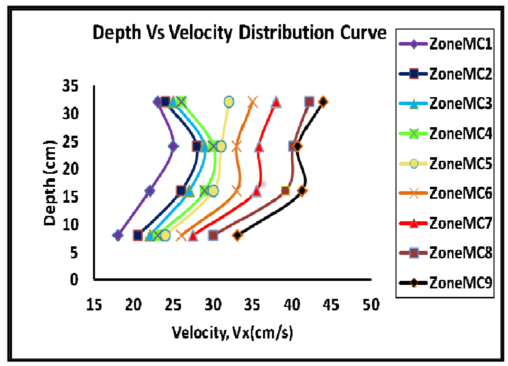

U/S Bend Section, Depth ratio 0.35
C1S1R3

U/S Bend Section, Depth ratio 0.40
C1S1R4

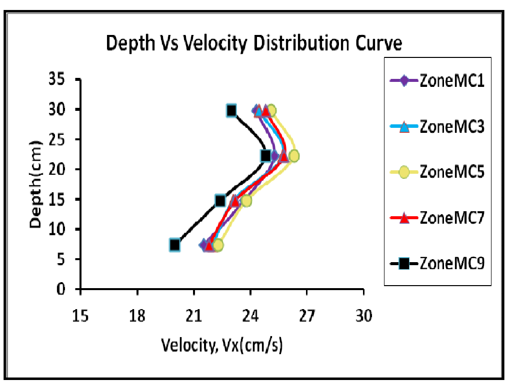

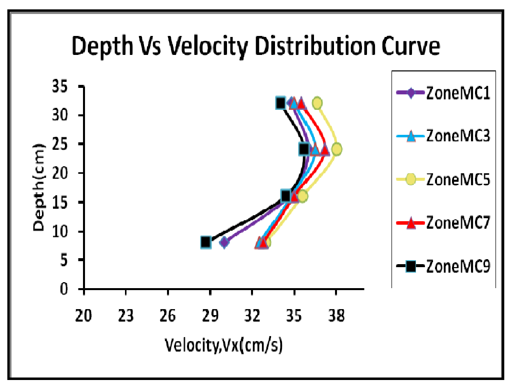

U/S Crossover Section, Depth ratio 0.35
C1S2R3

U/S Crossover Section, Depth ratio 0.40
C1S2R4

Figure 4.1: Longitudinal Velocity Profile for Case 1 (Wr=1) i.e. No Floodplain Condition

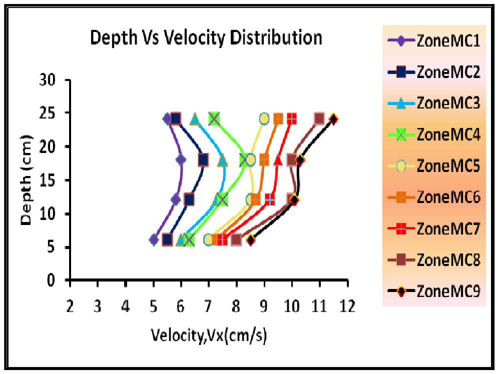

U/S Bend Section, Depth ratio 0.20
C2S1R1 (MC)

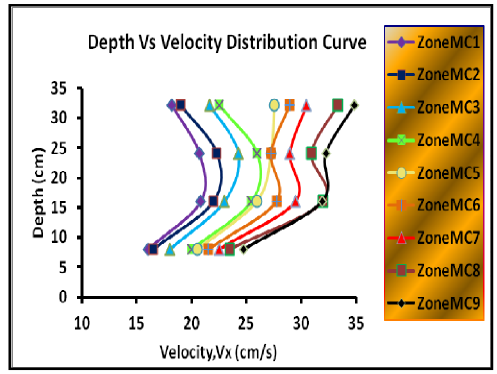

U/S Bend Section, Depth ratio 0.40
C2S1R4 (MC)

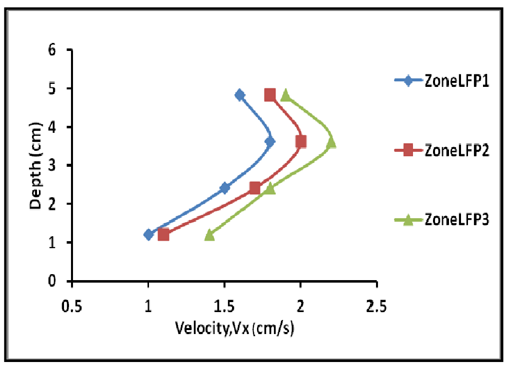

U/S Bend Section, Depth ratio 0.20
C2S1R1 (LFP i.e. Outer Bend)

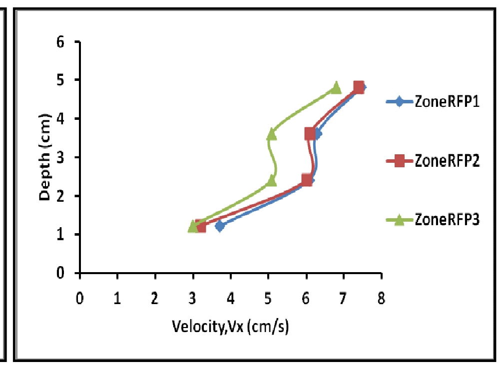

U/S Bend Section, Depth ratio 0.20
C2S1R1 (RFP i.e. Inner Bend)

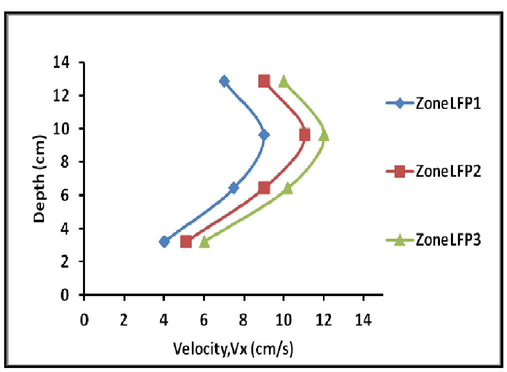

U/S Bend Section, Depth ratio 0.40
C2S1R1 (LFP i.e. Outer Bend)

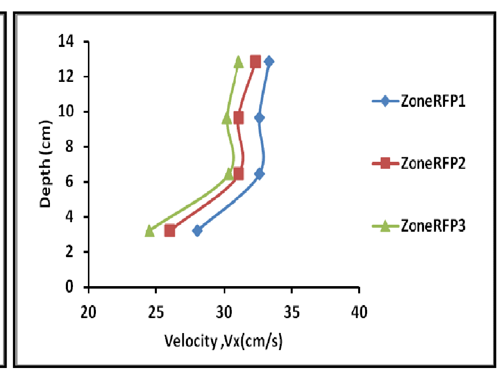

U/S Bend Section, Depth ratio 0.40
C2S1R1 (RFP i.e. Inner Bend)

Figure 4.2: Longitudinal Velocity Profile for Case 2 (Wr=1.67) i.e. floodplain width 15.30 cm

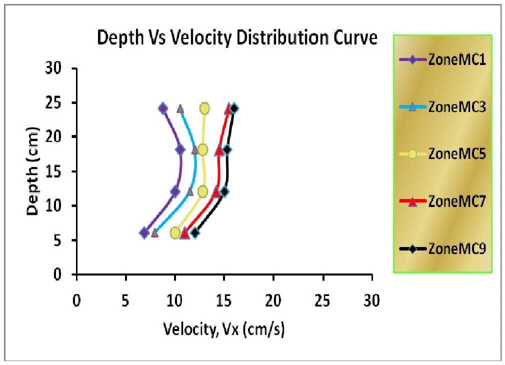

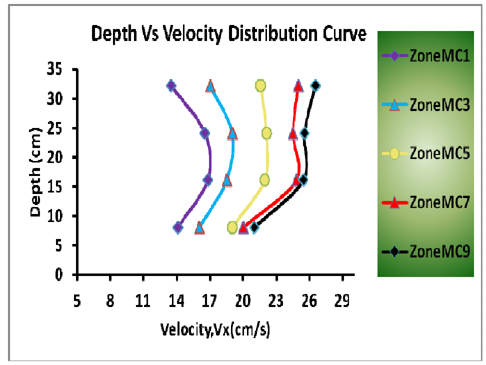

U/S Bend Section, Depth ratio 0.20
C3S1R1 (MC)

U/S Bend Section, Depth ratio 0.40
C3S1R4 (MC)

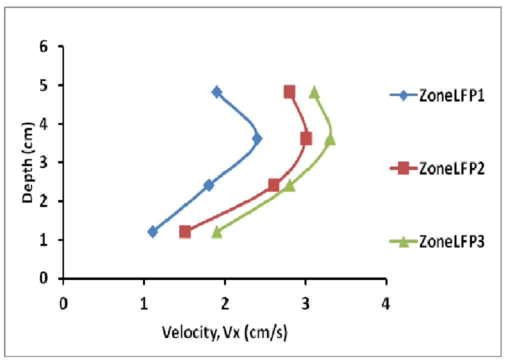

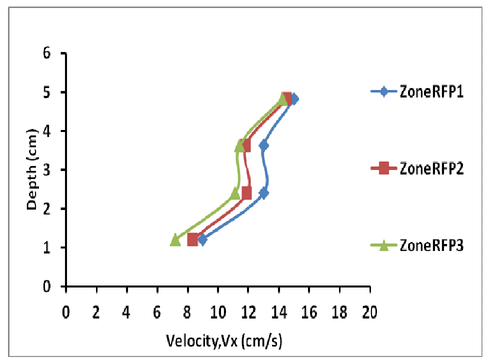

U/S Bend Section, Depth ratio 0.20
C3S1R1 (LFP i.e. Outer Bend)

U/S Bend Section, Depth ratio 0.20
C3S1R1 (RFP i.e. Inner Bend)

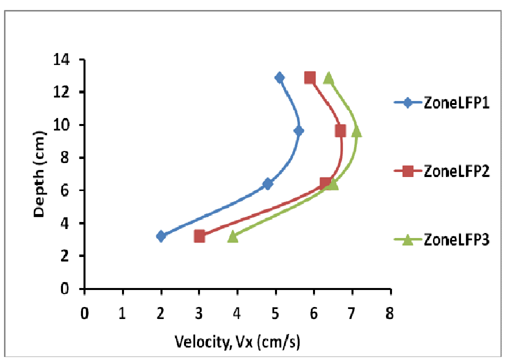

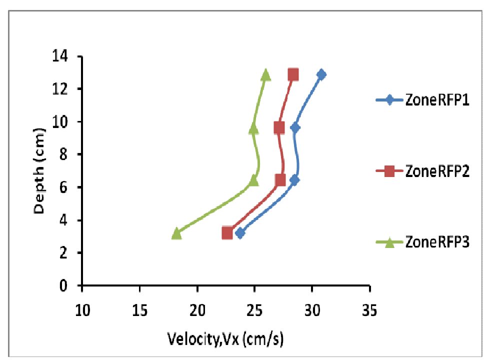

U/S Bend Section, Depth ratio 0.40
C3S1R4 (LFP i.e. Outer Bend)

U/S Bend Section, Depth ratio 0.40
C3S1R4 (RFP i.e. Inner Bend)

Figure 4.3: Longitudinal Velocity Profile for Case 3 (Wr=2.33) i.e. Floodplain width 30.50 cm

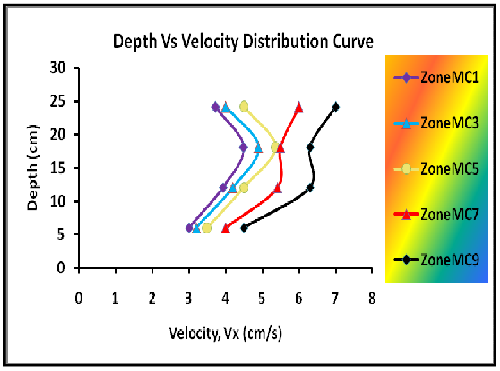

U/S Bend Section, Depth ratio 0.20
C4S1R1 (MC)

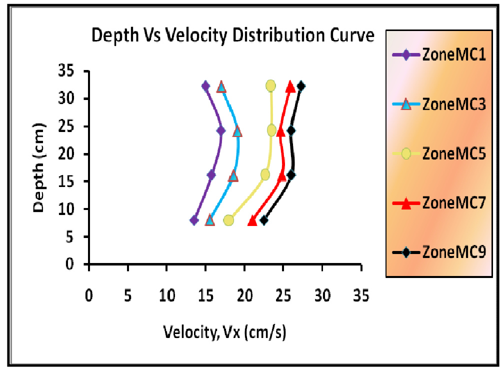

U/S Bend Section, Depth ratio 0.40
C4S1R4 (MC)

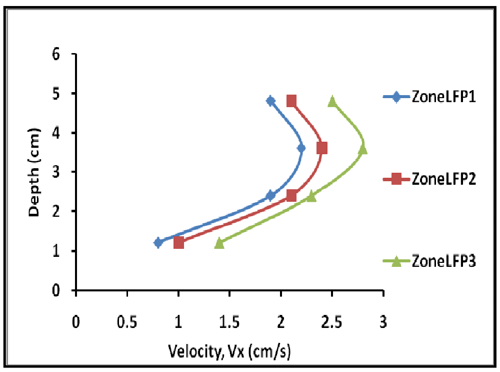

U/S Bend Section, Depth ratio 0.20
C4S1R1 (LFP i.e. Outer Bend)

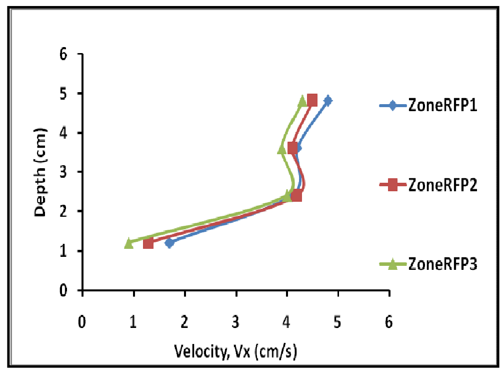

U/S Bend Section, Depth ratio 0.20
C4S1R1 (RFP i.e. Inner Bend)

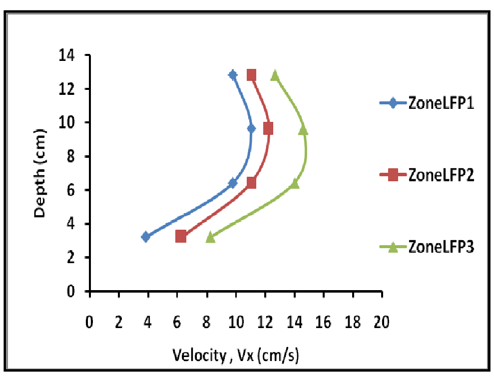

U/S Bend Section, Depth ratio 0.40
C4S1R4 (LFP i.e. Outer Bend)

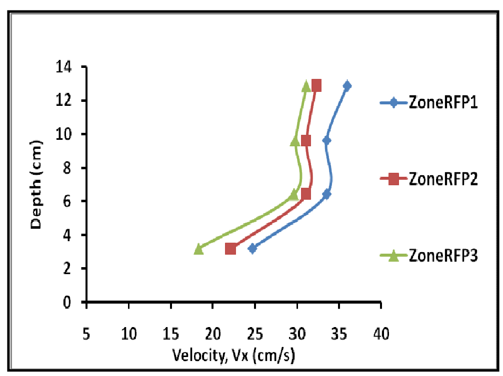

U/S Bend Section, Depth ratio 0.40
C4S1R4 (RFP i.e. Inner Bend)

Figure 4.4: Longitudinal Velocity Profile for Case 4 (Wr=3) i.e. floodplain width 45.70 cm

4.2.2 Individual Isovels Profile

In this section, isovels of different depth and width ratios for some locations are presented and all other isovels are given in the figures B-1 to B-8 at Appendix B.

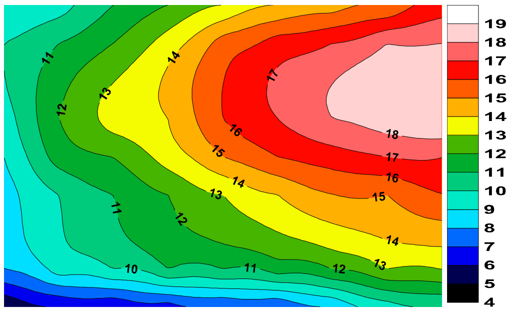

U/S Bend section, Depth ratio 0.30
(C1S1R2)

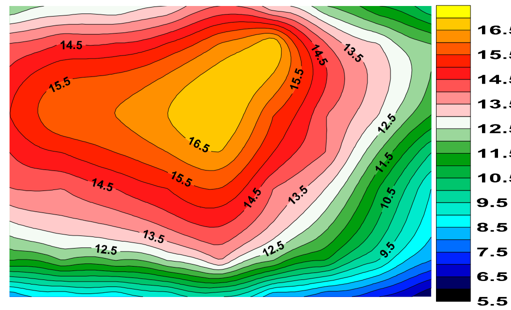

U/S Cross-over section, Depth Ratio 0.30
(C1S2R2)

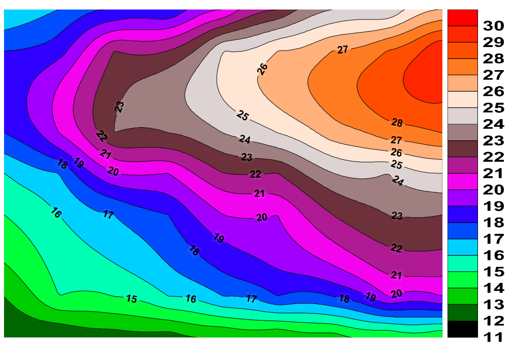

U/S Bend section, Depth ratio 0.35
(C1S1R3)

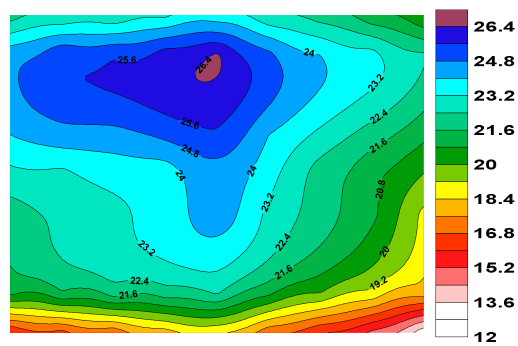

U/S Cross-over section, Depth Ratio 0.35
(C1S2R3)

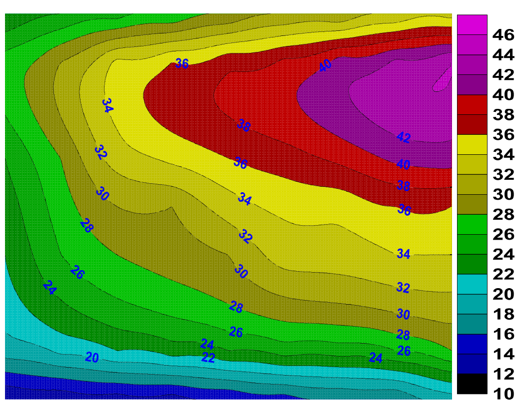

U/S Bend section, Depth ratio 0.40
(C1S1R4)

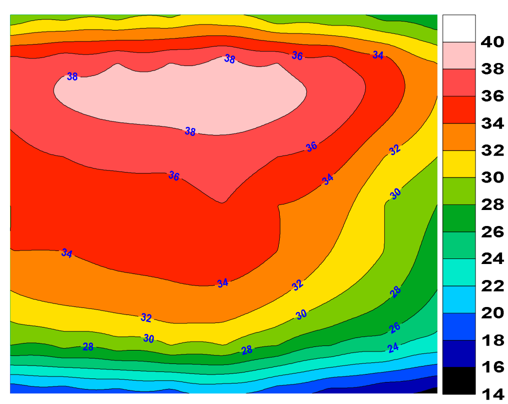

U/S Cross-over section, Depth Ratio 0.40
(C1S2R4)

Figure 4.5: Isovels Profile for Case 1 (Wr=1) i.e. No floodplain Condition

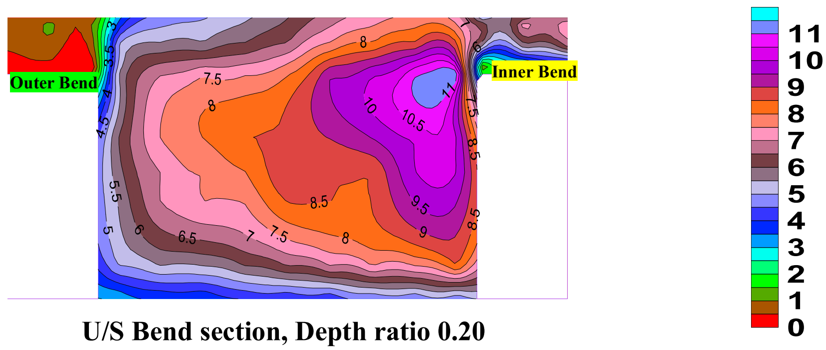

U/S Bend section, Depth ratio 0.20
(C2S1R1)

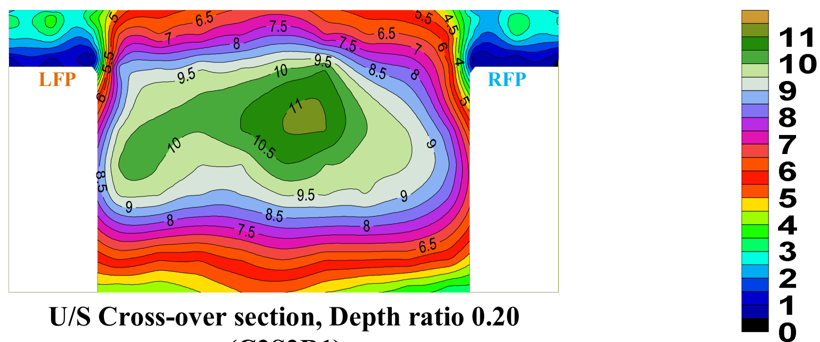

U/S Cross-over section, Depth ratio 0.20
(C2S2R1)

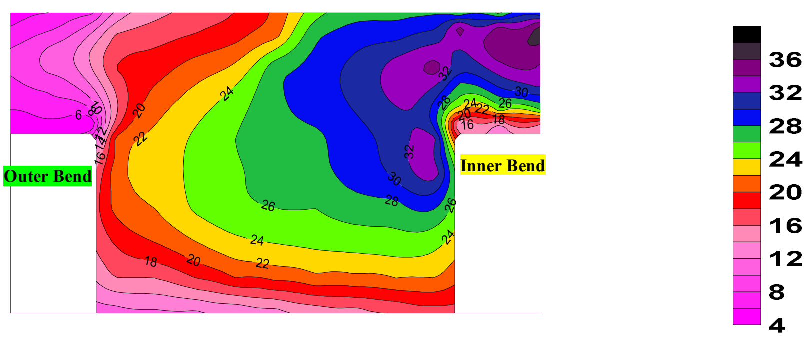

U/S Bend section, Depth ratio 0.40
(C2S1R4)

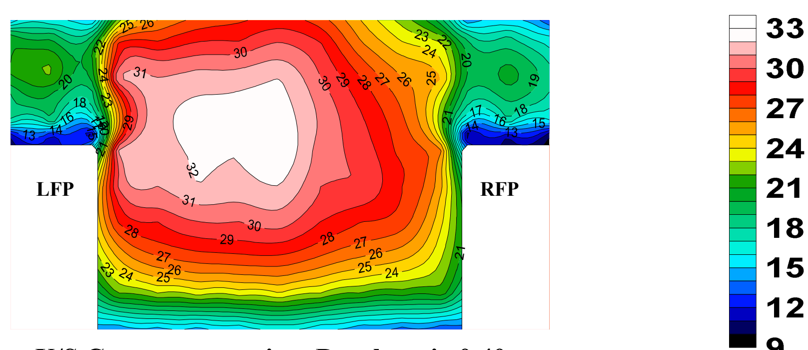

U/S Cross-over section, Depth ratio 0.40
(C2S2R4)

Figure 4.6: Isovels Profile for Case 2 (Wr=1.67) i.e. floodplain width 15.3 cm

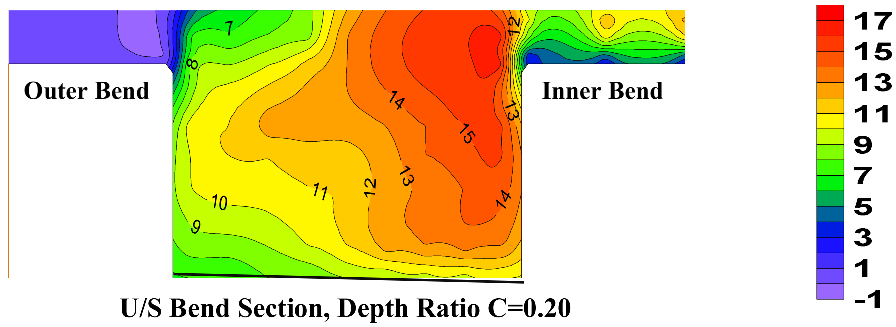

U/S Bend Section, Depth Ratio C=0.20
(C3S1R1)

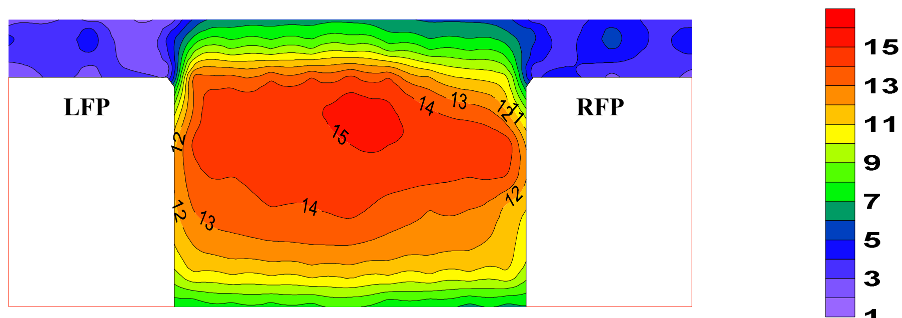

U/S Cross-over section, Depth ratio C=0.20
(C3S2R1)

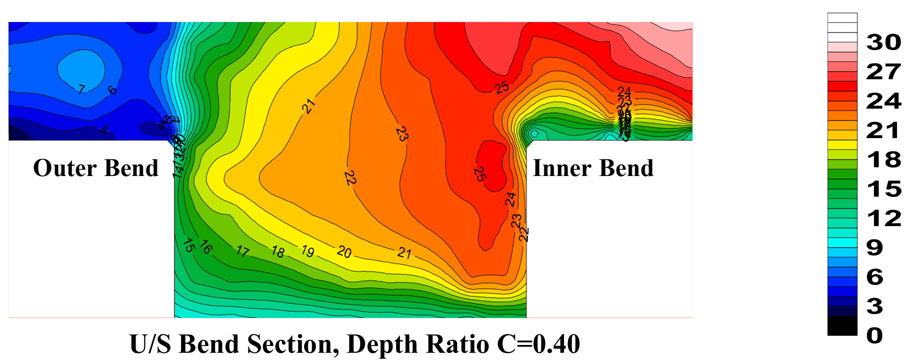

U/S Bend Section, Depth Ratio C=0.40
(C3S1R4)

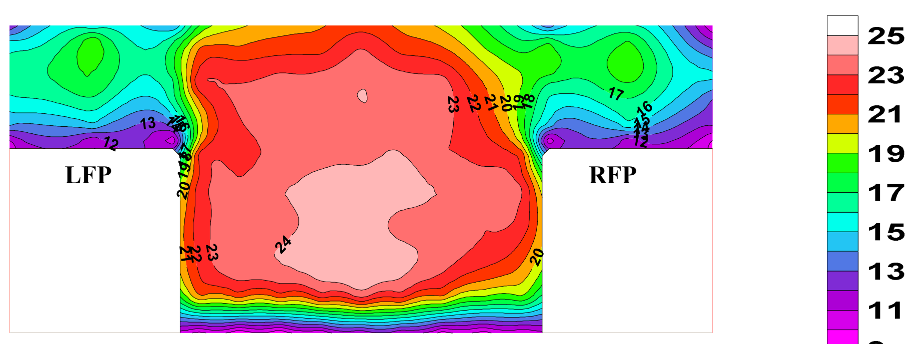

U/S Cross-over Section, Depth Ratio C=0.40
(C3S2R4)

Figure 4.7: Isovels Profile for Case 3 (Wr=2.33) i.e. floodplain width 30.5 cm

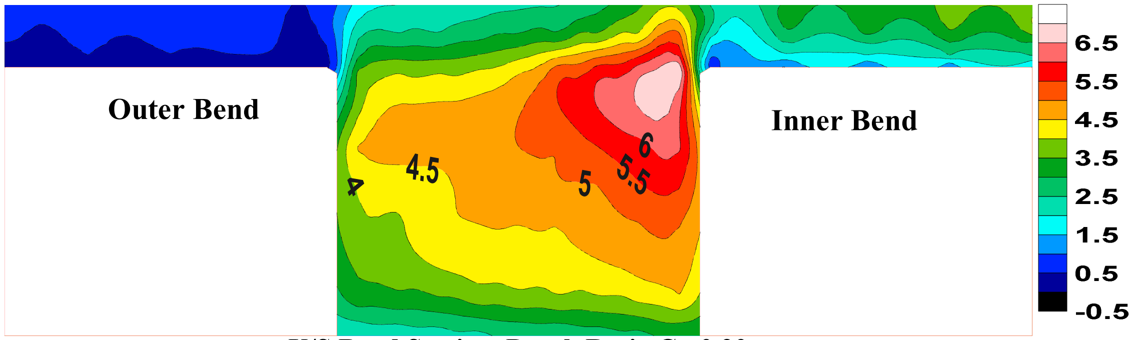

U/S Bend Section, Depth Ratio C =0.20
(C4S1R1)

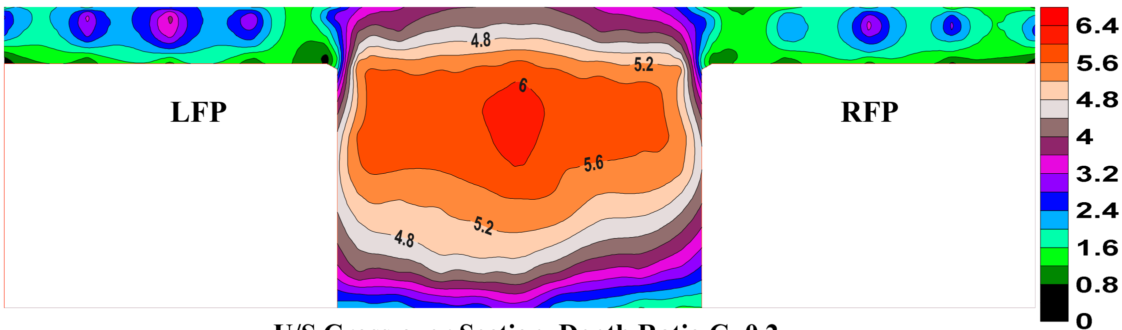

U/S Cross-over Section, Depth Ratio C=0.2
(C4S2R1)

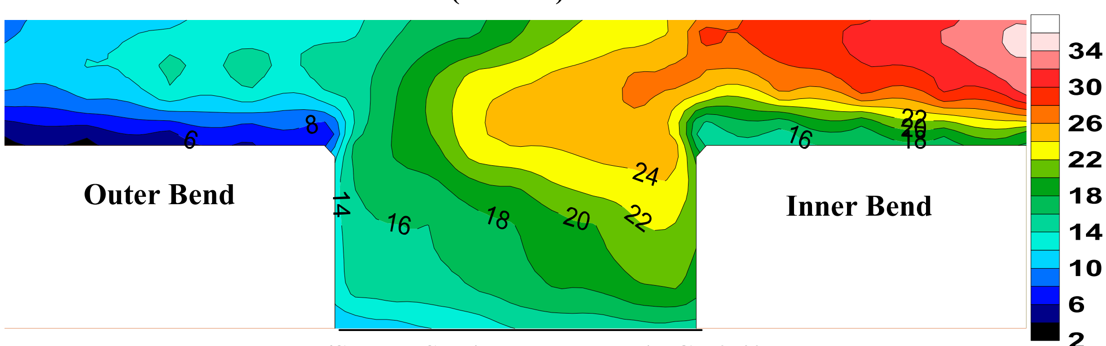

U/S Bend Section, Depth Ratio C =0.40
(C4S1R4)

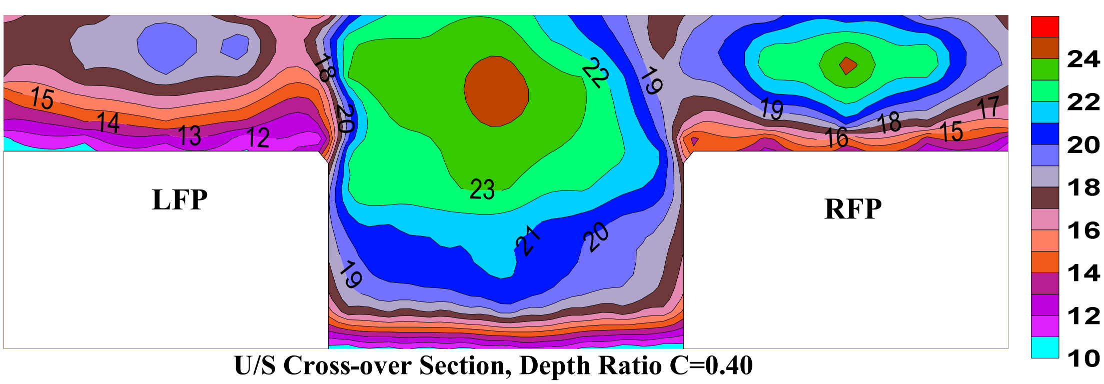

U/S Cross-over Section, Depth Ratio C=0.40
(C4S2R4)

Figure 4.8: Isovels Profile for Case 4 (Wr=3) i.e. floodplain width 45.7 cm

4.2.3 Illustrations of Velocity Distribution

Cross section (1-1) i.e. U/S Bend Section:

For all cases and depth ratio, velocity is increasing in the inner bend and decreasing in the outer bend. In C1S1R1, C2S1R1, C3S1R1, C4S1R1, C1S1R2, C2S1R2, C3S1R2, C4S1R2, C1S1R3, C2S1R3, C3S1R3, C4S1R3, C1S1R4, C2S1R4, C3S1R4, C4S1R4 maximum velocity is obtained in between the zone8 & zone9 at a vertical distance 0.05~0.10 of the total depth of flow.

Cross section (2-2) i.e. U/S Cross-over Section:

In the crossover, velocity is increasing and decreasing towards the mid section and boundary of the channel respectively for all cases and depth ratios. In C1S2R1, C2S2R1, C3S2R1, C4S2R1, C1S2R2, C2S2R2, C3S2R2, C4S2R2, C1S2R3, C2S2R3, C3S2R3, C4S2R3, C1S2R4, C2S2R4, C3S2R4, C4S2R4 maximum velocity is obtained in between the zone4 & zone5 at a vertical distance 0.10~0.15 of the total depth of flow.

Cross section (3-3) i.e. Middle Bend Section:

For all cases and depth ratio, velocity is decreasing in the outer bend and increasing in the inner bend. In C1S3R1, C2S3R1, C3S3R1, C4S3R1, C1S3R2, C2S3R2, C3S3R2, C4S3R2, C1S3R3, C2S3R3, C3S3R3, C4S3R3, C1S3R4, C2S3R4, C3S3R4, C4S3R4 maximum velocity is obtained in between the zone1 & zone2 at a vertical distance 0.05~0.10 of the total depth of flow.

From the observation of velocity profiles and isovels for all cases and depth ratio, it is shown that the maximum and minimum velocity is obtained nearest to the inner and outer bend respectively in the bend section of a compound meandering channel. In the crossover section, velocity is maximum nearest to the midsection of the channel. Velocity distribution shows the pattern of the natural river or channel velocity distribution in the outer bend and the logarithmic velocity distribution in the inner bend of a compound meandering channel. Because in the inner bend flow accelerate i.e. surface wind friction does not dominate and no secondary current is developed but in the outer bend flow decelerate i.e. surface wind resistance dominates intensively and secondary current is developed.

4.3 Discharge

Cross-sectional discharge is calculated by area velocity method from observed velocity profile. For all the cross-sections, discharge are calculated separately for the main channel, right and left flood plain; and then total discharge is obtained. Stage discharge curves with varying width ratios are as shown in figure 4.9, figure 4.10 and figure 4.11. In all cases (except case 3) discharge increases with the increase of width ratio for the discharge just above the bank level of the main channel. For the discharges just above the bank level, the retarding influence of the flood plain takes its toll on the overall discharge of the channel. As the depth ratio increases, the retarding effect of the floodplain is counter balanced by the increase in greater flow area provided by the floodplain. So for the higher water level (depth ratio), the discharge increases with the increase in depth of flow.

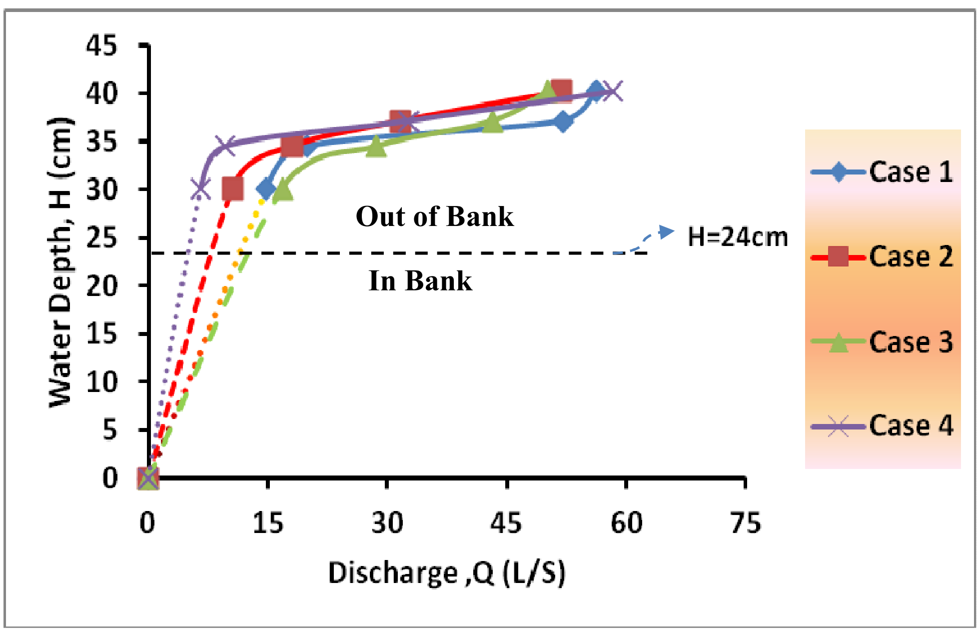

Figure 4.9: Stage Discharge Curve at U/S Bend Section

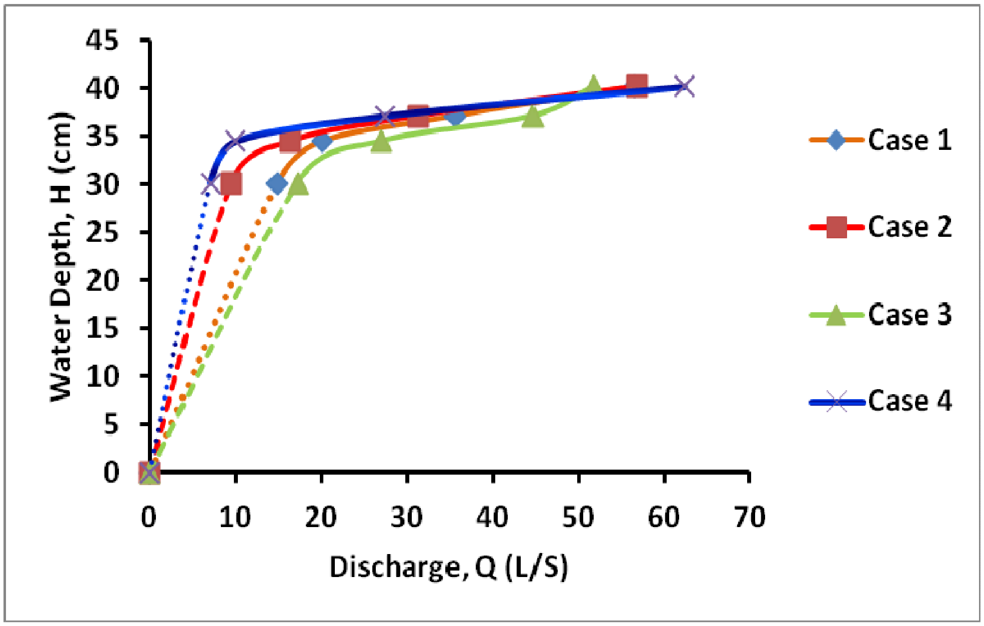

Figure 4.10: Stage Discharge Curve at U/S Cross-over Section

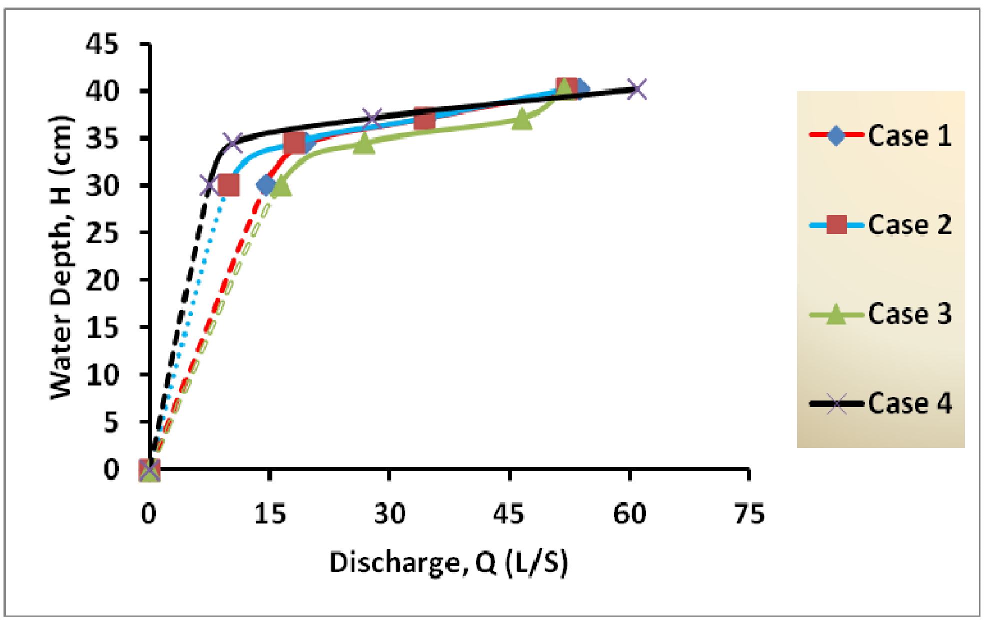

Figure 4.11: Stage Discharge Curve at Middle Bend Section

4.4 Flow Distribution

Flow distribution in a compound meandering channel is strongly dependent on the interaction between the flow in the main channel and that in the floodplain. Table C-1 to C-3 in the Appendix-C shows the experimental data in terms of % of flow for different depth and width ratios. Here flow distribution curve with respect to width ratio and depth ratio for some location is presented and all other flow distribution curves are given in the figure A-32 and A-33 at Appendix-A.

Salient features of flow distribution:

In C4S1R4, the percentage of flow in the main channel is 62.93% where it gradually increases with decrease of depth ratio and obtained maximum value 84.96% for depth ratio C=0.2. The total % of flow increase in the main channel is 22.03% from the depth ratio 0.4 to 0.2.The percentage of flow in the left floodplain(outer bend) is 7.12% where it gradually decreases with the decrease of depth ratio and obtained minimum value 3.5% for depth ratio C=0.2.In the right floodplain, the percentage of flow for the depth ratio(C=0.4) is 29.95% where it gradually decreases with the decrease of depth ratio and obtained a minimum value 11.55% for the depth ratio C=0.2. The total % of flow decreases in the left and right floodplain is 3.62% & 18.4% respectively from the depth ratio 0.4 to 0.2.

In C4S2R4, the percentage of flow in the main channel is 57.76% where it gradually increases with decrease of depth ratio and reaches maximum value 92% for depth ratio C=0.2. The total % of flow increase in the main channel is 34.24% from the depth ratio 0.4 to 0.2. In the floodplain reverse condition is observed. In the left flood plain, the percentage of flow is 19.65% where it gradually decreases with the decrease of depth ratio and obtained minimum value 3.92% for depth ratio C=0.2. In the right floodplain, the percentage of flow for the depth ratio(C=0.4) is 22.6% where it gradually decreases with the decrease of depth ratio and obtained a minimum value 4.08% for the depth ratio C=0.2. The total % of flow decreases in the left and right floodplain is 15.73% & 18.5% respectively from the depth ratio 0.4 to 0.2.

In C4S3R4, the percentage of flow in the main channel is 54.42% where it gradually increases with decrease of depth ratio and reaches maximum value 85.11% for the depth ratio C=0.2. The total % of flow increase in the main channel is 30.69% from the depth ratio 0.4 to 0.2. In the floodplain reverse condition is observed. In the left flood plain, the percentage of flow is 32.54% where it gradually decreases with the decrease of depth ratio and obtained minimum value 10.9% for depth ratio C=0.2. In the right floodplain, the percentage of flow for the depth ratio(C=0.4) is 13.04% where it gradually decreases with the decrease of depth ratio and obtained a minimum value 3.99% for the depth ratio C=0.2. The total % of flow decreases in the left and right floodplain is 21.64% & 9.05% respectively from the depth ratio 0.4 to 0.2.

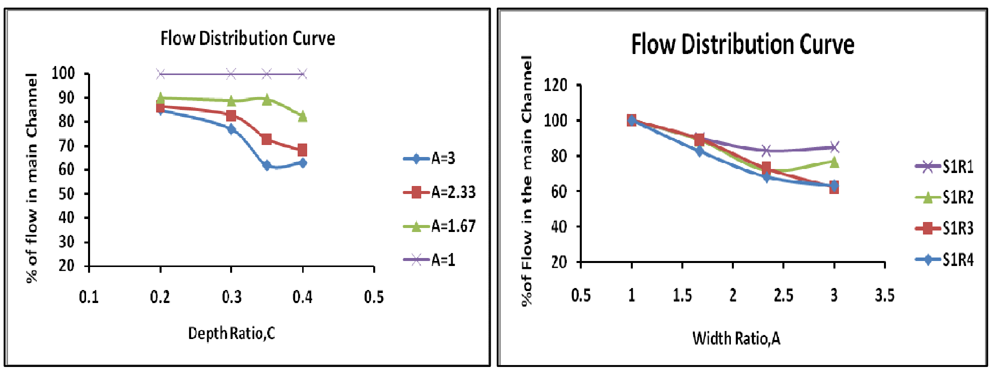

Figure 4.12: Variation in Percentage of Flow in the Main Channel at U/S Bend Section

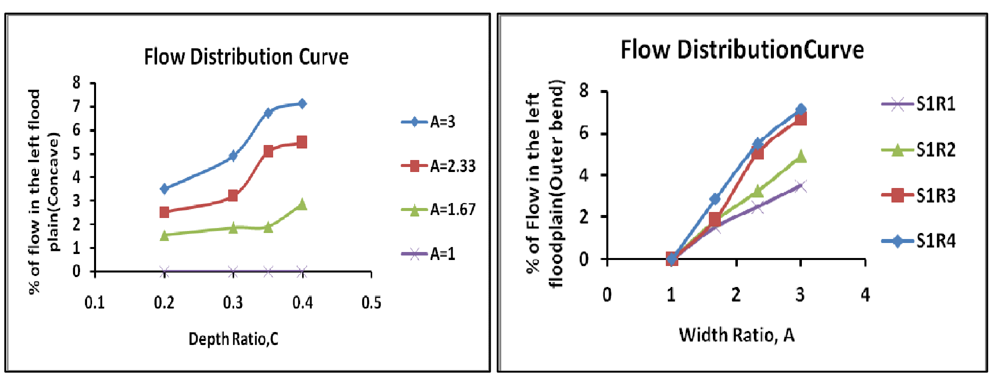

LFP LFP

Figure 4.13: Variation in Percentage of Flow in the Left Floodplain at U/S Bend Section

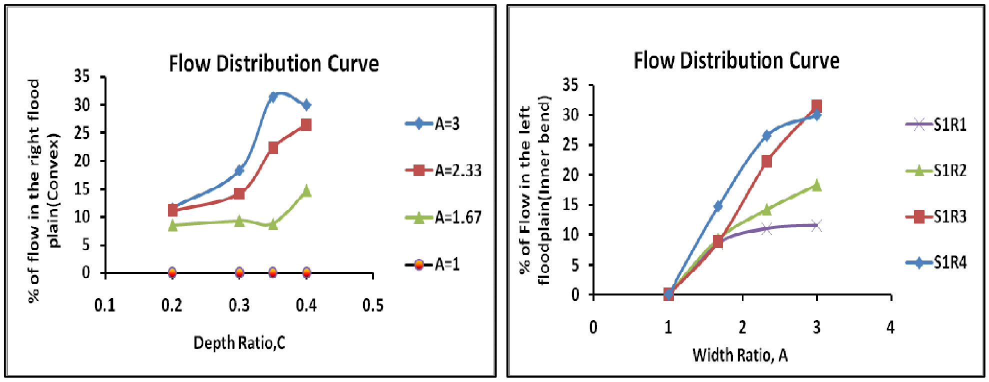

RFP RFP

Figure 4.14: Variation in Percentage of Flow in the Right Floodplain at U/S Bend Section

4.5 Shear Stress Distribution

Shear stress is a better predictor of erosion potential than velocity because it considers the actual force of the water on the boundary of the channel. Tabular form of total shear stress and shear stress distribution of a compound meandering channel are presented in the table C-4 to C-7 at Appendix C. Here variation of total shear stress curves in a channel section with respect to depth and width ratio are presented in the figure 4.15 and individual shear stress distribution curves of a compound meandering channel section for different depth ratio are presented in the figure 4.16 to figure 4.18.

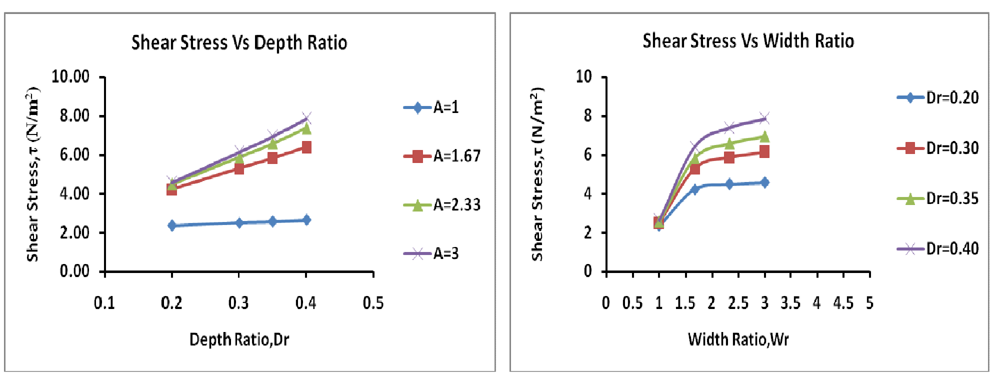

Figure 4.15: Variation of Total Shear Stress in terms of Depth and Width Ratio

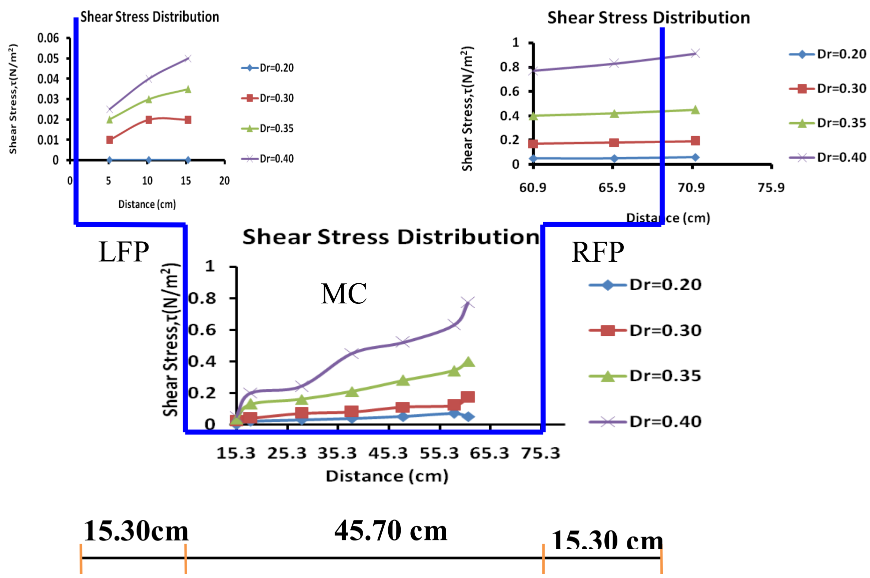

Figure 4.16: Shear Stress Distribution at U/S Bend Section for Case2 (Wr=1.67)

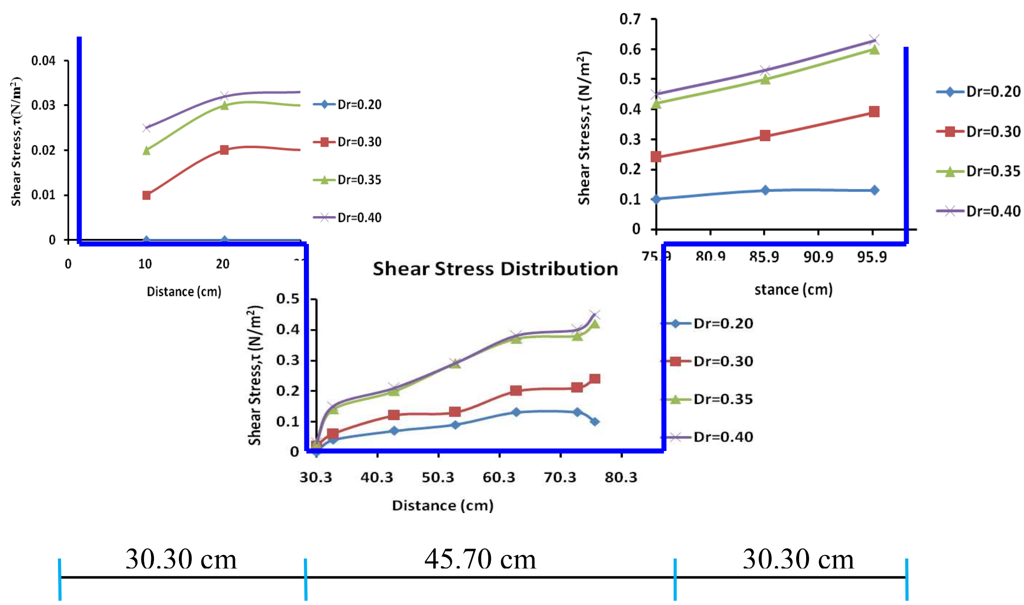

Figure 4.17: Shear Stress Distribution at U/S Bend Section for Case3 (Wr=2.33)

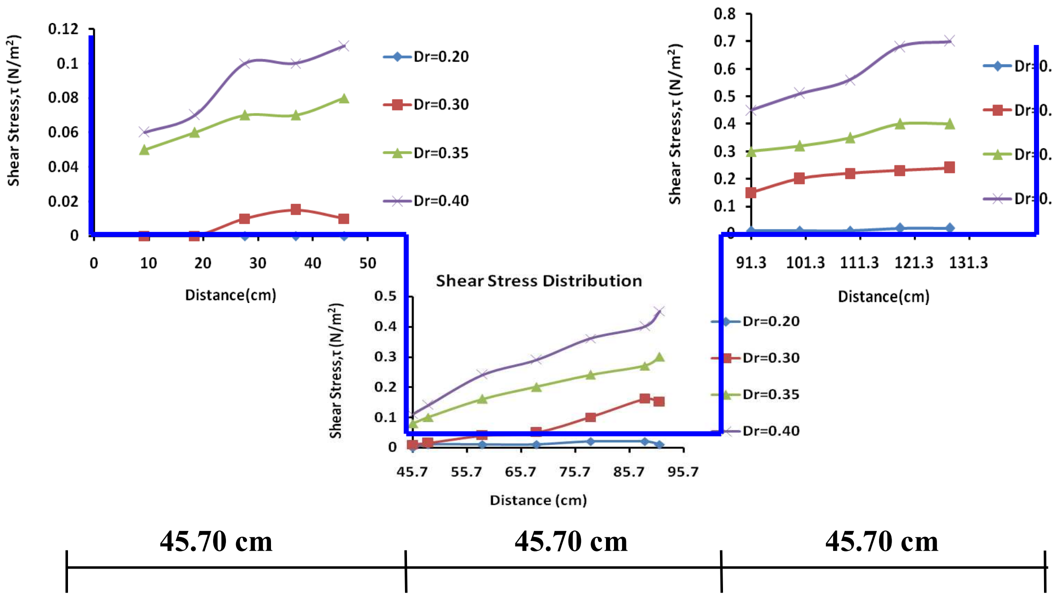

Figure 4.18: Shear Stress Distribution at U/S Bend Section for Case4 (Wr=3)

From the observation of shear stress distribution curve, it is seen that the shear stress increases with the increase of depth and width ratio. Because shear stress depend on the hydraulic radius as well as velocity distribution of a channel section. Hydraulic radius increases with the increase of depth and width ratio. In a compound meandering channel, the shear stress is increasing and decreasing in the inner and outer bend respectively. The maximum value of shear stress occurs along the inner bend of the main channel at low water depth ratio. But for higher depth ratio, the maximum shear stress occurs along the inner bend of the floodplain. Because at low over bank depths, the slow moving flow in the floodplain interact with the fast moving main channel intensely and considerable momentum exchange takes place giving rise to large non uniformity in the longitudinal velocity distribution. As the depth ratio increases, the intensity of interaction diminishes considerably.

4.6 Velocity Distribution Coefficients

As a result of non uniform distribution of velocities over channel section, velocity distribution coefficients (Coriolis Coefficient & Boussinesq Coefficient) are introduced. Coriolis Coefficient termed as Energy Coefficient (α) is the indicative of energy flux and Boussinesq Coefficient termed as Momentum Coefficient (β) indicates the momentum flux. The values of α & β are always greater than 1, which shows that the kinetic energy and momentum computed by the integration of each subarea is greater than the kinetic energy and momentum considering the entire flow area of the compound meandering channel to be a single section. The energy coefficient and momentum coefficient for the main channel and floodplain are computed using the depth-averaged velocity distributions. Table C-7 to C-9, in the Appendix-C shows the energy coefficient and momentum coefficient for different depth and width ratios. Here velocity coefficient distribution curve with respect to depth ratio in different sections are presented in the figure 4.19 to 4.21. The salient features of velocity distribution coefficients are as follows:

Cross section (1-1) i.e. U/S Bend Section:

From the experiment, it is observed that the values of energy coefficient in the section (1-1) of a compound meandering channel varies 1.32~1.33 for case1, 1.36~1.40 for case2, 1.36~1.47 for case3, 1.39~1.48 for case4 at different depth ratios. The momentum coefficient in that section for case1, case2, case3, case4 varies 1.14~1.15, 1.16~1.17, 1.16~1.21, 1.17~1.20 respectively at different depth ratios. Here Energy and Momentum coefficient are increasing due to the increase of floodplain width.

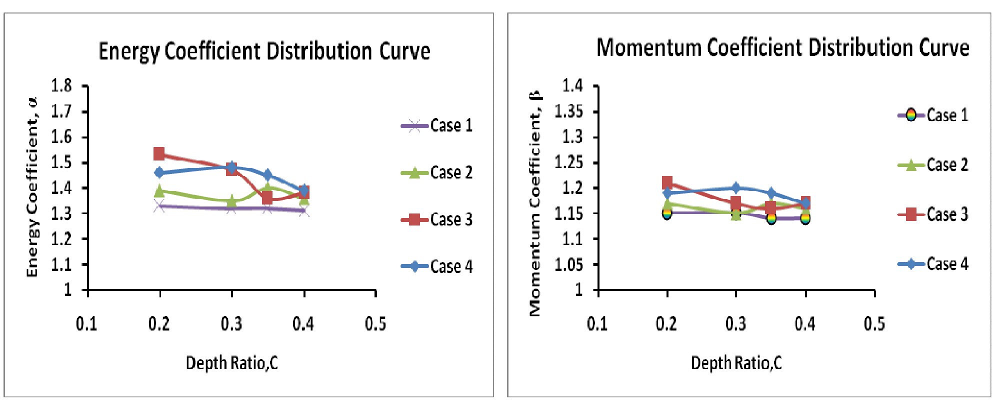

Figure 4.19: Energy Coefficient Distribution at U/S Bend Section

Cross section (2-2) i.e. U/S Cross-over Section:

In the section 2-2, Energy coefficient α varies from 1.32~1.35, 1.31~1.44, 1.31~1.45, 1.34~1.47 for the case1, case2, case3, case4 respectively and Momentum coefficient β varies from 1.15~1.16, 1.14~1.19, 1.17~1.19, 1.16~1.20 for the case1, case2, case3, case4 respectively at different depth ratios. Here energy coefficients are increasing with the increase of width ratio.

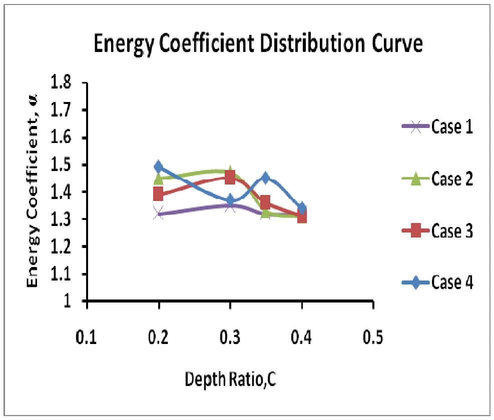

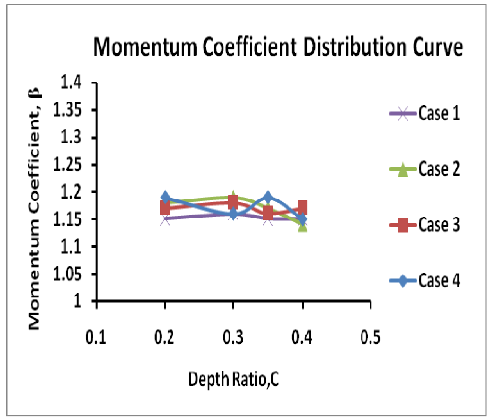

Figure 4.20: Energy Coefficient Distribution at U/S Cross-over Section

In the section 3-3, Energy coefficient α varies from 1.31~1.33, 1.35~1.43, 1.39~1.50, 1.37~1.49 for the case1, case2, case3, case4 respectively and Momentum coefficient β varies from 1.14~1.15, 1.15~1.18, 1.17~1.19, 1.16~1.19 for the case1, case2, case3, case4 respectively at different depth ratios. Here energy coefficients are increasing with the increase of width ratio.

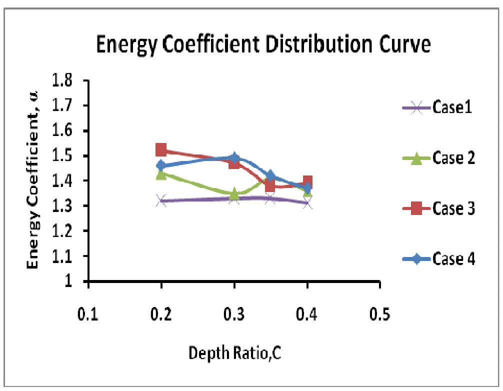

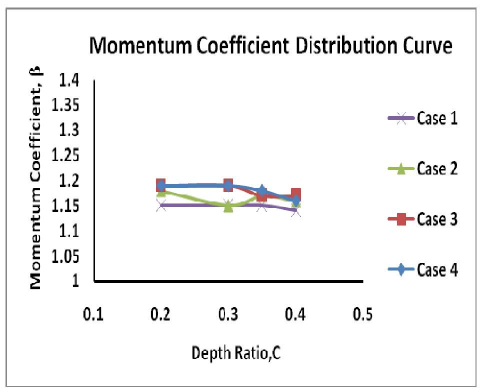

Figure 4.21: Energy Coefficient Distribution at Middle Bend Section

CHAPTER FIVE

CONCLUSIONS AND RECOMMENDATIONS

5.1 General

Flow parameters in a compound meandering channel in the actual field conditions are very complex in nature. Reviewing the research works done in the last three decades across the world, it was necessary for such a research work is initiated in Bangladesh. There is a genuine lack of proper research work in this field in Bangladesh. So it is the intention of the author to study the flow characteristics in a compound meandering channel's experimental observations which could be used in actual field observations in the days to come.

5.2 Conclusions

1. The longitudinal velocity distribution of a compound meandering main channel shows two characteristics for all cases and depth ratios. Velocity is increasing in the inner bend (convex) and decreasing in the outer bend (concave). Similar nature is observed in the floodplain boundary for all cases (except case1) and depth ratios. Maximum and minimum velocity is obtained nearest to the inner bend and outer bend respectively.

2. The vertical velocity profile of a compound meandering channel follows two shapes. In the outer bend the velocity profile follows the regular shape which is similar to the velocity profile observed in the natural channel. On the other hand, in the inner bend velocity profile follows logarithmic velocity distribution i.e. the point velocity at any vertical in the inner bend increase from the bed up to some level then at certain distance nearly constant velocity and increase until the water surface is reached.

3. For all cases discharge increases with the increase of width ratio but for the discharges just above the bank level of the main channel. For the discharges just above the bank level, the retarding influence of the floodplain takes its

toll on the overall discharge in the channel. As the depth ratio increases, the retarding effect of the floodplain is counter balanced by the increase in greater flow area provided by the floodplain.

4. The percentage of flow in the inner bend is greater than that of the percentage of flow in the outer bend. There is a significant effect of depth and width ratio on the percentage of flow in a compound meandering channel. The percentage of flow in the main channel is decreasing with the increase of depth ratio and the percentage of flow in the main channel is increasing with the decrease of width ratio.

5. Shear stress increases with the increase of depth ratio for all cases. Low magnitude of boundary shear stress is obtained at the outer bend as compare to that at the inner bend.

6. The value of both the energy and momentum coefficient of a compound meandering channel decrease with the increase of depth ratio at the same relative width ratio.

5.3 Recommendation

The present study creates a wide scope for the future researchers to explore many other aspects of compound meandering channel analysis. Analysis of velocity, discharge, shear stress, flow distribution, energy coefficient distribution has been performed in a compound meandering channel. Here the experimental channel is rigid. So further investigation is required to study the flow characteristics in a compound meandering channel with mobile bed, encroachment at floodplain and compound meandering channels of different sinuosity and geometry.

REFERENCES

Ackers, P. (1993). "Stage-Discharge Functions for Two-Stage Channels: The Impact of New Research." *Journal of the Institute of Water and Environmental Management*, 7(1), 52-61.

Afzalimehr, H., and Singh, V. P. (2009). "Influence of Meandering on the Estimation of Velocity and Shear Velocity in Cobble-Bed Channels." *Journal of Hydrologic Engineering*, ASCE, 14(10), 1126-1135.

Atabay, S., and Knight, D. W. (2002). "The Influence of Floodplain Width on the Stage-Discharge Relationship for Compound Channel." *Proceedings of the International Conference on Fluvial Hydraulics*, River flow 2002, 197-204.

Bhattacharya, A. K. (1995). "Mathematical Model of Flow in Meandering Channel." PhD thesis, IIT, Kharagpur, India.

Bousmar, D., and Zech, Y. (1999). "Momentum transfer for practical flow computation in compound channels." *Journal of Hydrologic Engineering*, ASCE, 125(7), 696–706.

Ching, E., and Luo, R. (2012). "Energy and Momentum Coefficients in Straight Symmetric Compound Channel Flows." *Journal of Hydraulic Engineering*, 1(3), 15-20

Chow, V. T. (1959). *Open channel hydraulics*, McGraw-Hill, New York.

Das, A. K. (1984). ''A study of River Floodplain and Boundary Shear Stress Distribution in Meander Channels with One side Flood plain.'' PhD thesis, IIT, Kharagpur, India.

Ervine, D. A., Willetts, B. B., Sellin, R. J., and Lorena, M. (1993). “Factors Affecting Conveyance in Meandering Compound Flows.” *Journal of Hydraulics Engineering*, ASCE, 119(12), 1383-1399.

Ervine, D. A., Koopaei, K. B., and Sellin, R. J. (2000). “Two-Dimensional Solution for Straight and Meandering Over-bank Flows.” *Journal of Hydraulic Engineering*, ASCE, 126(9), 653-669.

Fares, Y. (1995). “Boundary Shear in Curved Channel with Side Overflow.” *Journal of Hydraulic Engineering*, ASCE, 121(1), 2–14.

Ghosh, S.N., and Kar, S.K. (1975). “River Flood Plain Interaction and Distribution of Boundary Shear in a Meander Channel with Flood Plain.” *Proceedings of the Institution of Civil Engineers,* London, 59(2), 805-811.

James, C. S. (1994). “Evaluation of Methods for Predicting Bend Loss in Meandering Channels.” *Journal of Hydraulic Engineering*, ASCE, 120(2), 245-253.

James, C. S., and Wark, J. B. (1992). “Conveyance Estimation for Meandering Channels.” *Rep. SR 329*, HR Wallingford, Wallingford, U.K., Dec.

Johannesson, H., and Parker, G. (1989). “Velocity Distribution in Meandering Rivers.” *Journal of Hydraulic Engineering*, ASCE, 115(8), 1019-1039.

Kar, S. K. (1977). “A Study of Distribution of Boundary Shear in Meander Channel with and without Floodplain and River Floodplain Interaction.” PhD Thesis, IIT, Kharagpur, India.

Khan, S. M., (1999). “A Study of Flow Characteristics in a Compound Channel.” M.Sc Engineering Thesis, BUET, Dhaka, Bangladesh.

Khatua, K. K., and Patra, K. C. (2007). “Interaction of Flow and Estimation of Discharge in two Stage Meandering Compound Channels”, PhD Thesis, National Institute of Technology Rourkela, India.

Khatua, K. K., Patra, K. C., and Mohanty, P. K. (2012). “Stage-Discharge Prediction for Straight and Smooth Compound Channels with Wide Floodplains.” *Journal of Hydraulic Engineering*, ASCE, 138(1), 193-199.

Kiely, G. (1990). “Overbank Flow in Meandering Channels the Important Mechanisms.” *Proceedings of the Institution Conference on River Flood Hydraulics*, W. R. White, ed., Wiley, Chichester, U.K., 207–217.

Knight, D. W. (1981). “Boundary Shear in Smooth and Rough Channels.” *Journal of Hydraulic Engineering,* ASCE, 107(7), 839-851.

Knight, D. W., and Demetriou, J. D. (1983). “Floodplain and Main Channel Flow Interaction.” *Journal of Hydraulic Engineering*, ASCE, 109(8), 1073-1092.

Knight, D. W., and Hamed, M. E. (1984). “Boundary Shear in Symmetrical Compound Channels.” *Journal of Hydraulic Engineering*, ASCE, 110(10), 1412-1430.

McKeogh, E. J., and Kiley, G. K. (1989). “Experimental Study of Mechanism of Flood Flow in Meandering Channels.” *Proceeding of 23rd IAHR congress*, Ottawa, Canada, Vol-B, pp.491-498.

Mohaghegh, A., and Kouchakzadeh, S. (2008). “Evalution of Stage-Discharge Relationship in Compound Channels.” *Journal of Hydrodynamics*, 20(1), 81-87.

Morvan, H., Pender, G., Wright, N. G., and Ervine, D. A. (2002). “Three-Dimensional Hydrodynamics of Meandering Compound Channels.” *Journal of Hydraulic Engineering*, ASCE, 128(7), 674-682.

Myers, W. R. C. (1987). "Velocity and Discharge in Compound Channels." *Journal of Hydraulic Engineering*, ASCE, 113(6), 753-766.

Myers, W. R. C., and Elsawy, E. M. (1975). “Boundary Shear in Channel with Floodplain.” *Journal of Hydraulic Engineering*, ASCE, 101(7), 933-946.

Myers, W. R. C., and Lyness, J. F. (1997). “Discharge Ratios in Smooth and Rough Compound Channels.” *Journal of Hydraulic Engineering*, ASCE, 123(3), 182-188.

Myers, W. R. C., Lyness, J. F., and Cassells, J. (2001). “Influence of boundary roughness on velocity and discharge in compound river channels.” *Journal of Hydraulic Engineering*, ASCE, 39(3), 311-319.

Ozbek , T., and Cebe, K. (2003). “Comparison of Methods for Predicting Discharge in Straight Compound Channels Using the Apparent Shear Stress Concepts.” *Journal of Engineering and Environmental Science,* Tubitak, 101-109.

Pang, B. (1998). “River flood flow and its energy loss.” *Journal of Hydraulic Engineering*, ASCE, 124(2), 228-231.

Patra, K. C., and Kar, S. K. (2000). “Flow interaction of Meandering River with Flood plains.” *Journal of Hydraulic Engineering*, ASCE, 126(8), 593-604.

Patra, K. C. (2005). “Discharge Assessment for Two Stage Meandering and Straight Compound Channels.” *Journal of Hydraulic Engineering*, ISH, 11(3).125-140.

Patra, K. C., Kar, S. K., and Bhattacharya, A. K. (2004). “Flow and Velocity Distribution in Meandering Compound Channels.” *Journal of Hydraulic Engineering*, ASCE, 130(5), 398-411.

Prabir, K. M., Saine, S. D., and Khatua, K. K. (2012). "Flow Investigations in a Wide Meandering Compound Channel." *Journal of Hydraulic Engineering*, ASCE, 1(6), 83-94.

Rajaratnam, N., and Ahmadi, M. (1979). "Interaction between Main Channel and Flood Plain Flows." *Journal of Hydraulic Division*, ASCE, 105(5), 573-588.

Rajaratnam, N., and Ahmadi, M. (1981). "Hydraulics of Channels with Flood Plains." IAHR Journal of Hydraulic Research, 19(1), 43-60.

Sellin, R. H. J., Ervine, D. A., and Willetts, B. B. (1993). "Behavior of Meandering Two stage Channels." Proceedings of the Institution of Civil Engineers, Water, Maritime and Energy, 101(June), 99-111.

Shiono, K., Al-Romaih, J. S., and Knight, D. W. (1999). "Stage-Discharge Assessment in Compound Meandering Channels." Journal of Hydraulic Engineering, ASCE, 125(1), 66-77.

Shiono, K., and Muto, Y. (1998). "Complex flow mechanisms in compound meandering channels with overbank flow." J. Fluid Mech., 376, 221-261.

Shiono, K., Ishigaki, T., Muto, Y., and Imamoto, H. (1999). "Bed Shear Stress in Meandering channels for overbank flows." Proceedings of IAHR Congress in Graz, Austria, 22-27.

Shiono, K., Muto, Y., Knight, D. W., and Hyde, A. F. L. (1999). "Energy Losses due to Secondary Flow and Turbulence in Meandering Channels with Overbank Flow." *Journal of Hydraulic Research*, IAHR, 37(5), 641-664.

Shiono, K., Spooner, J., Chan, T., Rameshwaran, P., and Chandler, J. (2008). "Flow characteristics in meandering channels with non-mobile and mobile beds for overbank flows." *Journal of Hydraulic Research*, 46 (1), 113-132.

Stephenson, D., and Kolovopoulos, P. (1990). “Effects of Momentum Transfer in Compound Channels.” *Journal of Hydraulic Engineering*, ASCE, 116(12), 1512-1522.

Thornton, C., Abt, S., Morris, C., and Fischenich, J. (2000). ”Calculating Shear Stress at Channel-Overbank Interfaces in Straight Channels with Vegetated Floodplains.” *Journal of Hydraulic Engineering*, 126(12), 929–936.

Toebes, G. H., and Sooky, A. A. (1967). “Hydraulics of Meandering Rivers with Floodplains.” *Journal of the Waterways and Harbor Division*, ASCE, 93(2), 213-236.

Wark, J. B., and James, C. S. (1994). “An Application of New Procedure for Estimating Discharge in Meandering Overbank Flows to Field Data.” *2nd Intl. Conf. on River Flood Hydraulics*, March 22-25, Wiley, New York, 405-414.

Willetts, B. B., and Hardwick, R. I. (1993). “Stage Dependency for Over Bank Flow in Meandering Channels.” *Proceedings of the Institution of Civil Engineers Water Maritime and Energy*, 101, 45-54.

Wormleaton, P. R., Allen, J., and Hadjipanos, P. (1982). “Discharge Assessment in Compound Channel Flow.” *Journal of Hydraulic Engineering*, ASCE, 108(9), 975-994.

Wormleaton, P. R., and Hadjipanos, P. (1985). “Flow Distribution in Compound Channels.” *Journal of Hydraulic Engineering*, ASCE, 111(2), 357-361.

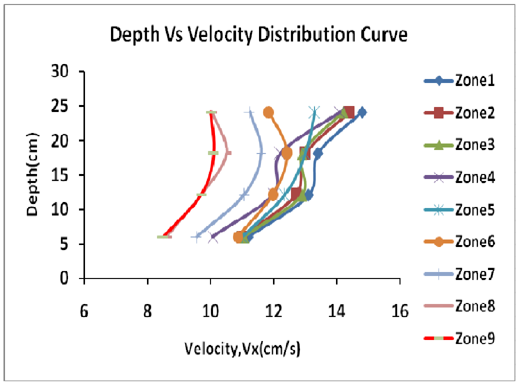

C1S1R1 (MC)

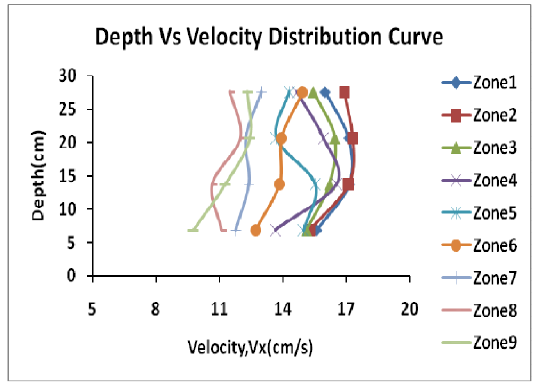

C1S3R2 (MC)

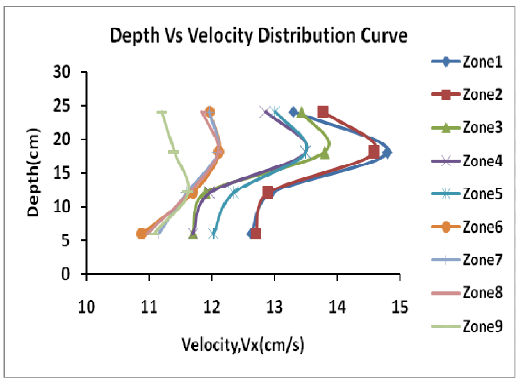

C1S2R2 (MC)

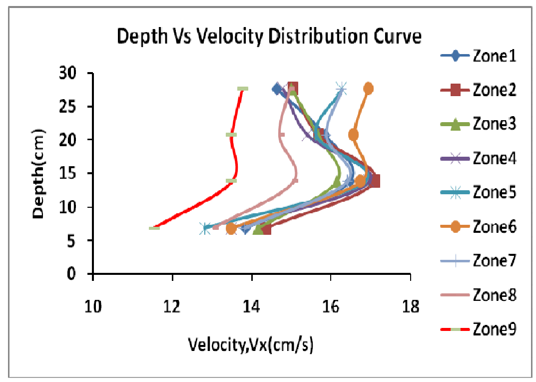

C1S2R3 (MC)

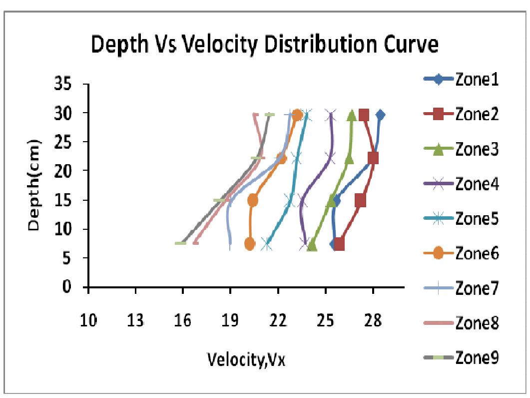

C1S3R3 (MC)

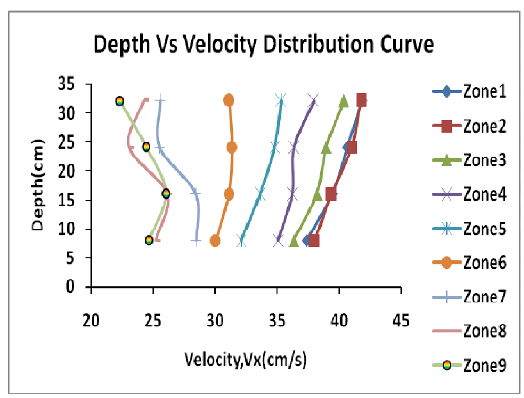

C1S3R4 (MC)

Figure A-1: Longitudinal Velocity Profile for Case 1(Wr=1)

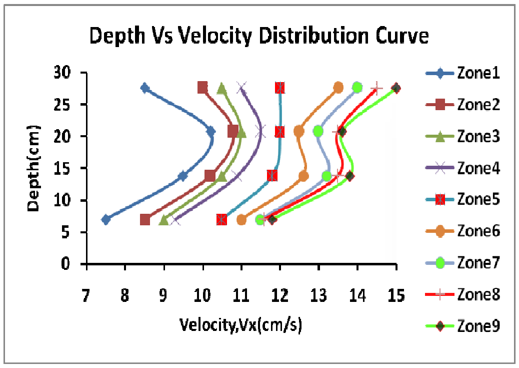

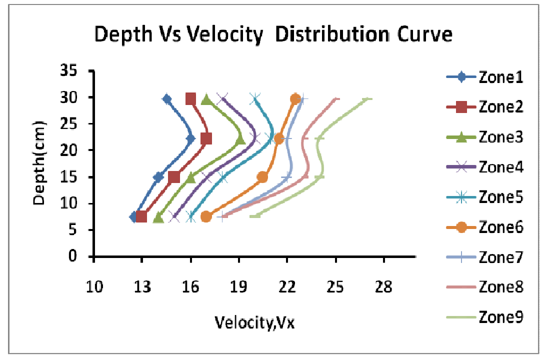

C2S1R2 (MC)

C2S1R3 (MC)

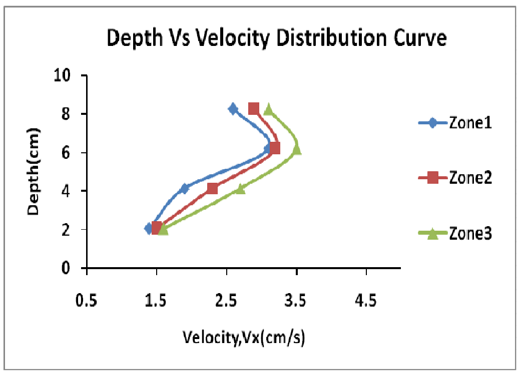

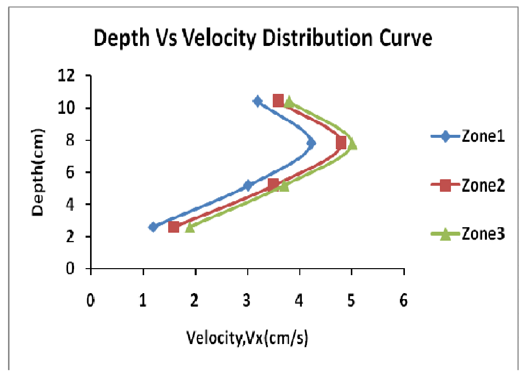

C2S1R2 (LFP)

C2S1R3 (LFP)

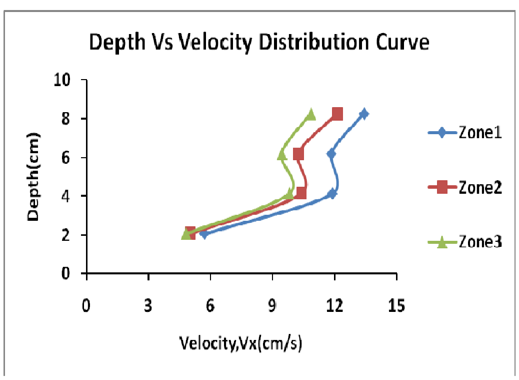

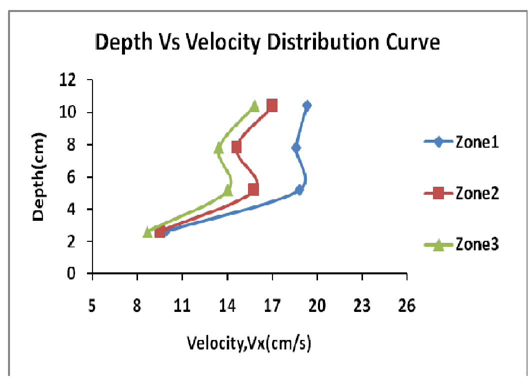

C2S1R2 (RFP)

C2S1R3 (RFP)

Figure A-2: Longitudinal Velocity Profile for C2S1R2

Figure A-3: Longitudinal Velocity Profile for C2S1R3

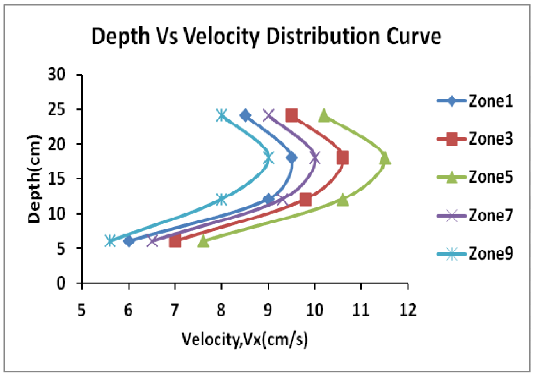

C2S2R1 (MC)

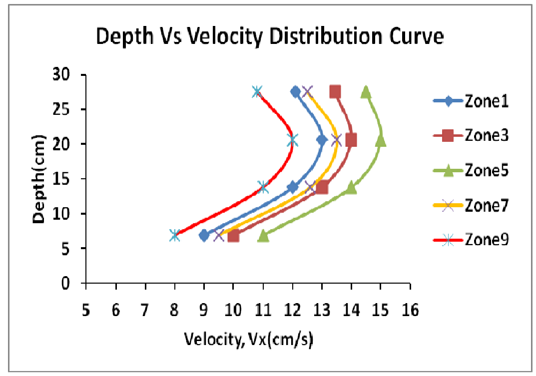

C2S2R2 (MC)

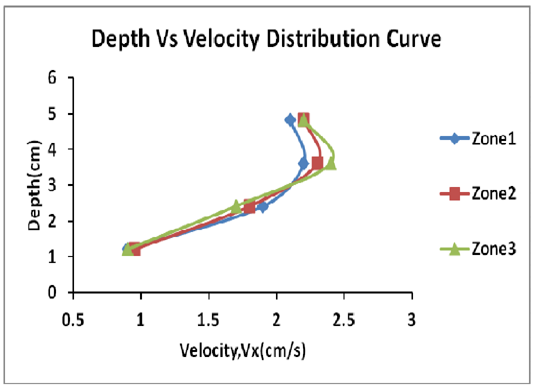

C2S2R1 (LFP)

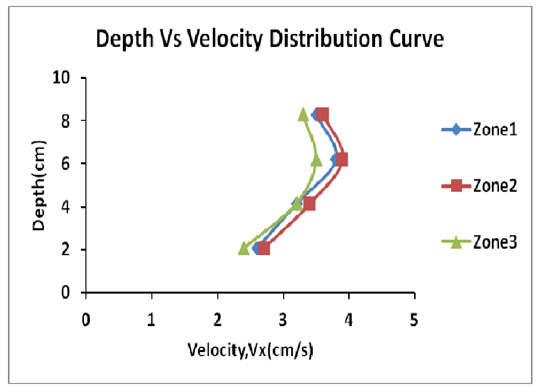

C2S2R2 (LFP)

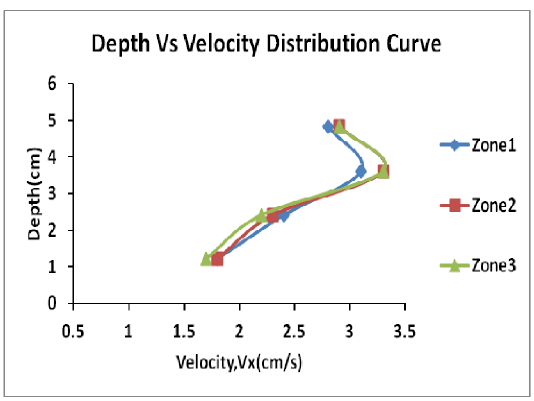

C2S2R1 (RFP)

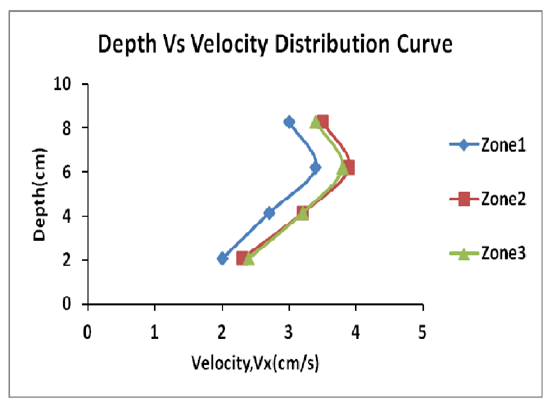

C2S2R2 (RFP)

Figure A-4: Longitudinal Velocity Profile for C2S2R1

Figure A-5: Longitudinal Velocity Profile for C2S2R2

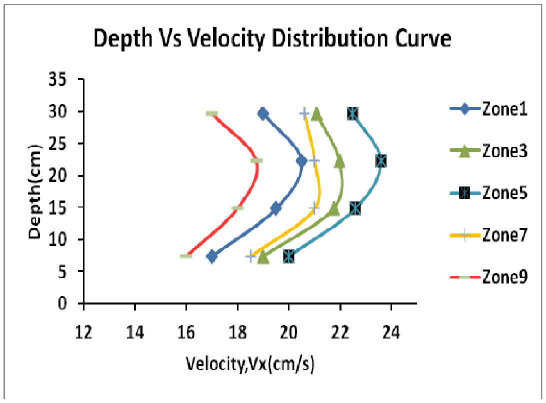

C2S2R3 (MC)

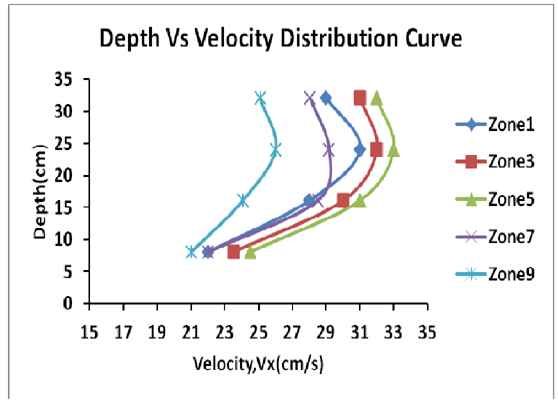

C2S2R4 (MC)

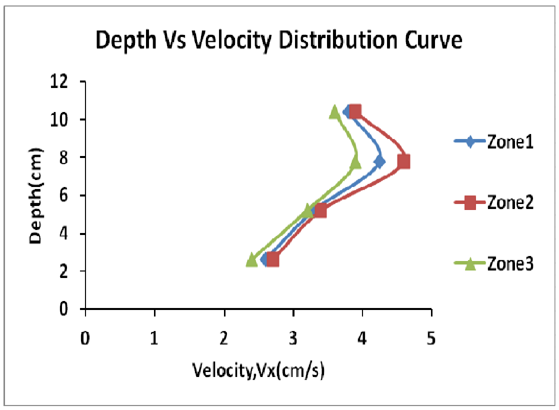

C2S2R3 (LFP)

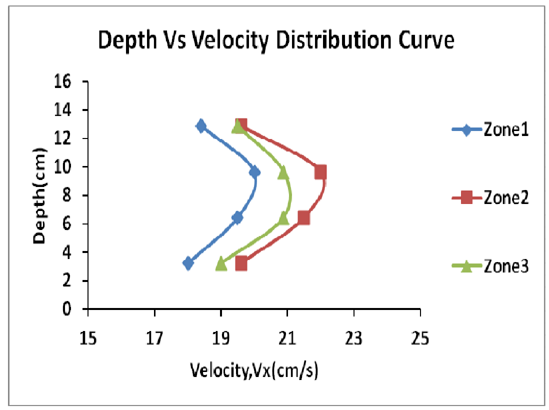

C2S2R4 (LFP)

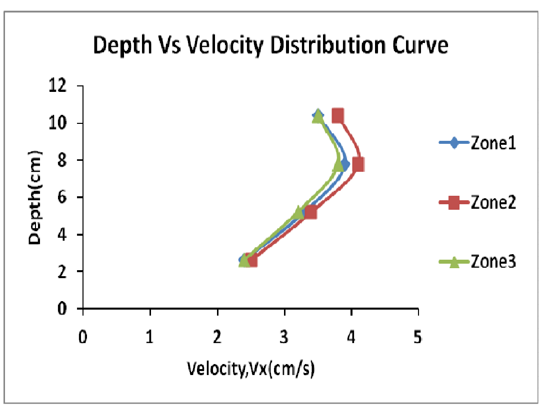

C2S2R3 (RFP)

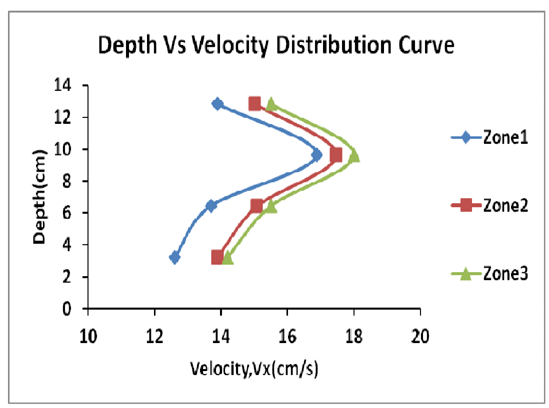

C2S2R4 (RFP)

Figure A-6: Longitudinal Velocity Profile for C2S2R3

Figure A-7: Longitudinal Velocity Profile for C2S2R4

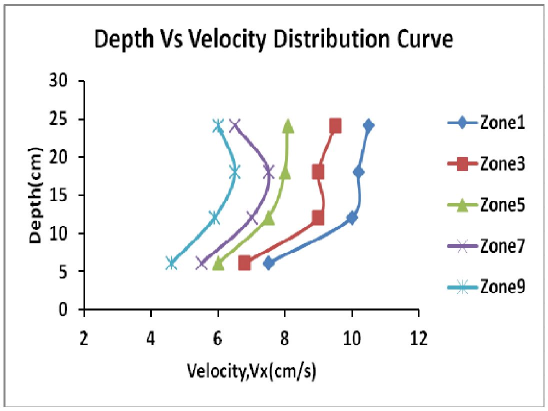

C2S3R1 (MC)

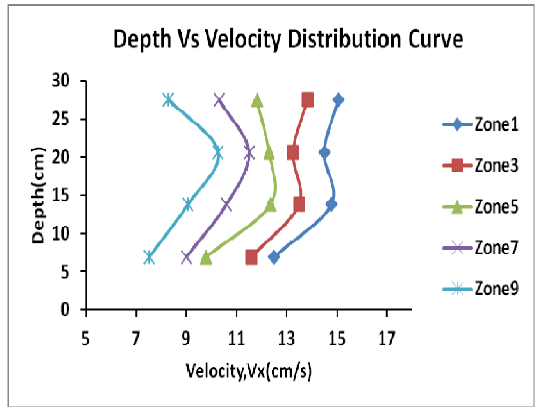

C2S3R2 (MC)

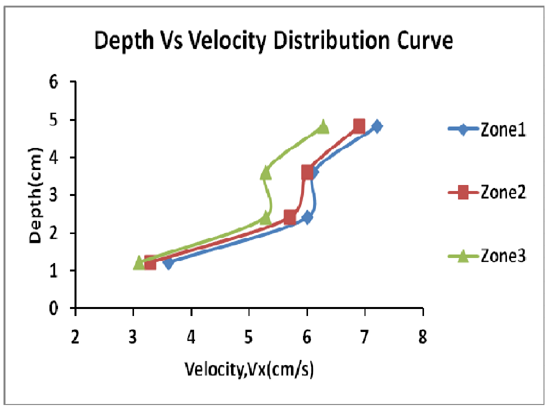

C2S3R1 (LFP)

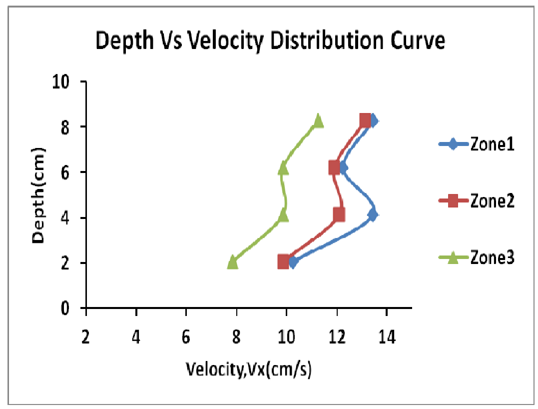

C2S3R2 (LFP)

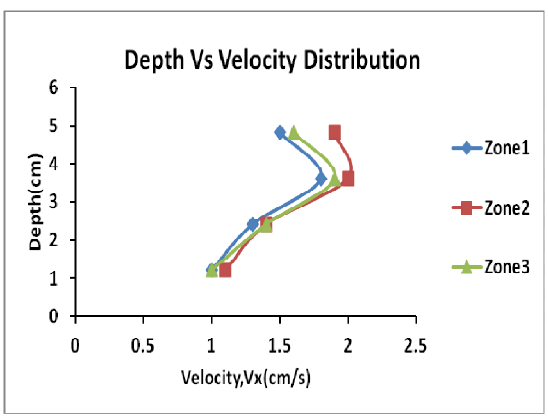

C2S3R1 (RFP)

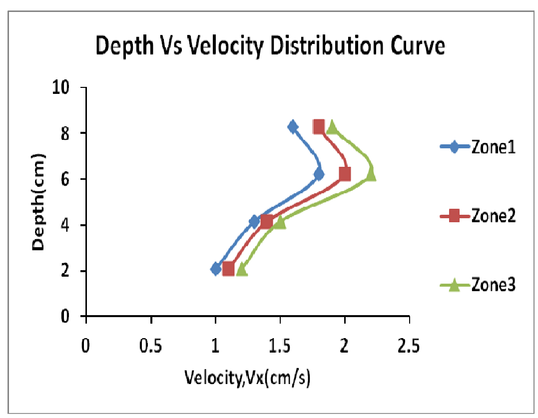

C2S3R2 (RFP)

Figure A-8: Longitudinal Velocity Profile for C2S3R1

Figure A-9: Longitudinal Velocity Profile for C2S3R2

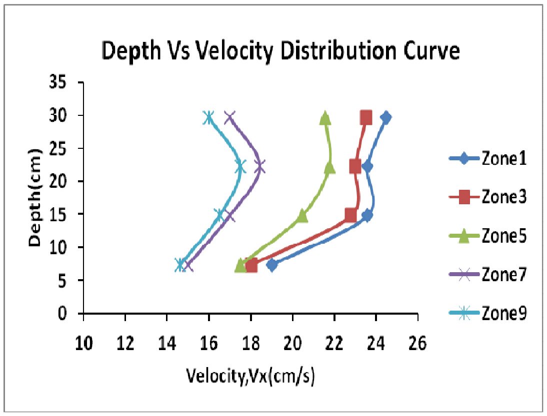

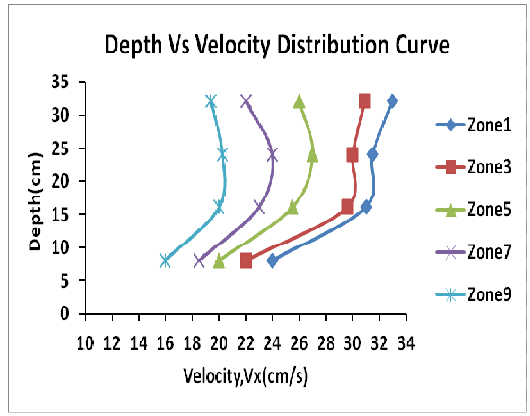

C2S3R3 (MC)

C2S3R4 (MC)

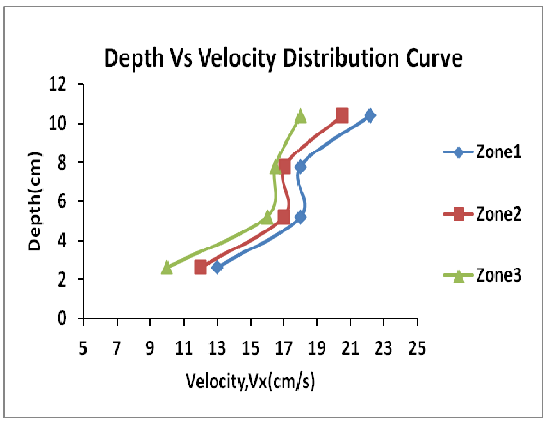

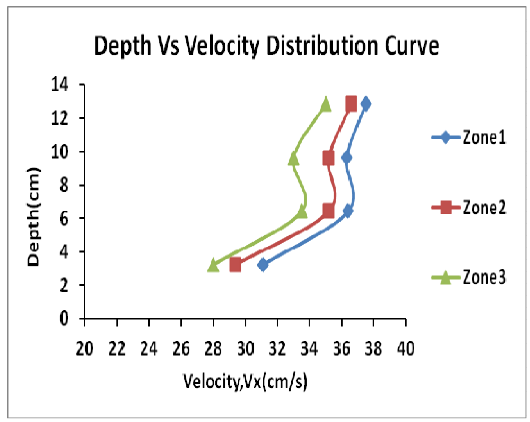

C2S3R3 (LFP)

C2S3R4 (LFP)

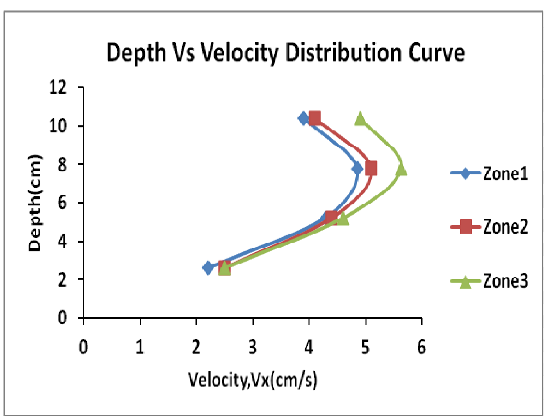

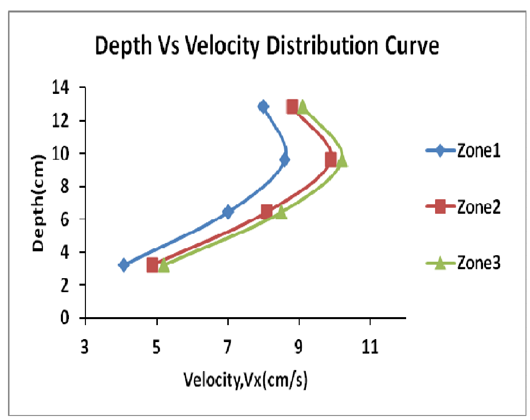

C2S3R3 (RFP)

C2S3R4 (RFP)

Figure A-10: Longitudinal Velocity Profile for C2S3R3

Figure A-11: Longitudinal Velocity Profile for C2S3R4

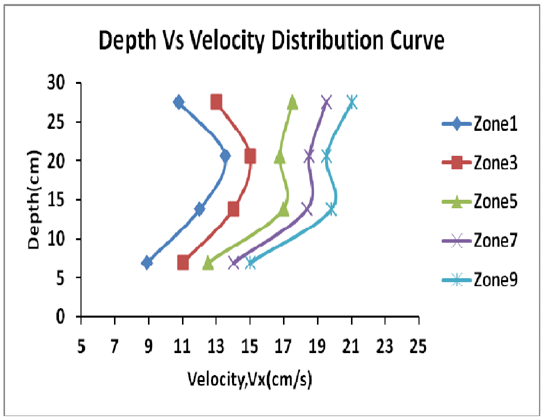

C3S1R2 (MC)

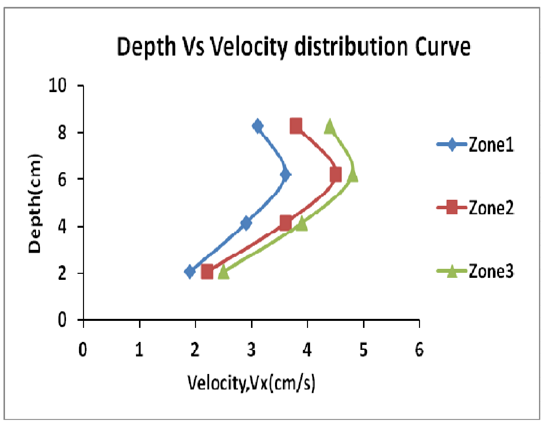

C3S1R2 (LFP)

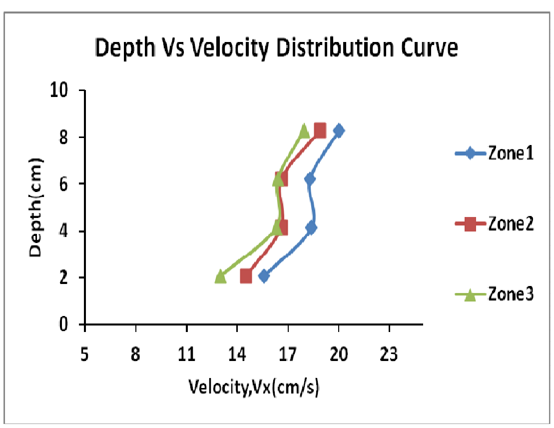

C3S1R2 (RFP)

Figure A-12: Longitudinal Velocity Profile for C3S1R2

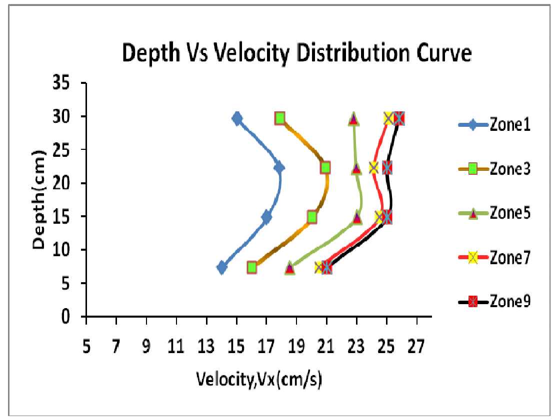

C3S1R3 (MC)

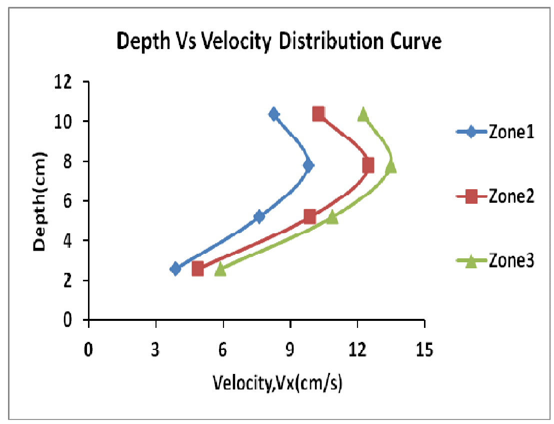

C3S1R3 (RFP)

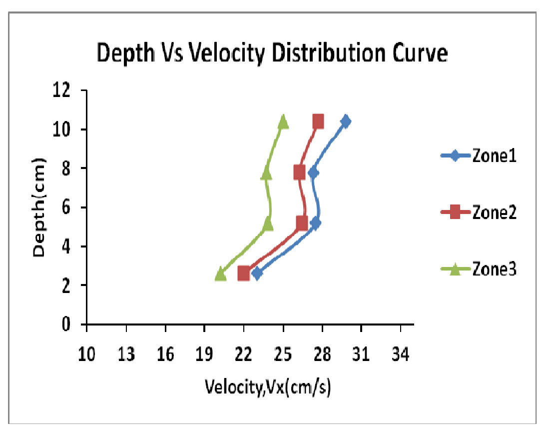

C3S1R3 (RFP)

Figure A-13: Longitudinal Velocity Profile for C3S1R3

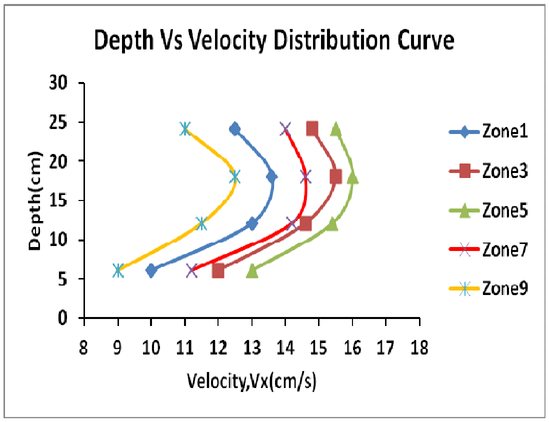

C3S2R1 (MC)

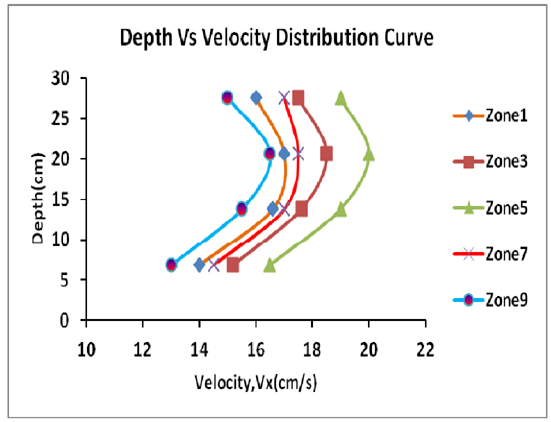

C3S2R2 (MC)

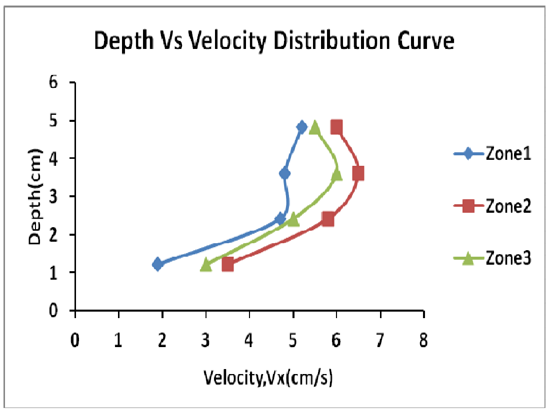

C3S2R1 (LFP)

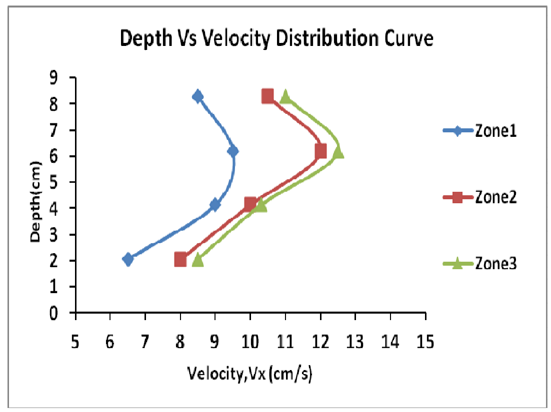

C3S2R2 (RFP)

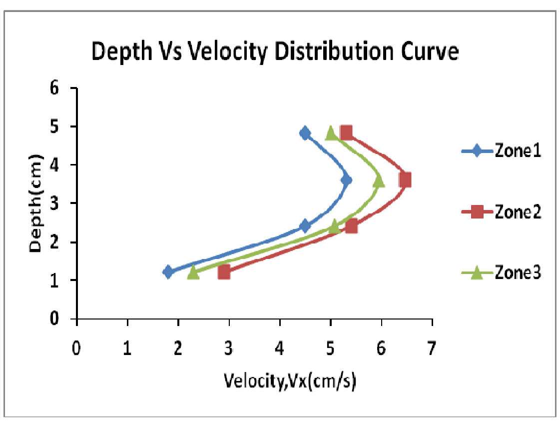

C3S2R1 (RFP)

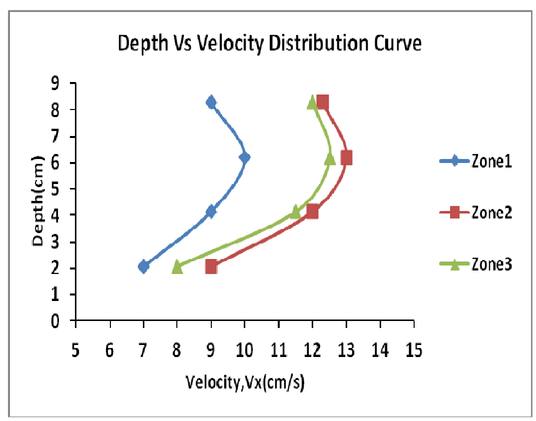

C3S2R2 (RFP)

Figure A-14: Longitudinal Velocity Profile for C3S1R2

Figure A-15: Longitudinal Velocity Profile for C3S1R3

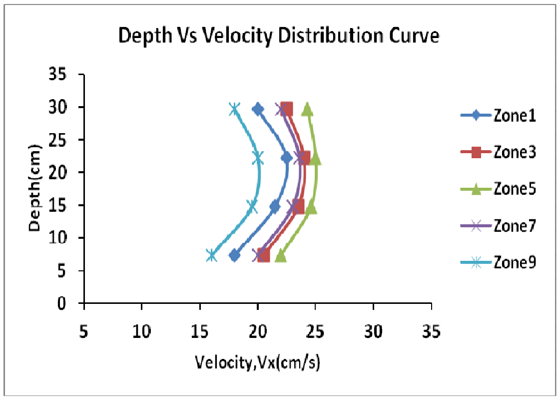

C3S2R3 (MC)

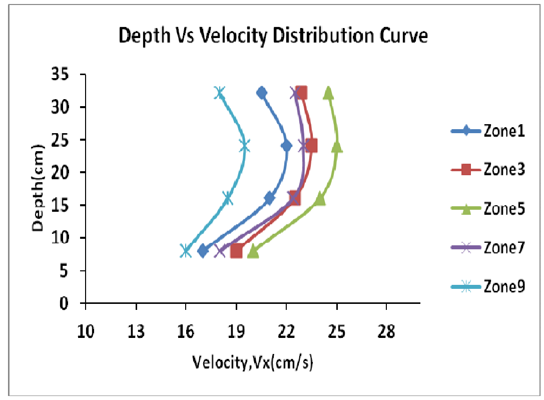

C3S2R4 (MC)

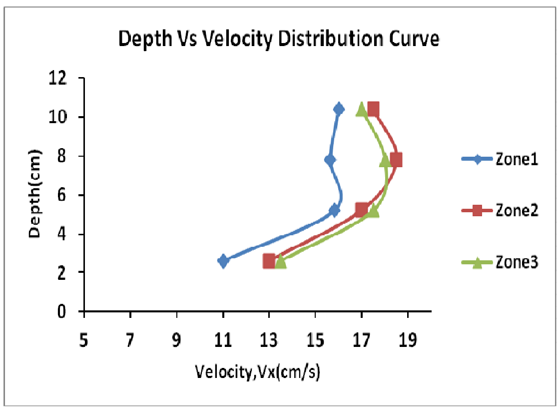

C3S2R3 (LFP)

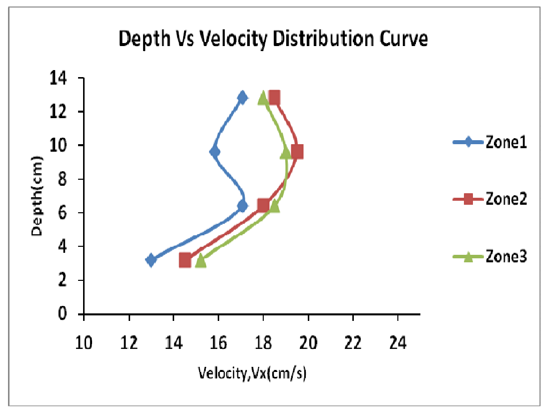

C3S2R4 (LFP)

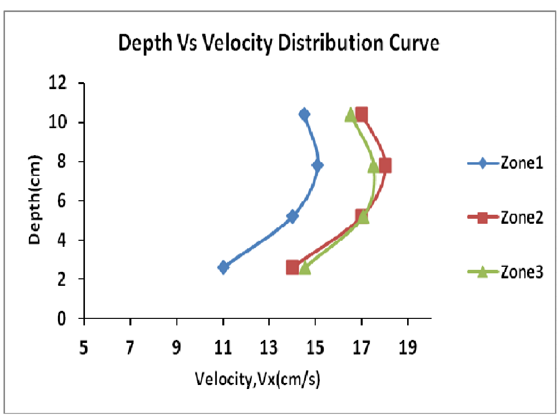

C3S2R3 (RFP)

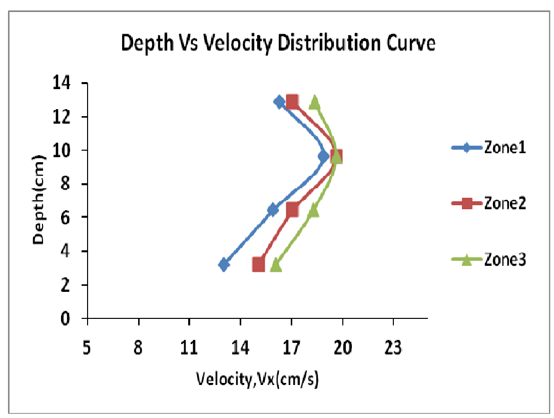

C3S2R4 (RFP)

Figure A-16: Longitudinal Velocity Profile for C3S2R3

Figure A-17: Longitudinal Velocity Profile for C3S2R4

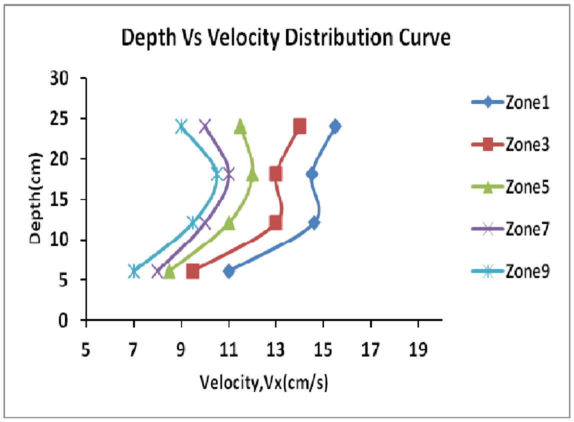

C3S3R1 (MC)

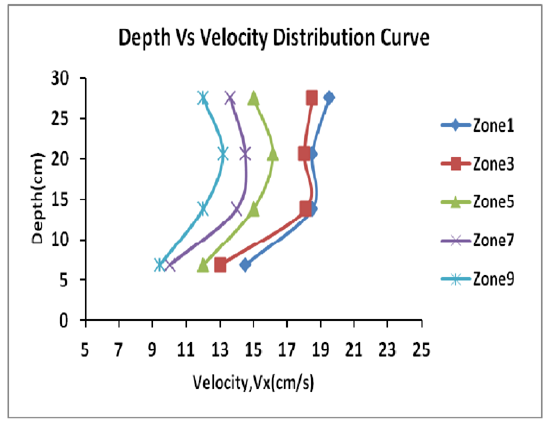

C3S3R2 (MC)

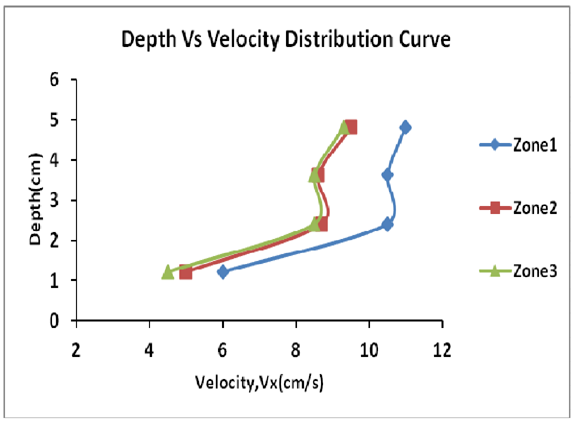

C3S3R1 (LFP)

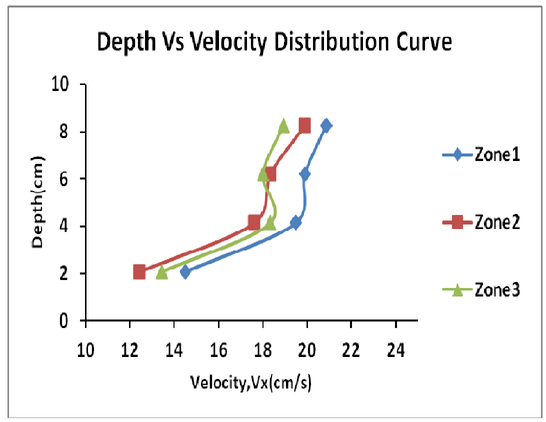

C3S3R2 (LFP)

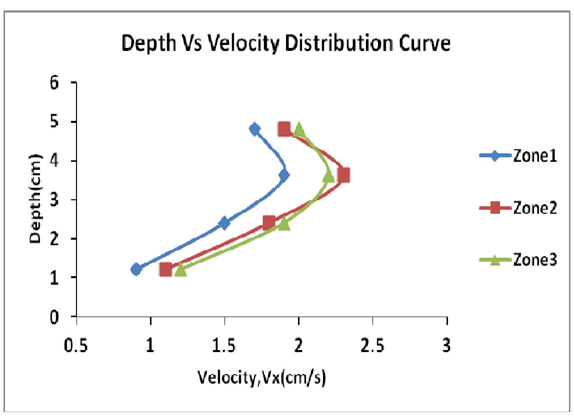

C3S3R1 (RFP)

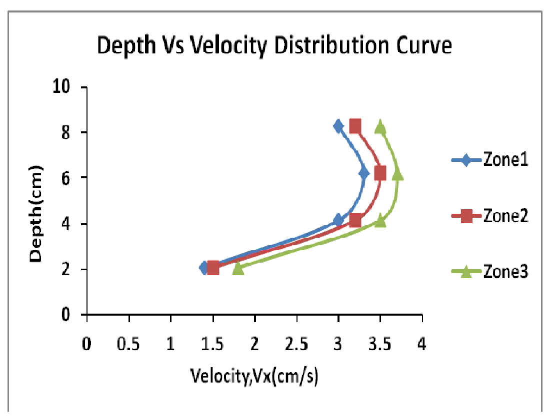

C3S3R2 (RFP)

Figure A-18: Longitudinal Velocity Profile for C3S2R1

Figure A-19: Longitudinal Velocity Profile for C3S2R2

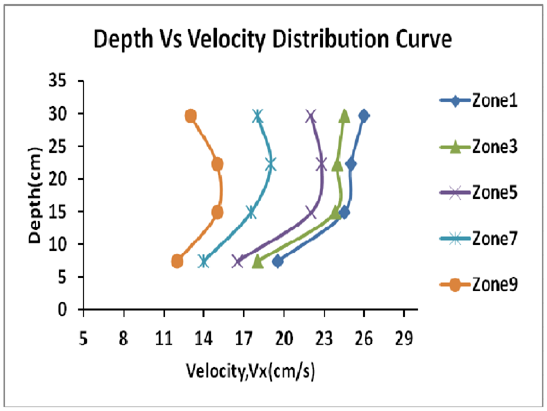

C3S3R3 (MC)

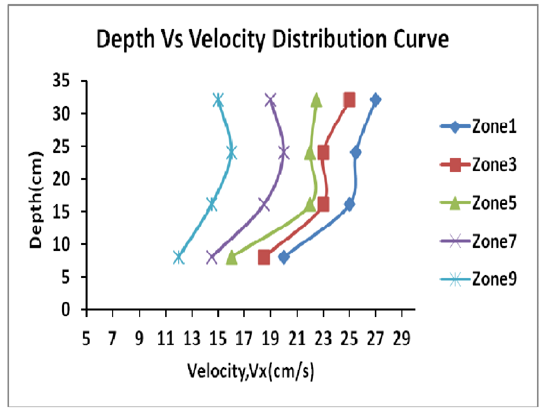

C3S3R4 (MC)

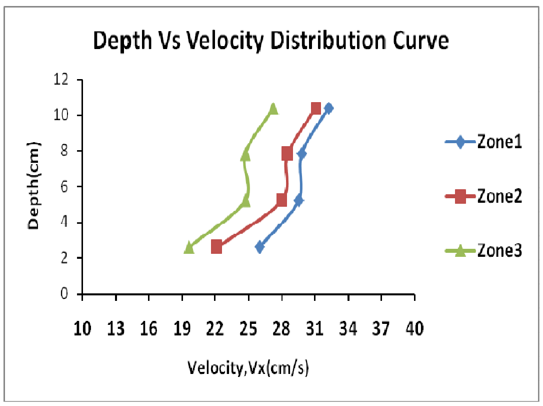

C3S3R3 (LFP)

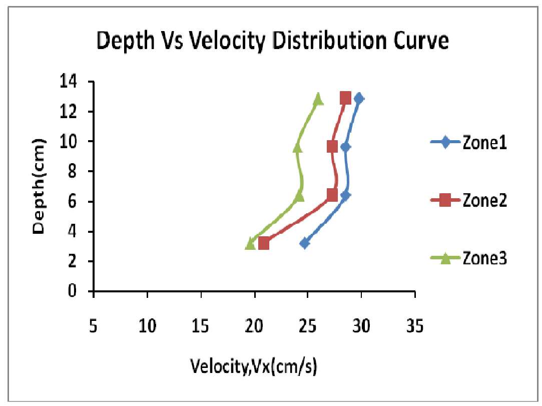

C3S3R4 (LFP)

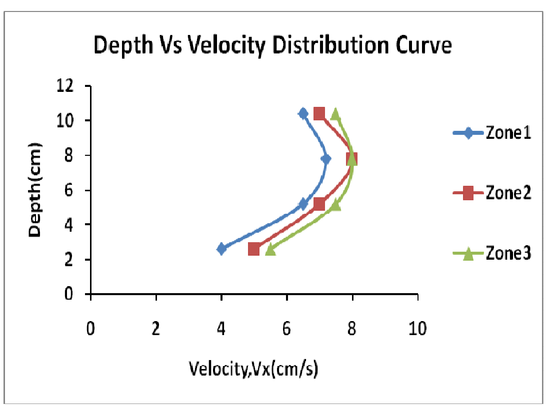

C3S3R3 (RFP)

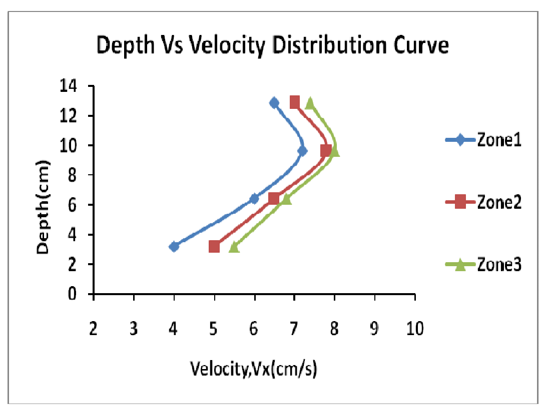

C3S3R4 (RFP)

Figure A-20: Longitudinal Velocity Profile for C3S3R3

Figure A-21: Longitudinal Velocity Profile for C3S3R4

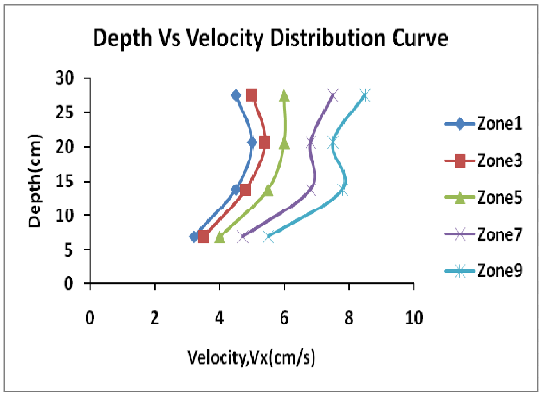

C4S1R2 (MC)

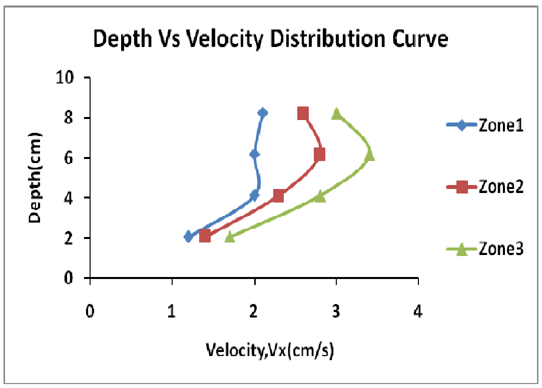

C4S1R2 (LFP)

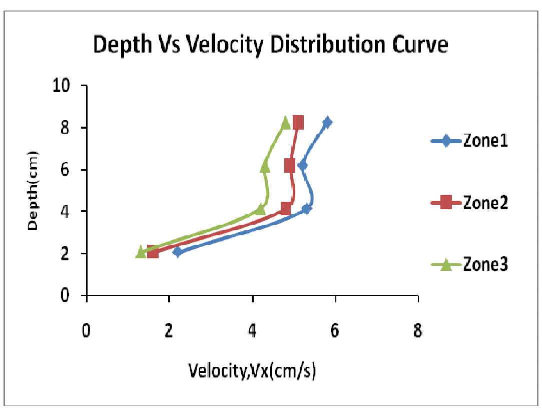

C4S1R2 (RFP)

Figure A-22: Longitudinal Velocity Profile for C4S1R2

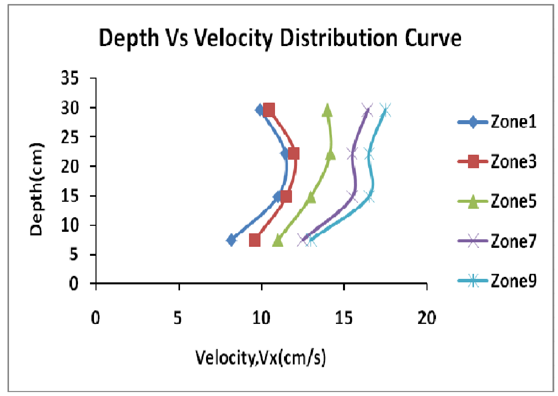

C4S1R3 (MC)

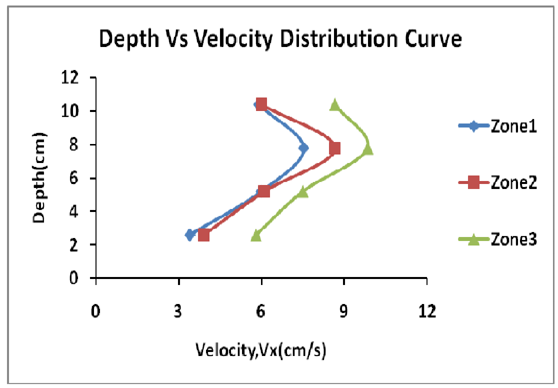

C4S1R3 (LFP)

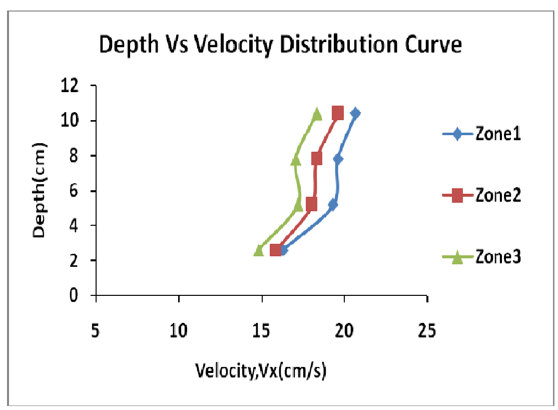

C4S1R3 (RFP)

Figure A-23: Longitudinal Velocity Profile for C4S1R3

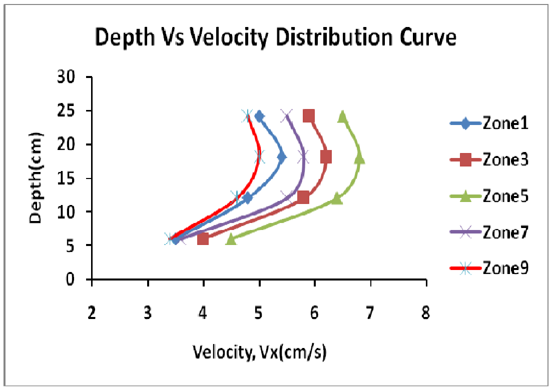

C4S2R1 (MC)

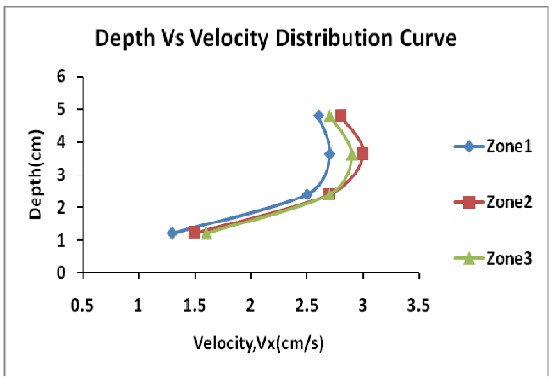

C4S2R1 (LFP)

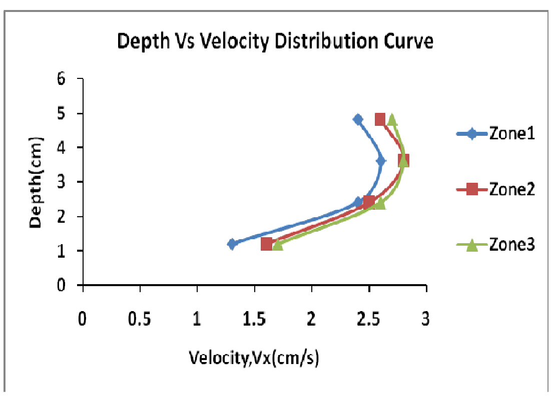

C4S2R1 (RFP)

Figure A-24: Longitudinal Velocity Profile for C4S2R1

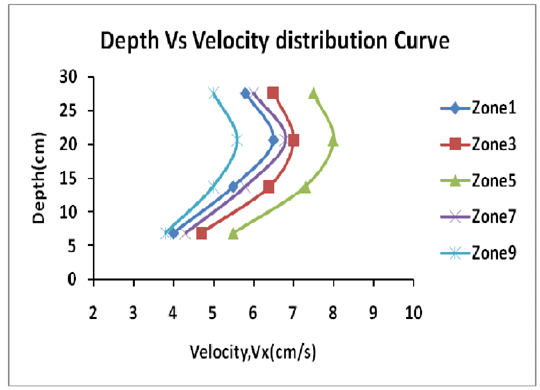

C4S2R2 (MC)

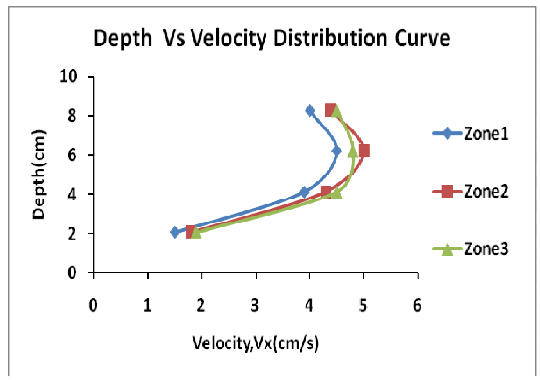

C4S2R2 (LFP)

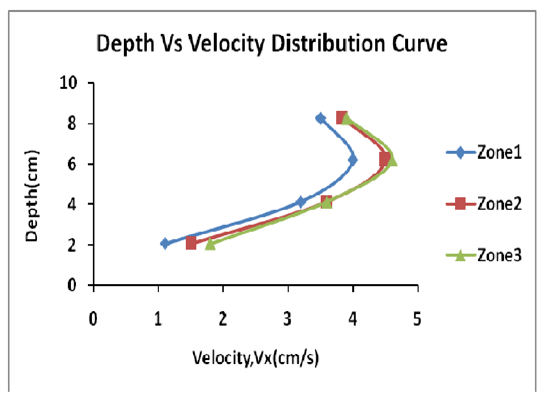

C4S2R2 (RFP)

Figure A-25: Longitudinal Velocity Profile for C4S2R2

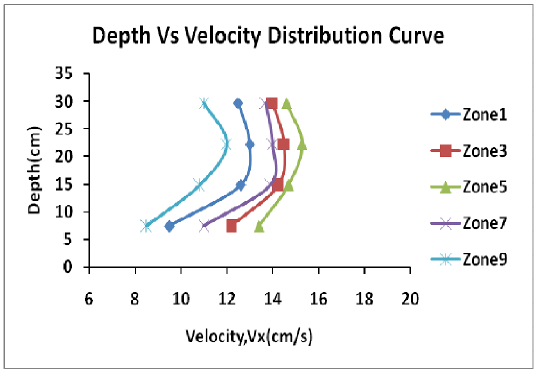

C4S2R3 (MC)

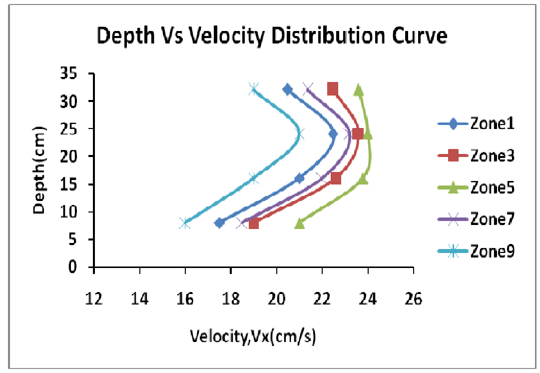

C4S2R4 (MC)

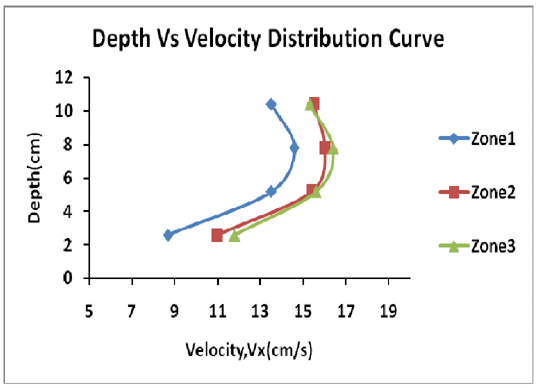

C4S2R3 (LFP)

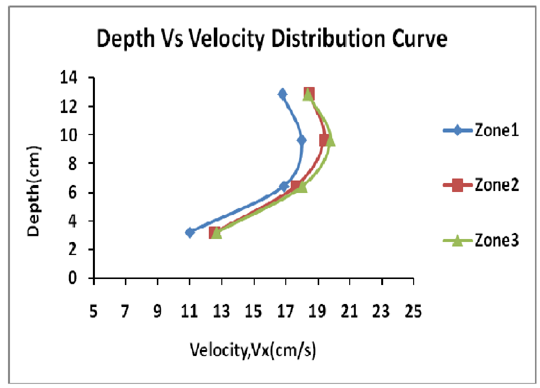

C4S2R4 (LFP)

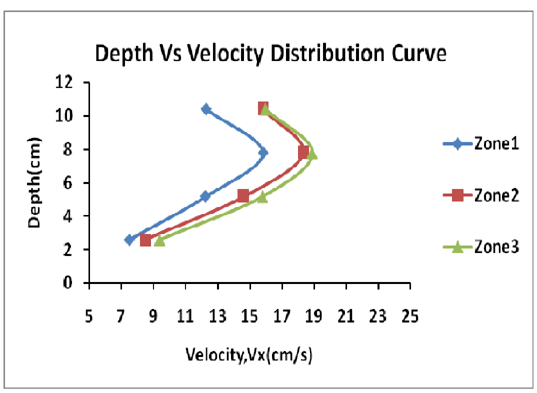

C4S2R3 (RFP)

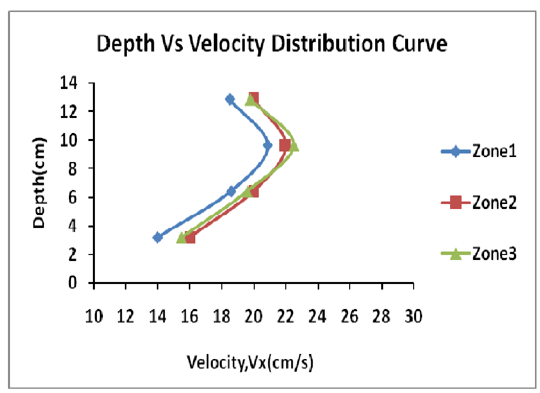

C4S2R4 (RFP)

Figure A-26: Longitudinal Velocity Profile for C4S2R1

Figure A-27: Longitudinal Velocity Profile for C4S2R2

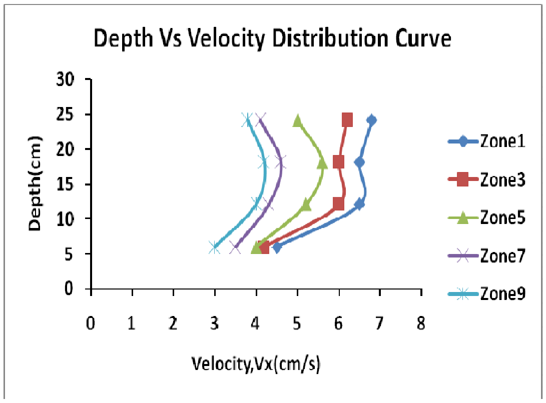

C4S3R1 (MC)

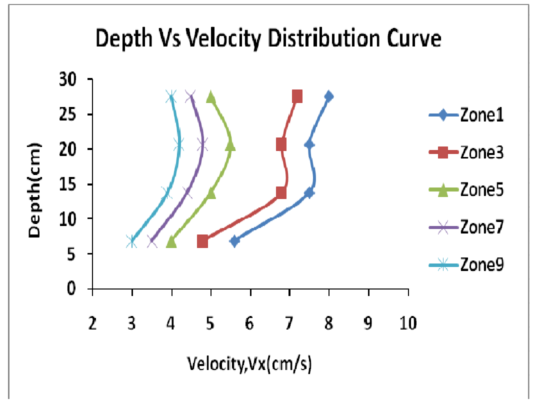

C4S3R2 (MC)

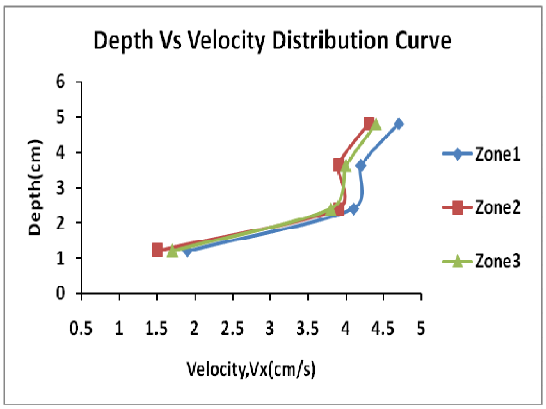

C4S3R1 (LFP)

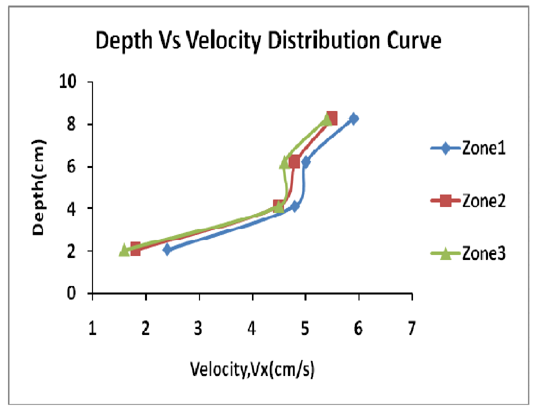

C4S3R2 (LFP)

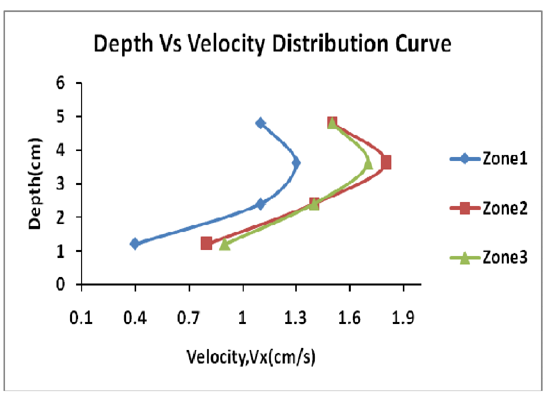

C4S3R1 (RFP)

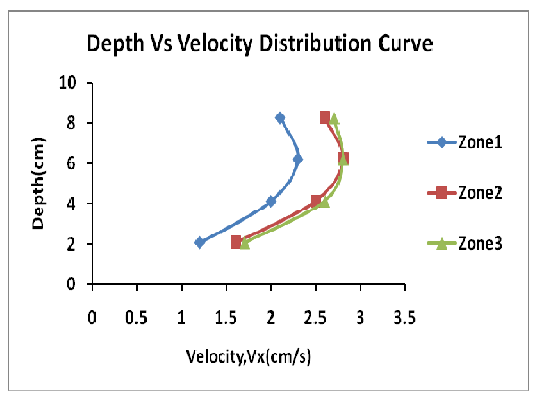

C4S3R2 (RFP)

Figure A-28: Longitudinal Velocity Profile for C4S3R1

Figure A-29: Longitudinal Velocity Profile for C4S3R2

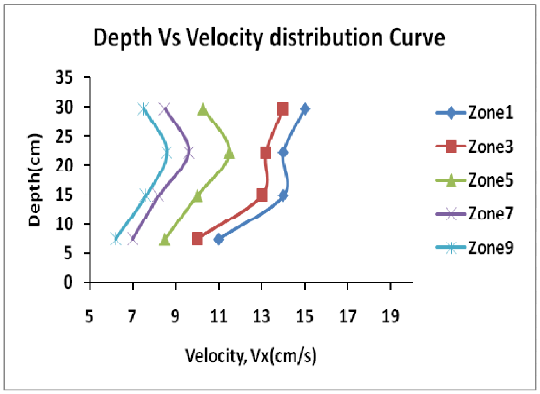

C4S3R3 (MC)

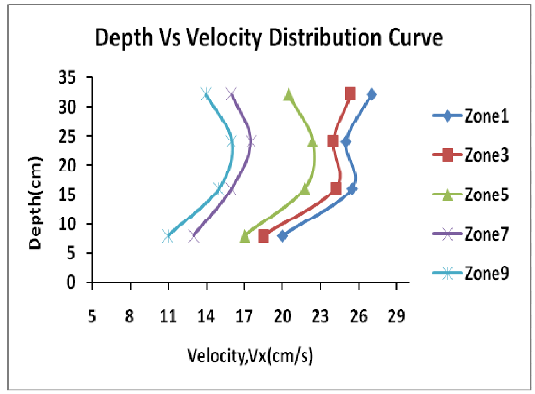

C4S3R4 (MC)

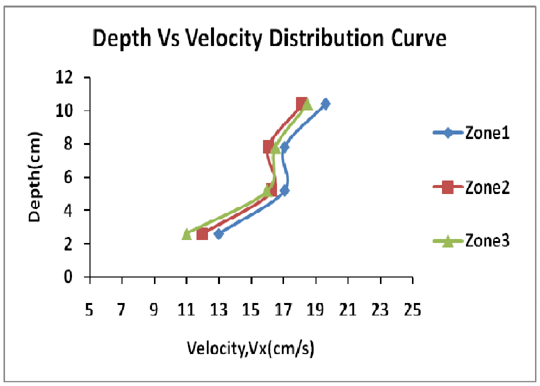

C4S3R3 (LFP)

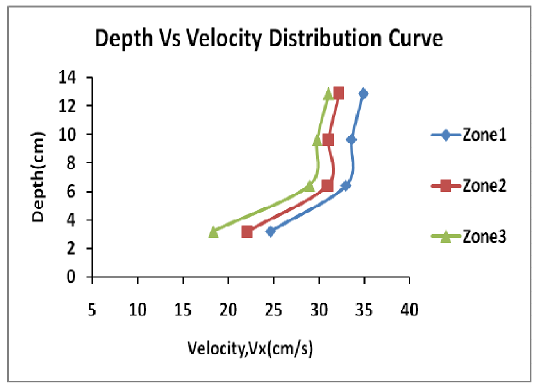

C4S3R4 (LFP)

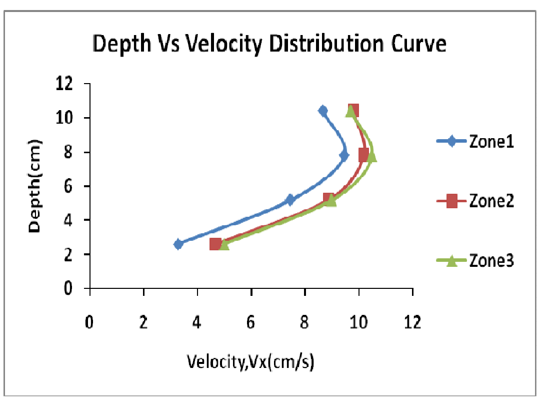

C4S3R3 (RFP)

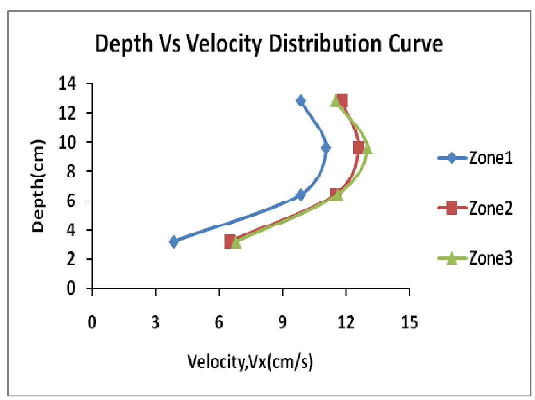

C4S3R4 (RFP)

Figure A-30: Longitudinal Velocity Profile for C4S3R1

Figure A-31: Longitudinal Velocity Profile for C4S3R2

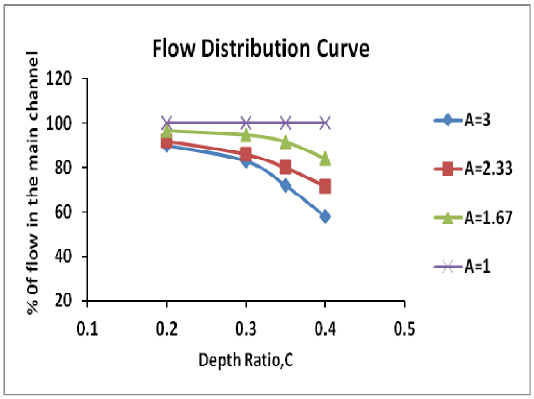

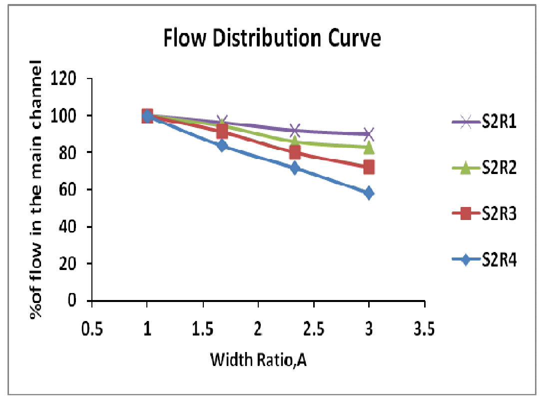

MC **MC**

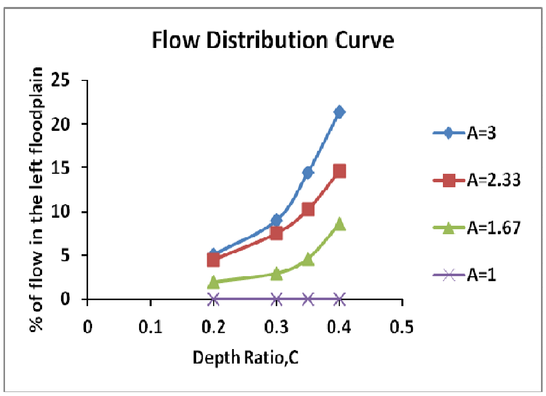

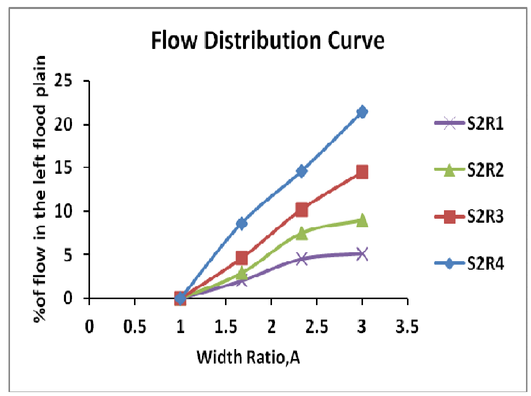

LFP **LFP**

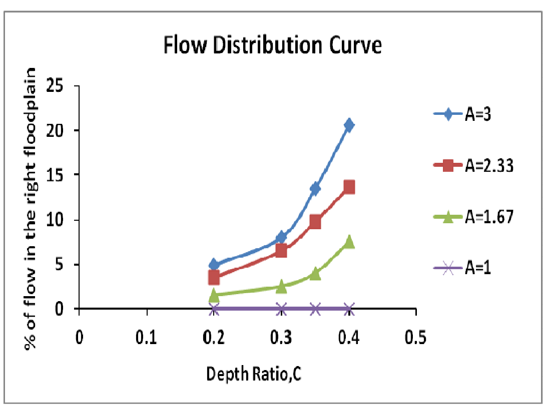

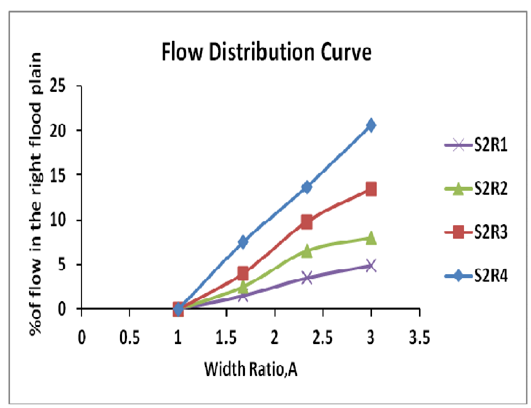

RFP **RFP**

Figure A-32: Flow Distribution Curve at U/S Cross-over Section (S2)

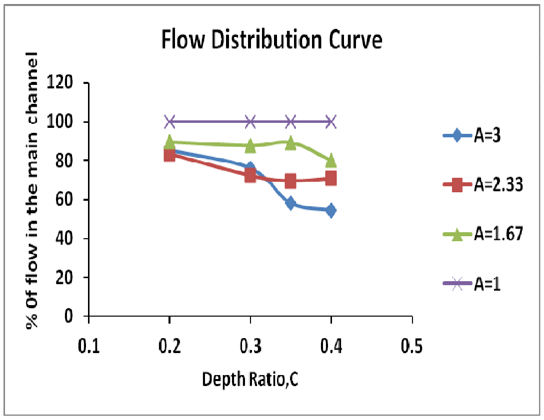

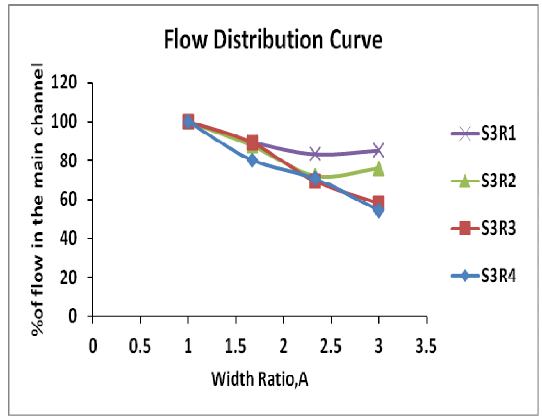

MC **MC**

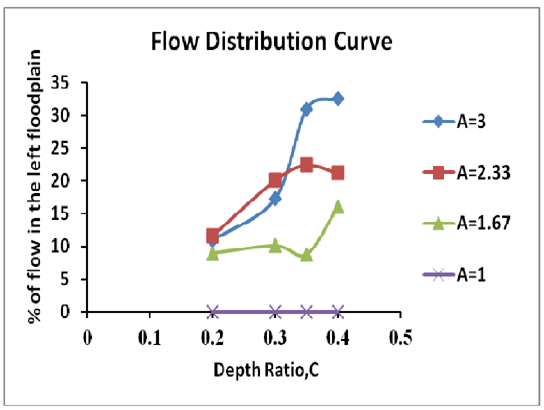

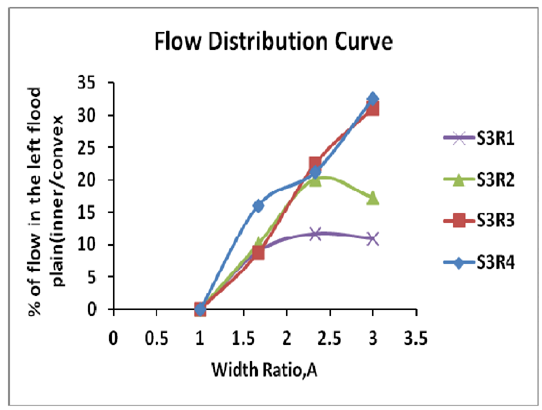

LFP **LFP**

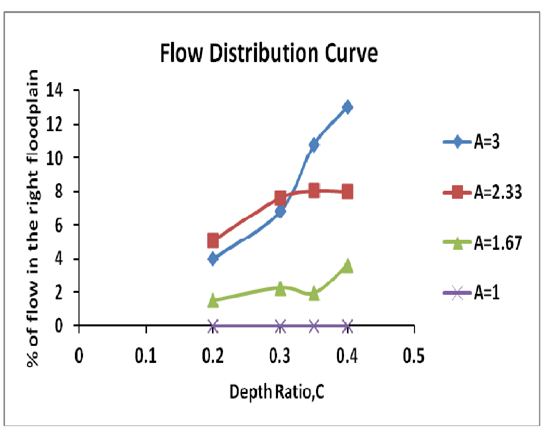

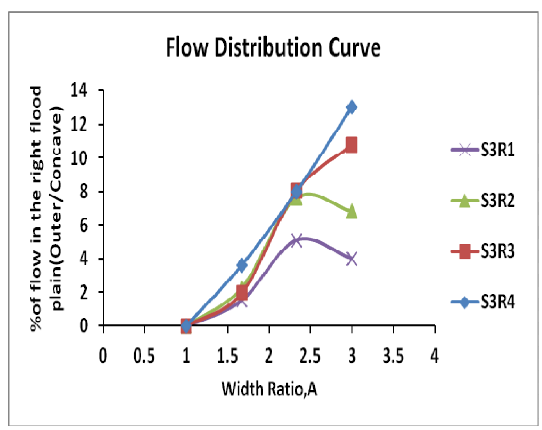

RFP **RFP**

Figure A-33: Flow Distribution Curve at Middle Bend Section (S3)

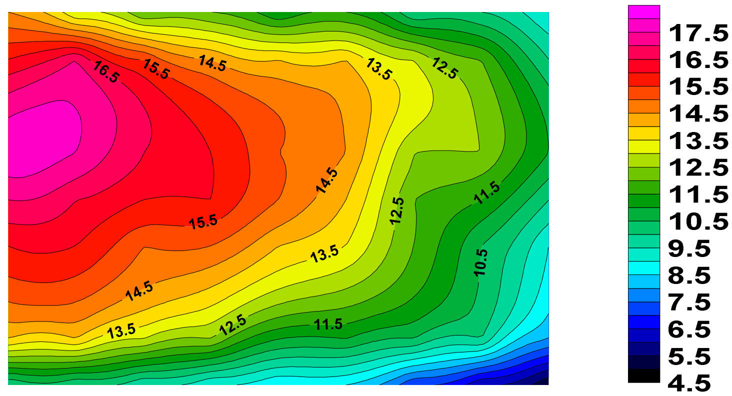

C1S3R2

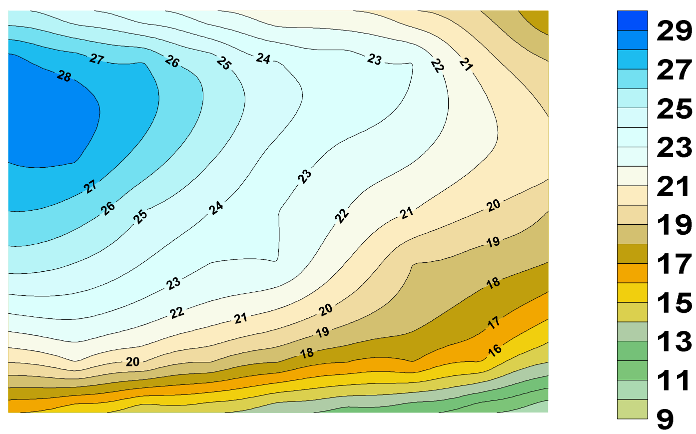

C1S3R3

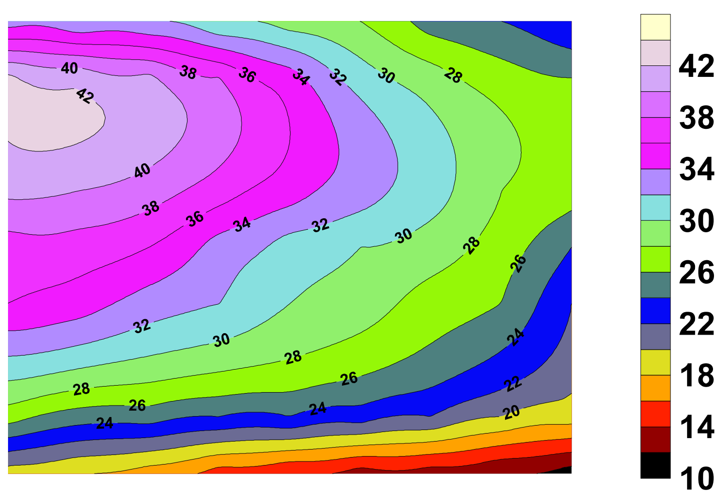

C1S3R4

Figure B-1: Isovel Profile for C1S3R2, C1S3R3, C1S3R4

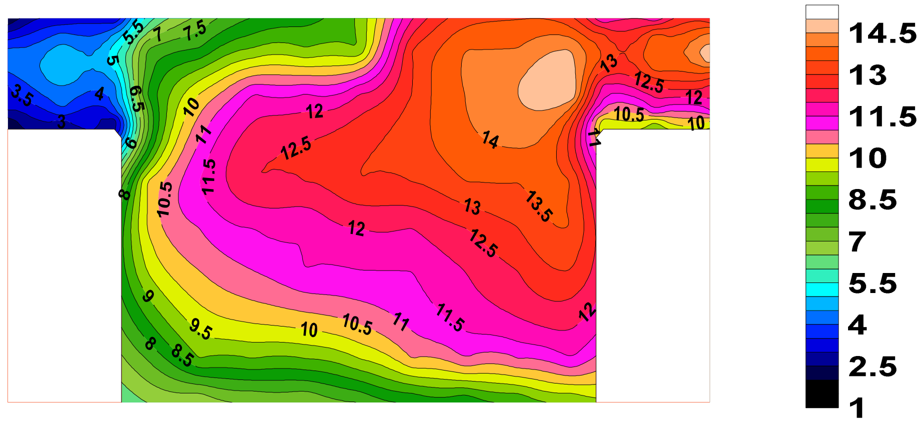

C2S1R2

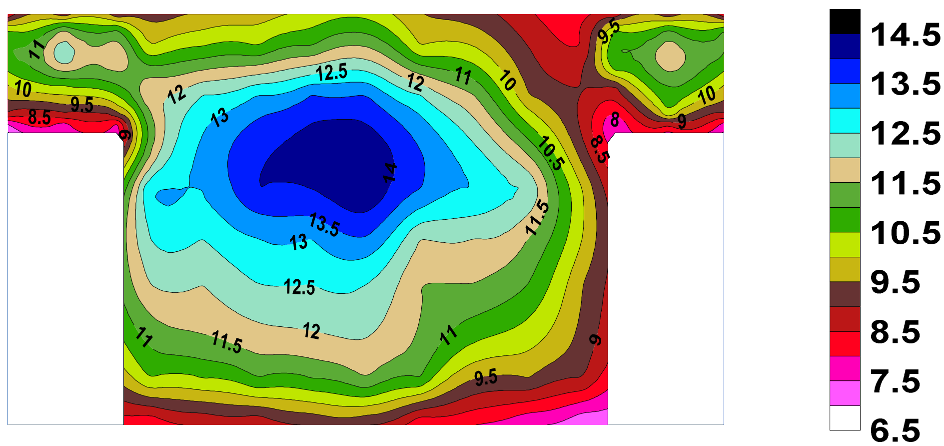

C2S2R2

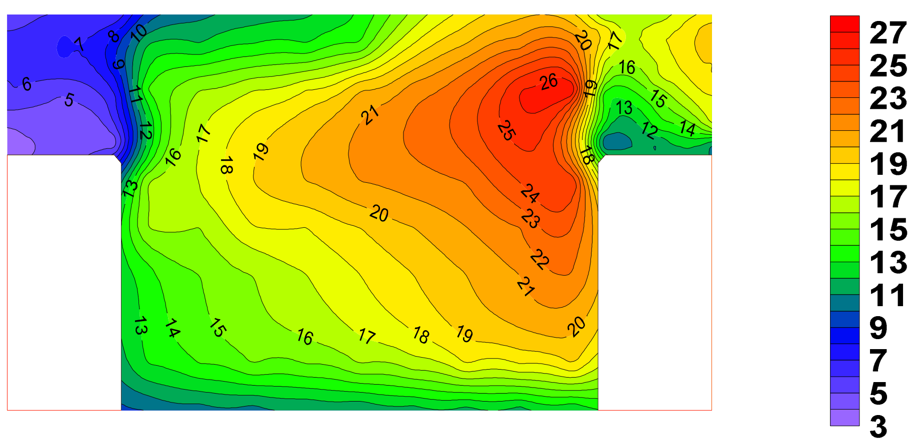

C2S1R3

Figure B-2: Isovel Profile for C2S1R2, C2S2R2, C2S1R3

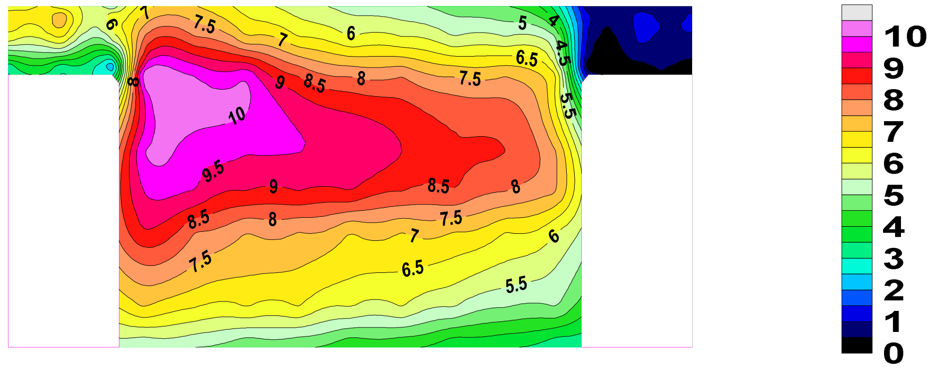

C2S3R1

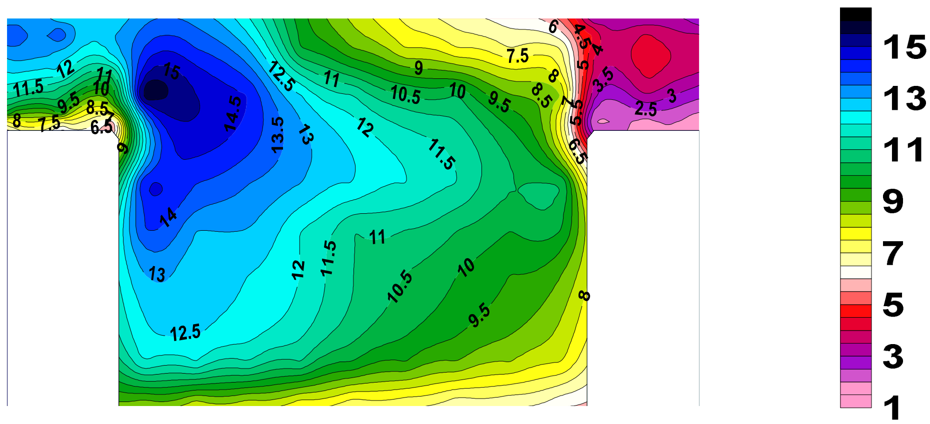

C2S3R2

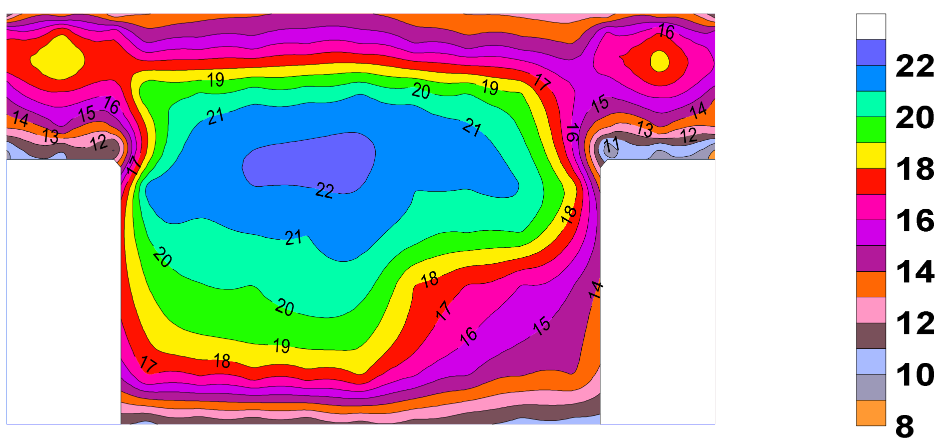

C2S2R3

Figure B-3: Isovel Profile for C2S3R1, C2S3R2, C2S2R3

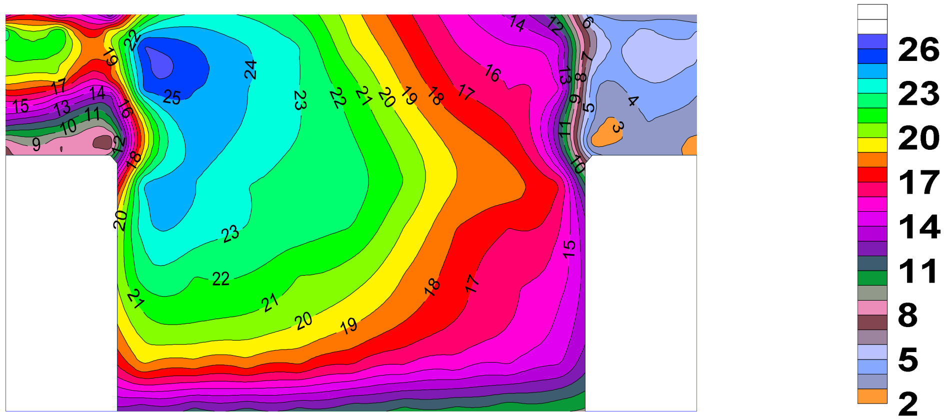

C2S3R3

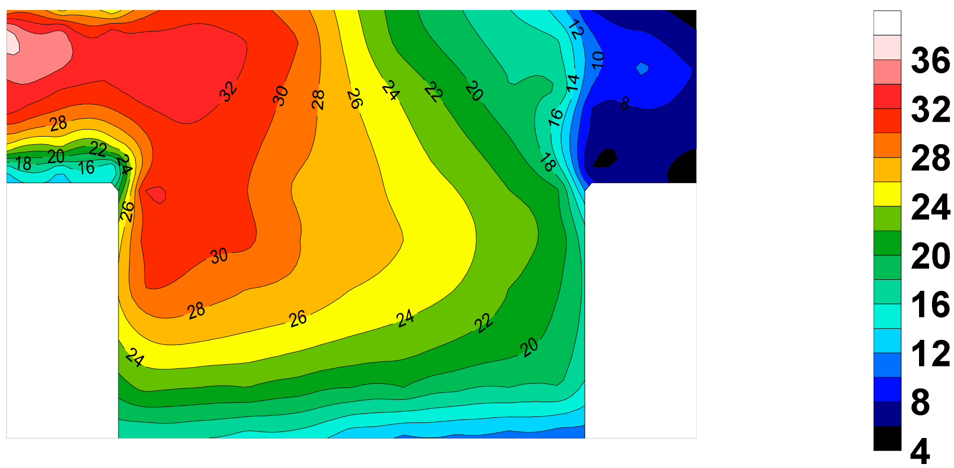

C2S3R4

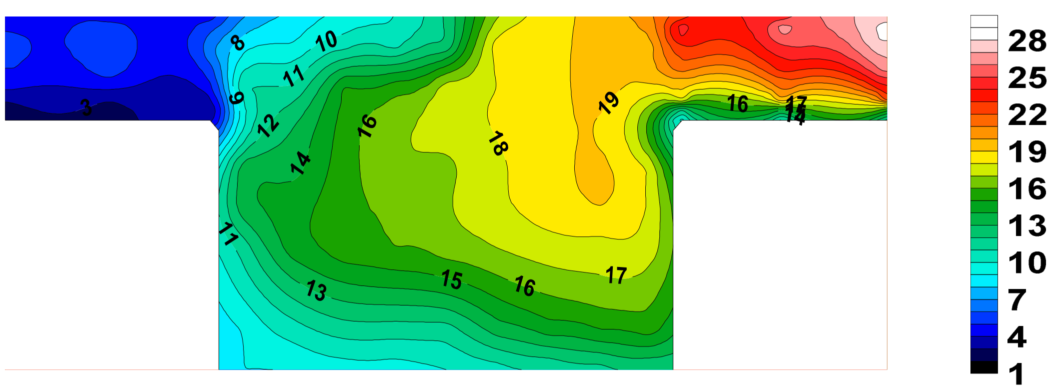

C3S1R2

Figure B-4: Isovel Profile for C2S3R3, C2S3R4, C3S1R2

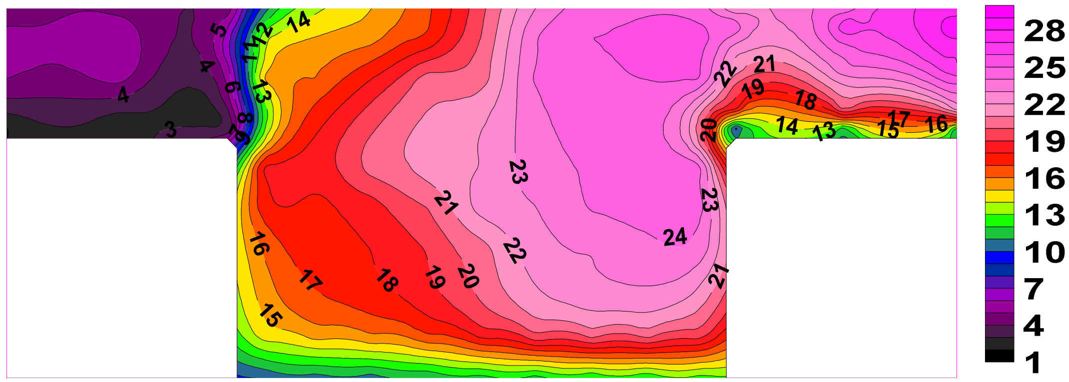

C3S1R3

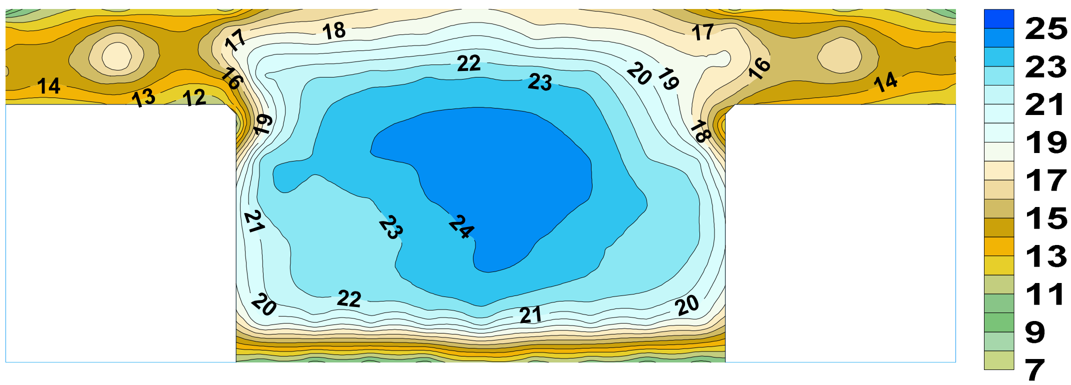

C3S2R2

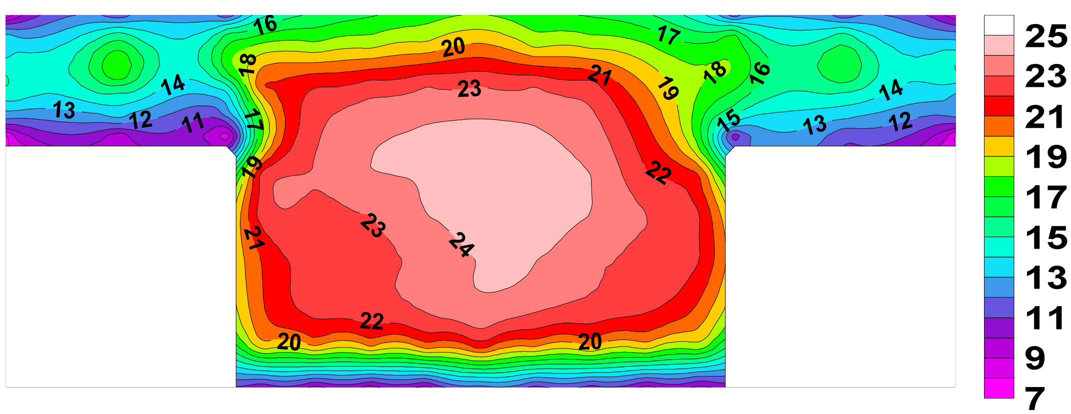

C3S2R3

Figure B-5: Isovel Profile for C3S1R3, C3S2R2, C3S2R3

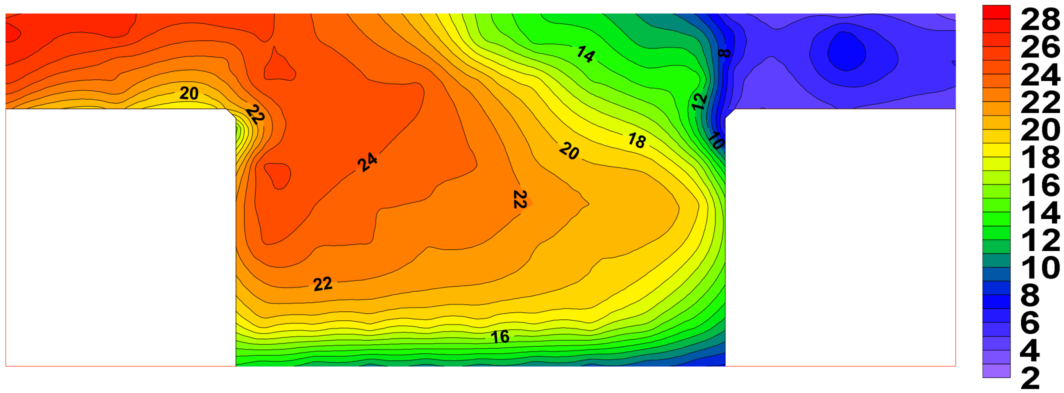

C3S3R2

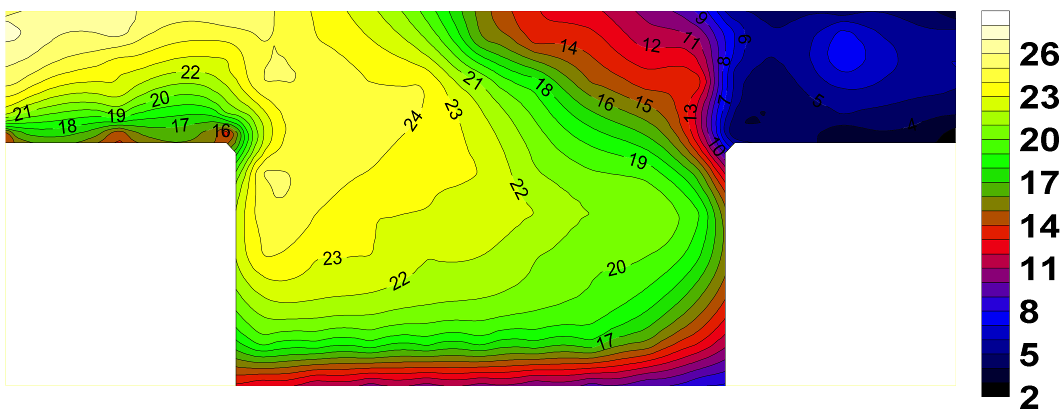

C3S3R3

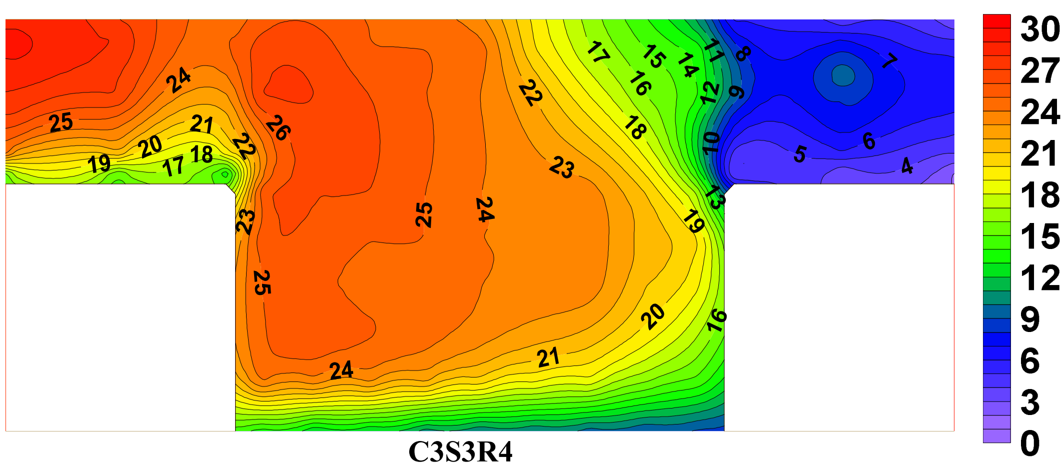

C3S3R4

Figure B-6: Isovel Profile for C3S3R2, C3S3R3, C3S3R4

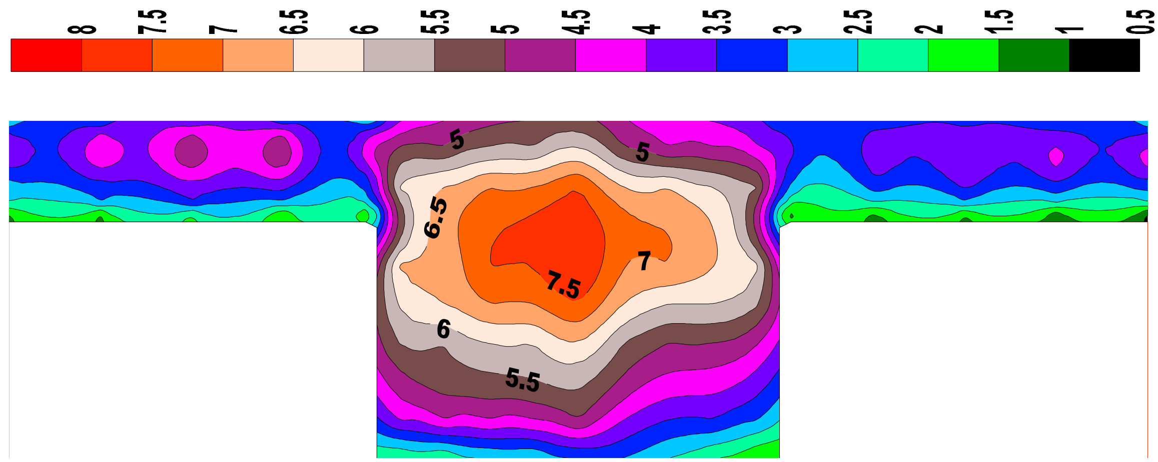

C4S2R2

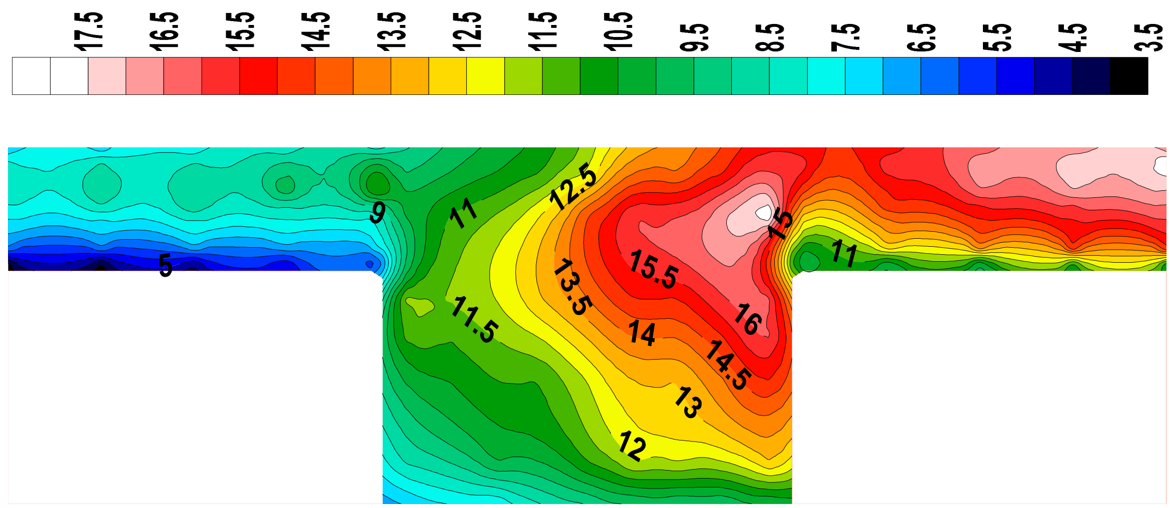

C4S1R3

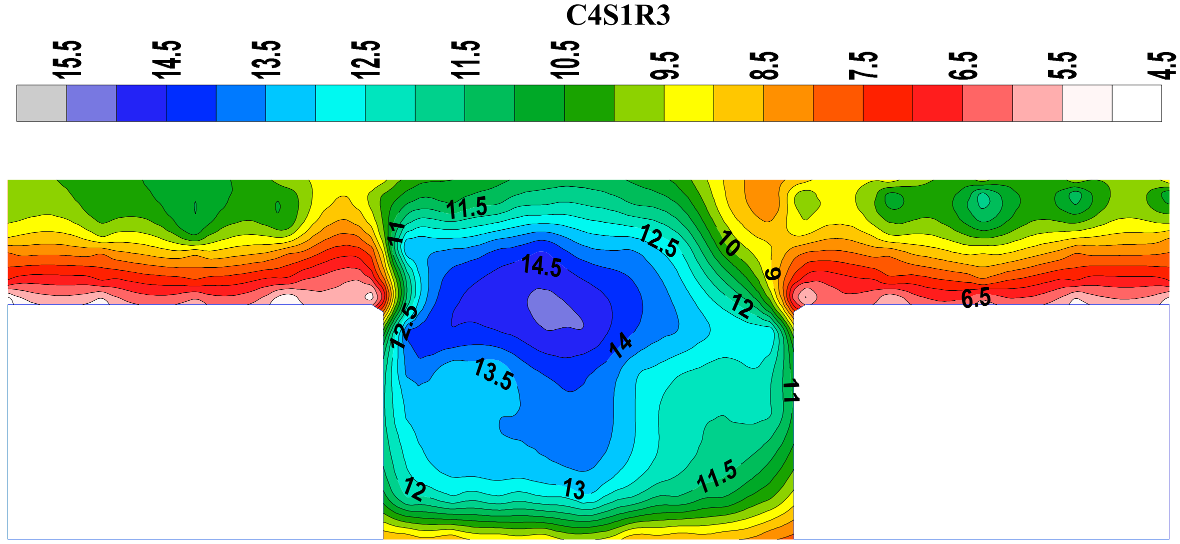

C4S2R3

Figure B-7: Isovel Profile for C4S2R2, C4S1R3, C4S2R3

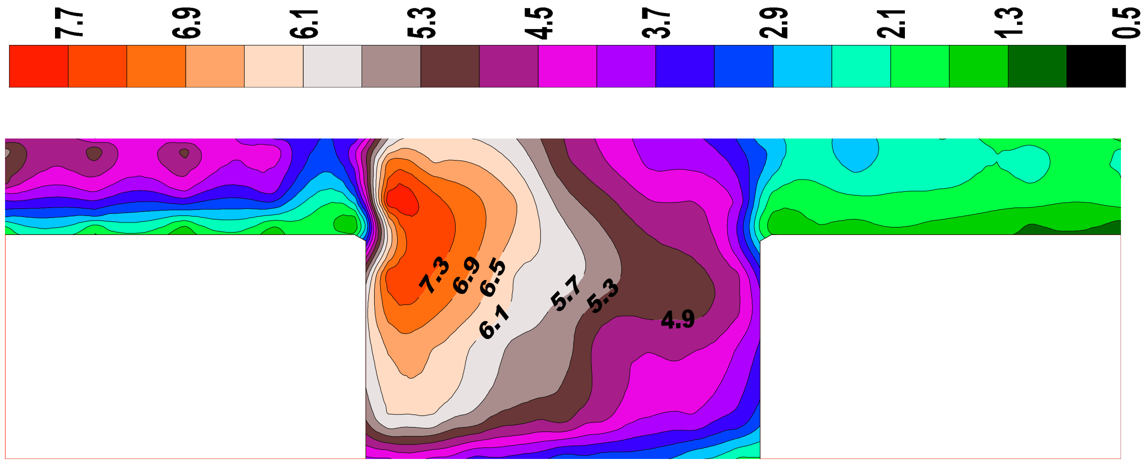

C4S3R2

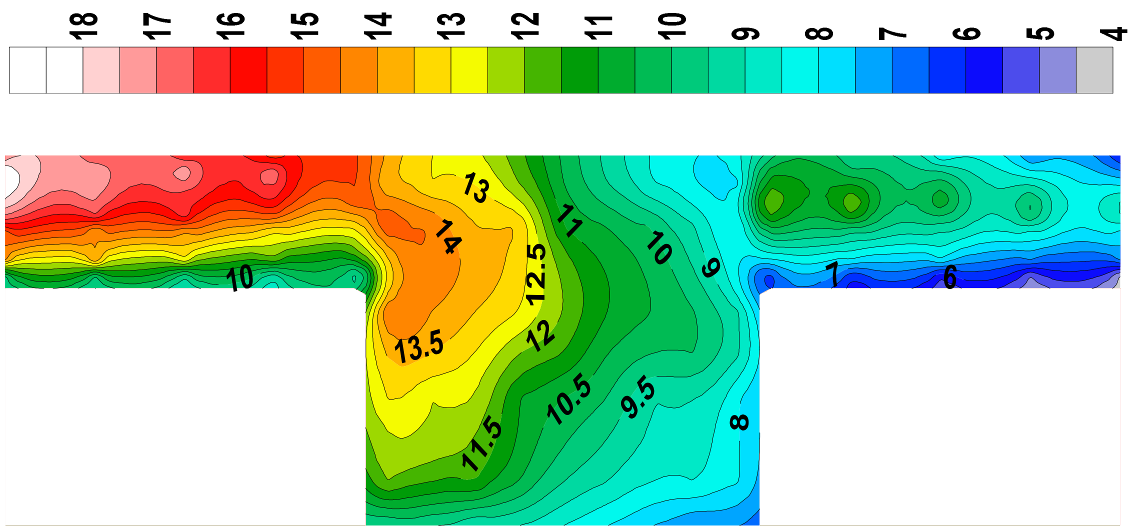

C4S3R3

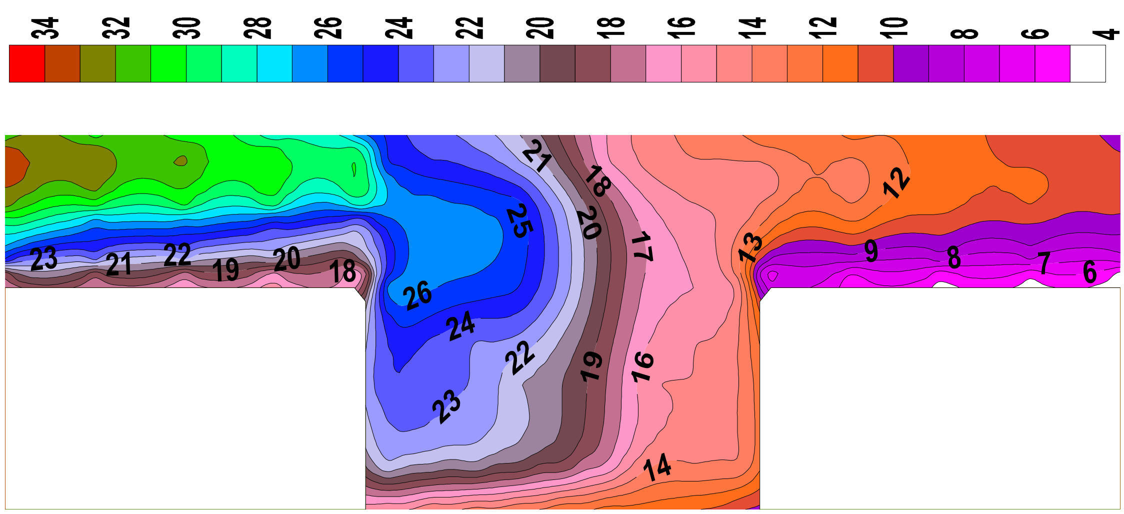

C4S3R4

Figure B-8: Isovel Profile for C4S3R2, C4S3R3, C4S3R3

Table C-1: Experimental Discharge Distribution at U/S Bend Section

Condition	Discharge,Q(cm^3/s)				% of Flow		
	Qmc	Q_{LFP}	Q_{RFP}	ΣQ	%Qmc	%Q_{LFP}	%Q_{RFP}
C1S1R1	14764.32	0	0	14764.32	100	0	0
C1S1R2	19872.95	0	0	19872.95	100	0	0
C1S1R3	51933.28	0	0	51933.28	100	0	0
C1S1R4	56227.24	0	0	56227.24	100	0	0
C2S1R1	9426.60	160.81	897.46	10484.87	89.91	1.53	8.56
C2S1R2	15867.05	330.94	1678.33	17876.32	88.76	1.85	9.39
C2S1R3	28299.70	605.22	2788.50	31693.42	89.29	1.91	8.80
C2S1R4	42728.80	1476.77	7616.66	51822.23	82.45	2.85	14.70
C3S1R1	14426.50	419.40	1845.20	16691.10	86.43	2.51	11.05
C3S1R2	23542.44	912.06	4050.00	28504.50	82.59	3.20	14.21
C3S1R3	31386.85	2188.40	9586.52	43161.77	72.72	5.07	22.21
C3S1R4	33994.27	2733.18	13254.21	49981.66	68.01	5.47	26.52
C4S1R1	5495.74	226.13	746.94	6468.81	84.96	3.50	11.55
C4S1R2	7377.60	470.47	1757.09	9605.16	76.81	4.90	18.29
C4S1R3	20157.36	2193.10	10264.72	32615.18	61.80	6.72	31.47
C4S1R4	36630.13	4146.39	17432.22	58208.74	62.93	7.12	29.95

Table C-2: Experimental Discharge Distribution at U/S Cross-over Section

Condition	Discharge,Q(cm^3/s)				% of Flow		
	Qmc	Q_{LFP}	Q_{RFP}	ΣQ	%Qmc	%Q_{LFP}	%Q_{RFP}
C1S2R1	14840.77	0	0	14840.77	100	0	0
C1S2R2	20132.14	0	0	20132.14	100	0	0
C1S2R3	35530.14	0	0	35530.14	100	0	0
C1S2R4	56443.12	0	0	56443.12	100	0	0
C2S2R1	9191.94	190.50	142.88	9525.32	96.50	2.00	1.50
C2S2R2	15437.23	473.23	407.96	16318.42	94.60	2.90	2.50
C2S2R3	28610.26	1439.90	1252.10	31302.26	91.40	4.60	4.00
C2S2R4	47660.32	4885.32	4260.46	56806.10	83.90	8.60	7.50
C3S2R1	15792.93	772.48	600.81	17166.22	92.00	4.50	3.50
C3S2R2	23180.13	2021.50	1751.98	26953.61	86.00	7.50	6.50
C3S2R3	35732.86	4555.94	4377.27	44666.07	80.00	10.20	9.80
C3S2R4	37202.61	7575.43	7108.45	51886.49	71.70	14.60	13.70
C4S2R1	6330.23	358.71	344.65	7033.59	90.00	5.10	4.90
C4S2R2	8298.25	899.81	799.83	9997.89	83.00	9.00	8.00
C4S2R3	19747.47	3976.88	3702.61	27426.96	72.00	14.50	13.50
C4S2R4	36190.80	13353.15	12853.96	62397.91	58.00	21.40	20.60

Table C-3: Experimental Discharge Distribution at Middle Bend Section

Condition	Discharge,Q(cm^3/s)				% of Flow		
	Qmc	Q_{LFP}	Q_{RFP}	ΣQ	%Qmc	%Q_{LFP}	%Q_{RFP}
C1S3R1	14488.83	0	0	14488.83	100	0	0
C1S3R2	19503.94	0	0	19503.94	100	0	0
C1S3R3	34604.09	0	0	34604.09	100	0	0
C1S3R4	53681.02	0	0	53681.02	100	0	0
C2S3R1	8884.25	885.21	150.09	9919.55	89.56	8.92	1.51
C2S3R2	15724.61	1804.41	404.48	17933.50	87.68	10.06	2.26
C2S3R3	30649.38	3006.14	670.31	34325.83	89.29	8.76	1.95
C2S3R4	41825.66	8345.25	1879.46	52050.37	80.36	16.03	3.61
C3S3R1	13552.75	1896.00	827.02	16275.77	83.27	11.65	5.08
C3S3R2	19370.09	5398.52	2040.07	26808.68	72.25	20.14	7.61
C3S3R3	32395.91	10456.77	3748.43	46601.11	69.52	22.44	8.04
C3S3R4	36684.11	12211.91	2881.85	51777.87	70.85	23.59	5.57
C4S3R1	6314.29	808.55	296.36	7419.20	85.11	10.90	3.99
C4S3R2	7887.32	1795.67	707.62	10390.61	75.91	17.28	6.81
C4S3R3	16114.61	9206.15	2393.56	27714.32	58.15	33.22	8.64
C4S3R4	33125.72	19805.54	7939.30	60870.56	54.42	32.54	13.04

Table C-4: Total Shear Stress Distribution

Condition	Location	b(cm)	h(cm)	A(cm^2)	P(cm)	R(m)	τ(N/m^2)
C1S1R1	MC	45.7	30.1	1375.57	105.90	0.13	2.35
C1S1R2	MC	45.7	34.5	1576.65	114.70	0.14	2.49
C1S1R3	MC	45.7	37.1	1695.47	119.90	0.14	2.56
C1S1R4	MC	45.7	40.2	1837.14	126.10	0.15	2.64
C2S1R1	MC	45.7	30.1	1375.57	93.90	0.15	2.65
	LFP	15.3	6	91.8	21.30	0.04	0.78
	RFP	15.3	6	91.8	21.30	0.04	0.78
C2S1R2	MC	45.7	34.5	1576.65	93.90	0.17	3.04
	LFP	15.3	10.4	159.12	25.70	0.06	1.12
	RFP	15.3	10.4	159.12	25.70	0.06	1.12
C2S1R3	MC	45.7	37.1	1695.47	93.90	0.18	3.27
	LFP	15.3	13	198.9	28.30	0.07	1.27
	RFP	15.3	13	198.9	28.30	0.07	1.27
C2S1R4	MC	45.7	40.2	1837.14	93.90	0.20	3.54
	LFP	15.3	16.1	246.33	31.30	0.08	1.42
	RFP	15.3	16.1	246.33	31.30	0.08	1.42
C3S1R1	MC	45.7	30.1	1375.57	93.90	0.15	2.65
	LFP	30.5	6	183	36.50	0.05	0.91
	RFP	30.5	6	183	36.50	0.05	0.91
C3S1R2	MC	45.7	34.5	1576.65	93.90	0.17	3.04
	LFP	30.5	10.4	317.2	40.90	0.08	1.40
	RFP	30.5	10.4	317.2	40.90	0.08	1.40
C3S1R3	MC	45.7	37.1	1695.47	93.90	0.18	3.27
	LFP	30.5	13	396.5	43.50	0.09	1.65
	RFP	30.5	13	396.5	43.50	0.09	1.65
C3S1R4	MC	45.7	40.2	1837.14	93.90	0.20	3.54
	LFP	30.5	16.1	491.05	46.60	0.11	1.91
	RFP	30.5	16.1	491.05	46.60	0.11	1.91
C4S1R1	MC	45.7	30.1	1375.57	93.90	0.15	2.65
	LFP	45.7	6	274.2	51.70	0.05	0.96
	RFP	45.7	6	274.2	51.70	0.05	0.96
C4S1R2	MC	45.7	34.5	1576.65	93.90	0.17	3.04
	LFP	45.7	10.4	475.28	56.10	0.08	1.53
	RFP	45.7	10.4	475.28	56.10	0.08	1.53
C4S1R3	MC	45.7	37.1	1695.47	93.90	0.18	3.27
	LFP	45.7	13	594.1	58.70	0.10	1.83
	RFP	45.7	13	594.1	58.70	0.10	1.83
C4S1R4	MC	45.7	40.2	1837.14	93.90	0.20	3.54
	LFP	45.7	16.1	735.77	61.80	0.12	2.15
	RFP	45.7	16.1	735.77	61.80	0.12	2.15

Table C-5: Shear Stress Distribution at U/S Bend Section (S1)

Condition	Location	τ_1(N/m^2)	τ_2(N/m^2)	τ_3(N/m^2)	$\tau 4$(N/m^2)	$\tau 5$(N/m^2)
C2S1R1	MC	0.02	0.03	0.04	0.05	0.07
	LFP	0.00	0.00	0.00	0.00	0.00
	RFP	0.06	0.05	0.04	0.00	0.00
C2S1R2	MC	0.04	0.07	0.08	0.11	0.12
	LFP	0.01	0.02	0.02	0.00	0.00
	RFP	0.19	0.18	0.17	0.00	0.00
C2S1R3	MC	0.13	0.16	0.21	0.28	0.34
	LFP	0.03	0.03	0.05	0.00	0.00
	RFP	0.35	0.22	0.22	0.00	0.00
C2S1R4	MC	0.20	0.24	0.45	0.52	0.63
	LFP	0.03	0.05	0.08	0.00	0.00
	RFP	0.91	0.83	0.77	0.00	0.00
C3S1R1	MC	0.04	0.07	0.09	0.13	0.13
	LFP	0.00	0.00	0.00	0.00	0.00
	RFP	0.13	0.13	0.10	0.00	0.00
C3S1R2	MC	0.06	0.12	0.13	0.20	0.21
	LFP	0.01	0.02	0.02	0.00	0.00
	RFP	0.39	0.31	0.24	0.00	0.00
C3S1R3	MC	0.14	0.20	0.29	0.37	0.38
	LFP	0.02	0.02	0.03	0.00	0.00
	RFP	0.67	0.57	0.47	0.00	0.00
C3S1R4	MC	0.15	0.21	0.29	0.37	0.37
	LFP	0.02	0.03	0.03	0.00	0.00
	RFP	0.62	0.53	0.43	0.00	0.00
C4S1R1	MC	0.01	0.01	0.01	0.02	0.02
	LFP	0.00	0.00	0.00	0.00	0.00
	RFP	0.02	0.02	0.01	0.01	0.01
C4S1R2	MC	0.01	0.01	0.02	0.02	0.03
	LFP	0.00	0.00	0.00	0.01	0.01
	RFP	0.02	0.02	0.02	0.01	0.01
C4S1R3	MC	0.05	0.08	0.13	0.15	0.17
	LFP	0.05	0.06	0.06	0.07	0.08
	RFP	0.28	0.27	0.25	0.22	0.19
C4S1R4	MC	0.14	0.24	0.29	0.36	0.42
	LFP	0.06	0.07	0.10	0.10	0.11
	RFP	0.84	0.68	0.56	0.51	0.48

Table C-6: Shear Stress Distribution at Crossover Section (S2)

Condition	Location	$\tau_1(N/m^2)$	$\tau_2(N/m^2)$	$\tau_3(N/m^2)$	$\tau 4(N/m^2)$	$\tau 5(N/m^2)$
C2S2R1	MC	0.04	0.04	0.05	0.03	0.03
	LFP	0.01	0.01	0.02	0.00	0.00
	RFP	0.01	0.01	0.01	0.00	0.00
C2S2R2	MC	0.09	0.10	0.10	0.06	0.06
	LFP	0.11	0.12	0.12	0.00	0.00
	RFP	0.12	0.13	0.10	0.00	0.00
C2S2R3	MC	0.28	0.28	0.29	0.24	0.18
	LFP	0.22	0.28	0.24	0.00	0.00
	RFP	0.20	0.25	0.22	0.00	0.00
C2S2R4	MC	0.55	0.59	0.60	0.51	0.37
	LFP	0.34	0.34	0.31	0.00	0.00
	RFP	0.24	0.30	0.27	0.00	0.00
C3S2R1	MC	0.11	0.11	0.12	0.09	0.08
	LFP	0.01	0.02	0.02	0.00	0.00
	RFP	0.02	0.03	0.03	0.00	0.00
C3S2R2	MC	0.17	0.17	0.17	0.14	0.14
	LFP	0.07	0.18	0.18	0.00	0.00
	RFP	0.04	0.10	0.15	0.00	0.00
C3S2R3	MC	0.32	0.34	0.34	0.34	0.22
	LFP	0.16	0.20	0.20	0.00	0.00
	RFP	0.15	0.20	0.26	0.00	0.00
C3S2R4	MC	0.31	0.33	0.34	0.30	0.24
	LFP	0.19	0.25	0.22	0.00	0.00
	RFP	0.16	0.27	0.25	0.00	0.00
C4S2R1	MC	0.02	0.02	0.02	0.02	0.02
	LFP	0.01	0.01	0.01	0.01	0.01
	RFP	0.00	0.01	0.01	0.01	0.01
C4S1R2	MC	0.03	0.03	0.03	0.03	0.02
	LFP	0.01	0.01	0.02	0.02	0.01
	RFP	0.01	0.01	0.01	0.01	0.01
C4S1R3	MC	0.11	0.12	0.12	0.11	0.07
	LFP	0.07	0.08	0.09	0.08	0.07
	RFP	0.08	0.09	0.10	0.09	0.07
C4S1R4	MC	0.28	0.31	0.32	0.30	0.26
	LFP	0.22	0.24	0.28	0.26	0.25
	RFP	0.27	0.35	0.42	0.35	0.30

Table C-7: Shear Stress Distribution at Middle Bend Section (S3)

Condition	Location	τ_1(N/m^2)	τ_2(N/m^2)	τ_3(N/m^2)	τ4(N/m^2)	τ5(N/m^2)
C2S1R1	MC	0.05	0.04	0.04	0.03	0.03
	LFP	0.04	0.04	0.03	0.00	0.00
	RFP	0.00	0.00	0.00	0.00	0.00
C2S1R2	MC	0.13	0.10	0.08	0.06	0.05
	LFP	0.17	0.16	0.13	0.00	0.00
	RFP	0.01	0.01	0.01	0.00	0.00
C2S1R3	MC	0.32	0.31	0.26	0.21	0.19
	LFP	0.31	0.29	0.23	0.00	0.00
	RFP	0.02	0.02	0.03	0.00	0.00
C2S1R4	MC	0.61	0.58	0.43	0.27	0.24
	LFP	0.88	0.80	0.75	0.00	0.00
	RFP	0.03	0.05	0.07	0.00	0.00
C3S1R1	MC	0.12	0.10	0.07	0.07	0.07
	LFP	0.14	0.11	0.10	0.00	0.00
	RFP	0.00	0.00	0.00	0.00	0.00
C3S1R2	MC	0.20	0.20	0.13	0.07	0.07
	LFP	0.37	0.33	0.31	0.00	0.00
	RFP	0.02	0.02	0.02	0.00	0.00
C3S1R3	MC	0.31	0.30	0.29	0.18	0.11
	LFP	0.64	0.57	0.52	0.00	0.00
	RFP	0.02	0.04	0.04	0.00	0.00
C3S1R4	MC	0.44	0.42	0.33	0.21	0.19
	LFP	0.67	0.57	0.46	0.00	0.00
	RFP	0.02	0.04	0.04	0.00	0.00
C4S1R1	MC	0.03	0.02	0.02	0.01	0.01
	LFP	0.01	0.01	0.01	0.01	0.00
	RFP	0.00	0.00	0.00	0.00	0.00
C4S1R2	MC	0.03	0.03	0.02	0.01	0.01
	LFP	0.02	0.02	0.02	0.01	0.01
	RFP	0.00	0.00	0.01	0.01	0.01
C4S1R3	MC	0.11	0.10	0.07	0.05	0.04
	LFP	0.27	0.24	0.24	0.22	0.18
	RFP	0.05	0.06	0.08	0.08	0.09
C4S1R4	MC	0.34	0.33	0.24	0.13	0.12
	LFP	0.83	0.75	0.71	0.64	0.60
	RFP	0.07	0.08	0.09	0.11	0.13

Table C-8: Velocity Distribution Coefficients at U/S Bend Section (S1)

Condition	Location	Δh	u1	u2	u3	u4	h	ū	α	β
C1S1R1	MC	6.03	13.3	13	12.35	11	24.13	10.75	1.33	1.15
C1S1R2	MC	6.89	16.5	16.8	15.9	14.5	27.58	13.85	1.32	1.15
C1S1R3	MC	7.42	25.5	23.50	23.00	20	29.7	19.80	1.33	1.15
C1S1R4	MC	8.04	37.5	36.20	34.40	31.6	32.16	30.24	1.32	1.15
C2S1R1	MC	6.03	9.36	8.94	8.67	6.7	24.13	7.24	1.37	1.16
	LFP	1.21	0.9	1.00	0.80	0.6	4.84	0.71	1.45	1.18
	RFP	1.21	6.28	7.50	6.30	4.5	4.84	5.36	1.44	1.18
C2S1R2	MC	6.89	11.98	12.34	12.3	9.6	27.58	10.05	1.35	1.16
	LFP	2.07	4	5.00	4.50	4	8.27	3.88	1.34	1.15
	RFP	2.07	9.85	13.44	13.44	11	8.27	10.71	1.36	1.16
C2S1R3	MC	7.42	21.1	20.00	18.60	16.4	29.7	16.38	1.34	1.15
	LFP	2.6	7	7.00	5.00	4.5	10.4	5.00	1.46	1.19
	RFP	2.6	15.8	17.10	14.60	11	10.4	12.65	1.41	1.17
C2S1R4	MC	8.04	29	29.35	28.60	25.7	32.16	24.54	1.32	1.15
	LFP	3.22	7.5	11.00	8.50	7.5	12.9	7.68	1.42	1.18
	RFP	3.22	28	33.60	32.30	28.5	12.9	27.06	1.33	1.15
C3S1R1	MC	6.03	13	13.95	13.4	10	24.13	10.96	1.37	1.16
	LFP	1.21	0.95	1.10	0.70	0.5	4.84	0.69	1.67	1.25
	RFP	1.21	12.2	14.63	14.60	7.5	4.84	10.71	1.54	1.22
C3S1R2	MC	6.89	15.5	16.9	16	11.55	27.58	13.04	1.39	1.17
	LFP	2.07	6.3	8.70	7.50	3.5	8.27	5.72	1.67	1.26
	RFP	2.07	15	18.30	19.60	15	8.27	15.12	1.36	1.16
C3S1R3	MC	7.42	20.9	21.50	21.44	19.3	29.7	18.16	1.32	1.15
	LFP	2.6	5.1	6.20	5.00	3.9	10.4	4.4125	1.42	1.18
	RFP	2.6	23.4	20.88	20.50	18.34	10.4	17.86	1.33	1.15
C3S1R4	MC	8.04	21.5	22.00	21.50	19.8	32.16	18.51	1.31	1.14
	LFP	3.22	8.6	9.05	7.30	5	12.9	6.40	1.50	1.20
	RFP	3.22	27.3	25.98	22.16	20.88	12.9	20.64	1.35	1.16
C4S1R1	MC	6.03	4.7	5.5	5.6	3.8	24.13	4.31	1.40	1.17
	LFP	1.21	0.8	0.80	0.60	0.5	4.84	0.58	1.46	1.19
	RFP	1.21	3.5	3.50	2.50	2	4.84	2.44	1.52	1.20
C4S1R2	MC	6.89	6.6	6.1	6.01	4.44	27.58	4.96	1.38	1.17
	LFP	2.07	2.5	2.80	2.20	1.5	8.27	1.94	1.50	1.20
	RFP	2.07	5	5.20	4.10	2.5	8.27	3.58	1.57	1.22
C4S1R3	MC	7.42	14.9	14.20	14.00	13	29.7	12.15	1.32	1.15
	LFP	2.6	8.6	9.90	7.50	3.9	10.4	6.4	1.69	1.26
	RFP	2.6	17	18.40	18.40	15.8	10.4	15.28	1.32	1.15
C4S1R4	MC	8.04	23.5	23.50	22.60	20	32.16	19.46	1.32	1.15
	LFP	3.22	11.05	12.25	11.05	6.3	12.9	8.77	1.52	1.21
	RFP	3.22	20.9	25.98	25.90	24.7	12.9	21.72	1.33	1.15

Table C-9: Velocity Distribution Coefficients at Cross-over Section (S2)

Condition	Location	Δh	u1	u2	u3	u4	h	ū	α	β
C1S2R1	MC	6.03	13	13.5	12.4	12	24.13	11.10	1.32	1.15
C1S2R2	MC	6.89	16.2	16.8	15.6	12.8	27.58	13.32	1.35	1.16
C1S2R3	MC	7.42	25.0	25.30	24.60	22.24	29.7	21.15	1.32	1.15
C1S2R4	MC	8.04	37.7	36.60	35.60	32.2	32.16	30.81	1.32	1.15
C2S2R1	MC	6.03	9.7	9.45	9.05	6.4	24.13	7.43	1.40	1.17
	LFP	1.21	2.2	2.50	2.10	1.4	4.84	1.78	1.47	1.19
	RFP	1.21	2.1	2.30	2.00	1.3	4.84	1.66	1.47	1.19
C2S2R2	MC	6.89	11.5	13	12.7	10.7	27.58	10.53	1.33	1.15
	LFP	2.07	5.1	9.90	7.50	5	8.27	6.25	1.63	1.23
	RFP	2.07	5	6.50	6.20	4	8.27	4.81	1.44	1.18
C2S2R3	MC	7.42	22.1	21.30	20.60	19.9	29.7	18.20	1.31	1.15
	LFP	2.6	18	19.00	16.50	15	10.4	14.875	1.34	1.15
	RFP	2.6	17	18.50	16.00	14	10.4	14.25	1.35	1.16
C2S2R4	MC	8.04	32.3	30.80	30.20	29.6	32.16	26.69	1.31	1.14
	LFP	3.22	19.5	22.00	20.00	19	12.9	17.66	1.32	1.15
	RFP	3.22	18	20.00	19.50	18	12.9	16.60	1.32	1.15
C3S2R1	MC	6.03	14.2	14.9	14.4	11.2	24.13	11.90	1.36	1.16
	LFP	1.21	5.8	6.50	6.30	4.1	4.84	4.95	1.42	1.18
	RFP	1.21	5	6.00	5.50	4	4.84	4.50	1.40	1.17
C3S2R2	MC	6.89	17.4	17.52	16.64	14.78	27.58	14.40	1.33	1.15
	LFP	2.07	9.9	14.60	11.00	7.5	8.27	9.52	1.55	1.21
	RFP	2.07	9.9	15.80	14.60	9.9	8.27	11.33	1.47	1.19
C3S2R3	MC	7.42	24.3	23.50	24.60	21.45	29.7	20.41	1.32	1.15
	LFP	2.6	19.6	18.34	18.30	13	10.4	14.86	1.39	1.17
	RFP	2.6	17	18.50	17.00	13.5	10.4	14.38	1.36	1.16
C3S2R4	MC	8.04	23.19	24.40	23.52	22.9	32.16	20.60	1.31	1.14
	LFP	3.22	15.83	18.34	14.63	11.05	12.9	12.96	1.45	1.18
	RFP	3.22	17	19.60	17.06	12.5	12.9	14.39	1.42	1.18
C4S2R1	MC	6.03	5.9	6.2	6.01	4.5	24.13	4.91	1.37	1.16
	LFP	1.21	4	3.50	3.00	2	4.84	2.63	1.52	1.21
	RFP	1.21	3	3.50	2.50	2	4.84	2.38	1.49	1.20
C4S2R2	MC	6.89	6.3	7.3	6.8	5.2	27.58	5.61	1.37	1.16
	LFP	2.07	4.5	5.00	4.00	3.5	8.27	3.69	1.38	1.16
	RFP	2.07	3.8	4.00	3.80	3	8.27	3.18	1.35	1.16
C4S2R3	MC	7.42	13.8	14.30	13.80	12.7	29.7	11.92	1.32	1.15
	LFP	2.6	9	9.80	6.30	5.8	10.4	6.6	1.52	1.20
	RFP	2.6	9.8	11.00	7.40	6.2	10.4	7.38	1.52	1.21
C4S2R4	MC	8.04	23.9	23.40	23.40	21.1	32.16	19.96	1.32	1.15
	LFP	3.22	17.1	18.40	14.60	13.4	12.9	13.72	1.38	1.16
	RFP	3.22	19.6	20.80	19.60	18	12.9	17.02	1.32	1.15

Table C-10: Velocity Distribution Coefficients at Middle Bend Section (S3)

Condition	Location	Δh	u1	u2	u3	u4	h	ū	α	β
C1S3R1	MC	6.03	13.3	13.1	11.8	10.9	24.13	10.61	1.33	1.15
C1S3R2	MC	6.89	14.7	16.5	15.9	13.7	27.58	13.35	1.33	1.15
C1S3R3	MC	7.42	25.3	25.20	23.50	21.3	29.7	20.65	1.33	1.15
C1S3R4	MC	8.04	35.4	34.80	33.60	32	32.16	29.53	1.31	1.14
C2S3R1	MC	6.03	8.9	9.6	9.14	6.8	24.13	7.49	1.37	1.16
	LFP	1.21	6.5	7.00	6.00	4.4	4.84	5.16	1.42	1.18
	RFP	1.21	0.9	1.10	1.00	0.6	4.84	0.79	1.49	1.20
C2S3R2	MC	6.89	11.8	12.3	12.3	9.8	27.58	10.07	1.34	1.15
	LFP	2.07	9.9	13.44	12.25	9.9	8.27	10.15	1.37	1.16
	RFP	2.07	4.0	5.00	4.00	4	8.27	3.75	1.35	1.15
C2S3R3	MC	7.42	21.5	22.80	20.50	18.5	29.7	18.13	1.33	1.15
	LFP	2.6	19.6	20.00	15.00	12	10.4	14.2	1.47	1.19
	RFP	2.6	5.5	6.00	4.50	4	10.4	4.31	1.42	1.17
C2S3R4	MC	8.04	26	27.50	26.00	23	32.16	22.38	1.32	1.15
	LFP	3.22	27.5	33.60	32.00	28	12.9	26.80	1.34	1.15
	RFP	3.22	8	10.50	8.00	7	12.9	7.36	1.42	1.18
C3S3R1	MC	6.03	11.5	14	12.44	10.5	24.13	10.67	1.36	1.16
	LFP	1.21	11	14.60	13.44	7.47	4.84	10.25	1.54	1.21
	RFP	1.21	0.9	1.10	0.70	0.5	4.84	0.69	1.66	1.25
C3S3R2	MC	6.89	14.8	16.2	16.8	12.8	27.58	13.29	1.35	1.16
	LFP	2.07	19.6	18.30	14.60	13.5	8.27	14.07	1.39	1.17
	RFP	2.07	6.0	8.50	6.30	3.5	8.27	5.33	1.68	1.25
C3S3R3	MC	7.42	21.0	25.00	22.80	21.5	29.7	19.94	1.33	1.15
	LFP	2.6	27	24.70	24.70	19.6	10.4	20.625	1.35	1.16
	RFP	2.6	7.5	8.60	7.40	5	10.4	6.19	1.45	1.19
C3S3R4	MC	8.04	22.7	23.50	23.50	19.67	32.16	19.51	1.33	1.15
	LFP	3.22	28.53	27.30	27.30	20.85	12.9	22.39	1.36	1.16
	RFP	3.22	6.3	8.70	8.00	5	12.9	6.20	1.49	1.20
C4S3R1	MC	6.03	5.4	5.8	5.6	3.7	24.13	4.45	1.42	1.18
	LFP	1.21	3	2.80	2.00	1.8	4.84	2.03	1.48	1.19
	RFP	1.21	0.6	0.70	0.50	0.4	4.84	0.48	1.49	1.20
C4S3R2	MC	6.89	5.3	6.9	6.8	4.5	27.58	5.21	1.43	1.18
	LFP	2.07	5.0	5.30	4.00	2.5	8.27	3.58	1.59	1.23
	RFP	2.07	2.5	2.40	2.00	1.5	8.27	1.79	1.44	1.18
C4S3R3	MC	7.42	10.3	12.05	11.20	10.7	29.7	9.77	1.32	1.15
	LFP	2.6	18.3	17.06	14.63	13.44	10.4	13.57	1.36	1.16
	RFP	2.6	8.66	6.30	6.30	3.8	10.4	5.18	1.58	1.22
C4S3R4	MC	8.04	23.5	24.90	24.70	23	32.16	21.09	1.31	1.14
	LFP	3.22	24.7	24.20	23.40	22.1	12.9	20.48	1.32	1.15
	RFP	3.22	9.85	11.05	8.70	6.28	12.9	7.73	1.48	1.19

Photo D-1: Compound Meandering Channel with Width Ratio 3

Photo D-2: Compound Meandering Channel with Width Ratio 2.33

Photo D-3: Compound Meandering Channel with Width Ratio 1.67

Photo D-4: Compound Meandering Channel with Width Ratio 1

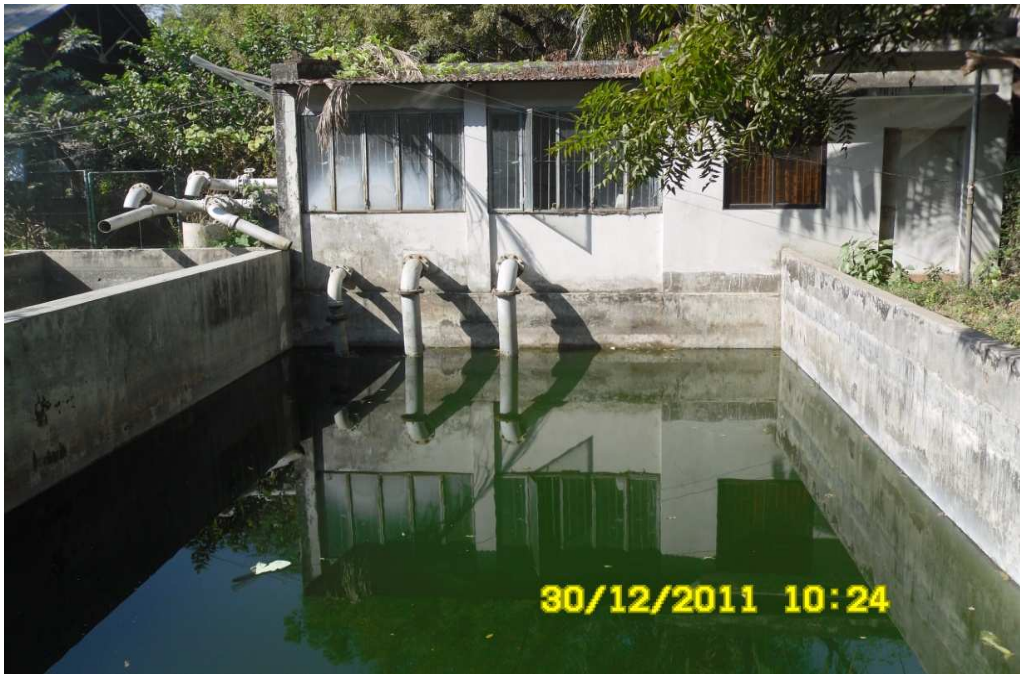

Photo D-5: The Storage Reservoir

Photo D-6: The Upstream Reservoir

Photo D-7: The Approach Channel

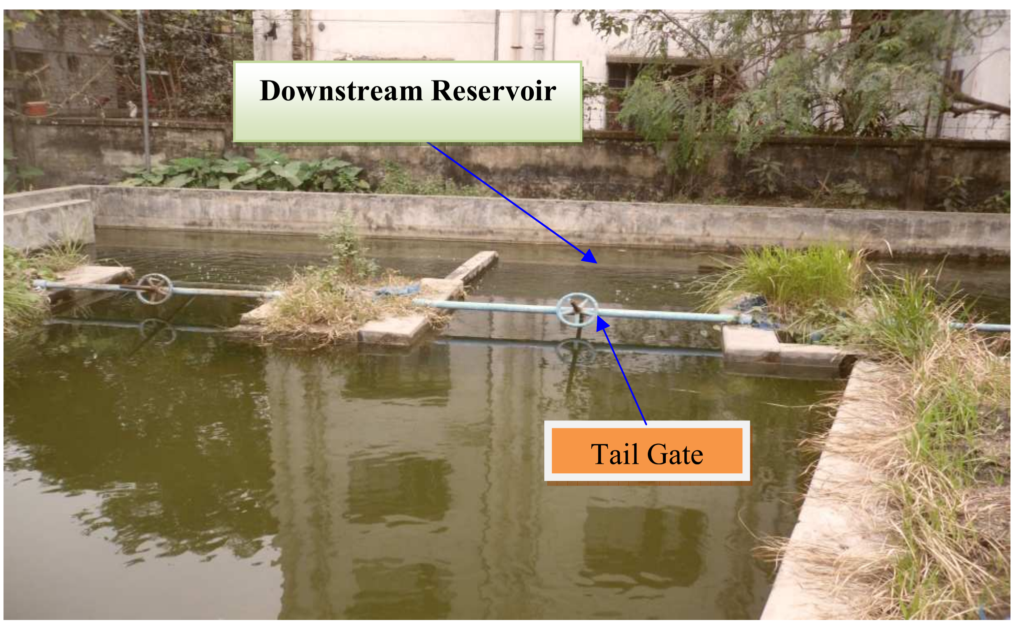

Photo D-8: The Downstream Reservoir

Photo D-9: The Transition Flume

Photo D-10: The Guide Vanes and Tubes